RESEARCH

UDOT Keeping Utah Moving

Utah Department of Transportation - Research Division
4501 South 2700 West - P.O. Box 148410 - SLC,UT 84114-8410

Report No. UT-24.15

MEASURING THE IMPACT OF ROADSIDE FEATURES ON ROAD DEPARTURE CRASHES AND PRIORITIZING SAFETY IMPROVEMENT PROJECTS

Prepared For:

Utah Department of Transportation
Research & Innovation Division

Final Report
November 2024

ACKNOWLEDGMENTS

The authors acknowledge the Utah Department of Transportation (UDOT) for funding this research, and the following individuals from UDOT on the Technical Advisory Committee for helping to guide the research:

- Jeff Lewis (Safety Programs Engineer)
- Carrie Jacobson (Region 1 Traffic Operations Engineer)
- Abdul Wakil (Asset Engineer for Maintenance)
- Suyanka Neupaney (Data and Safety Manager)
- Brad Palmer (UDOT Rail Division Director)
- Clancy Black (Traffic and Safety Division Consultant)

TECHNICAL REPORT ABSTRACT

1. Report No.	2. Government Accession No.	3. Recipient's Catalog No.
UT-24.15	N/A	N/A

4. Title and Subtitle	5. Report Date
Measuring the Impact of Roadside Features on Road-Departure Crashes and Prioritizing Safety Improvement Projects	September 2024
	6. Performing Organization Code N/A
7. Author(s) Abhishek Kumar Subedi, Nikola Markovic, Abbas Rashidi, Robert Chamberlin	8. Performing Organization Report No. N/A
9. Performing Organization Name and Address The University of Utah Department of Civil and Environmental Engineering 201 Presidents Circle Salt Lake City, Utah 84112	10. Work Unit No. 5H092 62H 11. Contract or Grant No. 24-8334
12. Sponsoring Agency Name and Address Utah Department of Transportation 4501 South 2700 West P.O. Box 148410 Salt Lake City, UT 84114-8410	13. Type of Report & Period Covered Final Sept 2023 to Nov 2024 14. Sponsoring Agency Code UT23.314

15. Supplementary Notes

Prepared in cooperation with the Utah Department of Transportation and the U.S. Department of Transportation, Federal Highway Administration

16. Abstract

This study investigated the impact of roadside features on road departure (RD) crashes and provided recommendations for safety improvements on Utah's highways. The research utilized a computer vision model originally developed in the UDOT project, Automated Safety Assessment of Rural Roadways Using Computer Vision (Mashhadi et al., 2023), which was initially trained on images from Mandli. The model was retrained on Pathway images to extract roadside features from across seven Utah roads, including non-interstate routes (US-6, SR-10, SR-12, US-40, SR-150) and interstate highways (I-15 and I-80). The retrained model achieved high classification accuracies, enabling the extraction of key roadside features such as clear zones, rigid obstacles, side slopes, and safety barriers using advanced computer vision techniques. Safety ratings were assigned based on the algorithm developed in accordance with FHWA roadside rating guidelines. The roadside feature dataset was merged with the crash database obtained from UDOT using the milepoints information to create a comprehensive view of crash occurrences and severities in relation to roadside features. Statistical analysis, including Spearman's Rank Correlation Coefficient, was conducted to identify the correlation between these features and RD crash rates. The study identified hotspots and provided targeted recommendations for safety improvements, such as installing safety barriers, improving clear zones, implementing high-friction surface treatments, and considering additional safety measures to enhance overall roadway safety.

17. Key Words	18. Distribution Statement	23. Registrant's Seal
Road Departure Crash, Roadside Safety, Machine Learning, Image Processing, Computer Vision, Statistical Analysis, Hotspot, Safety Measures	Not restricted. Available through: UDOT Research Division 4501 South 2700 West P.O. Box 148410 Salt Lake City, UT 84114-8410 www.udot.utah.gov/go/research	N/A

19. Security Classification (of this report)	20. Security Classification (of this page)	21. No. of Pages	22. Price
Unclassified	Unclassified	185	N/A

TABLE OF CONTENTS

LIST OF TABLES

LIST OF FIGURES

LIST OF ACRONYMS

AADT	Annual Average Daily Traffic
CMF	Crash Modification Factor
DOT	Department of Transportation
EPDO	Equivalent Property Damage Only
FHWA	Federal Highway Administration
GBDT	Gradient Boosting Decision Tree
GIS	Geographic Information System
HFST	High-Friction Surface Treatment
KABCO	Injury Classification Scale
MVMT	Million Vehicle Miles Traveled
PDO	Property Damage Only
RD	Roadway Departure
RHR	Roadside Hazard Ratings
RPM	Raised Pavement Marking
TSIV	Traffic Signs Information Volume
UDOT	Utah Department of Transportation
usRAP	United States Road Assessment Program
VGG16	Visual Geometry Group 16
VMT	Vehicle Miles Traveled
XGBoost	eXtreme Gradient Boosting

EXECUTIVE SUMMARY

Roadway departures (RD) are a major contributor to fatal highway crashes in the United States, highlighting the importance of identifying and understanding the elements that lead to these events, with a special focus on roadside features. While features like clear zones, rigid obstacles, side slopes, and safety barriers have been examined from a crash data perspective, there is still a lack of network-level analysis of existing roadside conditions. Such an analysis would allow for a more detailed review of crashes in relation to the roadside features present.

This project aims to understand the role of roadside features in rural RD crashes through statistical analysis, identify critical hotspot locations that need attention, and propose safety improvement measures to minimize the occurrence and severity of rural RD crashes. Additionally, this project addresses the problem of limited data availability on roadside features using a computer vision model developed in a previous study. The developed computer vision model helps to extract information on roadside features from images, saving time and resources.

The analysis focuses on seven roads in Utah: US-6, SR-10, I-15, SR-12, US-40, I-80, and SR-150. Roadside feature data along these routes are obtained using the computer vision model developed in the prior UDOT project, Automated Safety Assessment of Rural Roadways Using Computer Vision (Mashhadi et al., 2023). This model was initially trained on images collected by Mandli, UDOT's asset collection contractor, covering the five rural roads in Utah (US-6, SR-10, SR-12, US-40, and SR-150). To extend the analysis to two additional roads in Utah (I-15 and I-80), the computer vision model is retrained using images collected by Pathway, UDOT's new data collection vendor. Labels from the Mandli images for the initial five routes are transferred to Pathway images, and additional images from these routes and the new routes (I-15 and I-80) within the state are labeled. After the labeling of the images, the computer vision model is trained on these images and is used to extract roadside information for these routes.

Safety ratings are then assigned using an algorithm developed in the previous study, Automated Safety Assessment of Rural Roadways Using Computer Vision (Mashhadi et al., 2023), in collaboration with UDOT specialists. This algorithm is based on the FHWA roadside rating system and evaluates detailed roadside features and conditions to determine safety ratings. This detailed data on roadside features and safety ratings is integrated with a crash database from

UDOT, enabling an in-depth analysis of crash occurrence and severity related to rural RD crashes. After the analysis, hotspots are identified by locating the top 10 locations along each route, and safety measures are recommended based on conditions observed in the images.

1.0 INTRODUCTION

1.1 Background

The Federal Highway Administration (FHWA) describes a Roadway Departure (RD) crash as an event where a vehicle crosses over the edge line or centerline or leaves the traveled way (Donnell et al., 2019). According to the FHWA, these crashes account for over half of all highway fatalities in the United States (Hossain et al., 2023). This concerning statistic underscores the critical need for ongoing research and investigation into RD crashes and their contributing factors.

RD crashes arise from a multitude of reasons and factors, including human, roadway design, and environmental factors. Human factors such as distracted driving, drowsiness, and speeding; roadway features like curves, narrow lanes, and shoulder conditions; and environmental influences such as animal crossings or adverse weather conditions are all recognized contributors to RD crashes. These elements may act alone or collectively to cause such incidents (Taylor, 2005). Although there is substantial research on RD crashes and their association with these various factors (Islam & Pande, 2020; Jalayer et al., 2019; Lord et al., 2011), a comprehensive analysis of how roadside features specifically influence RD crashes is still lacking.

A comprehensive analysis that considers all roadside features is essential for formulating effective safety measures to address RD. These measures are typically implemented in locations where the most prevalent contributing factors to severe RD crashes are observed based on thorough analysis and need assessment. In this context, roadside characteristics are integral to the process of recommending countermeasures. The FHWA suggests six countermeasures with proven benefits: signage/markings, rumble strips, median cable barriers, safety edge, road widening, and raised median islands (Taylor, 2005). However, these countermeasures are not limited to these six options. Determining the need for specific countermeasures, such as guardrail installation, roadside clearance, or rumble strips on shoulders, relies on an analysis of roadside features alongside crash data. FHWA determines the need for guardrail installation based on whether the consequences of colliding with other objects on the roadside are more severe than those of hitting the guardrail. This decision hinges on factors such as the presence of fixed obstacles, clear zones, and embankments (Pigman & Agent, 1991). Stephens Jr. (2005) also emphasizes the importance of evaluating the probability of striking a hazard in comparison to the barrier when considering barrier installation. Consequently, determining the necessity of the mentioned countermeasures is contingent upon a comprehensive assessment of crash data in conjunction with roadside features.

Several studies have aimed to understand the relationship between roadside features and RD crashes, focusing on elements like clear zones, rigid obstacles, side slopes, and safety barriers. However, these studies frequently lack a comprehensive analysis that considers all these features together in relation to RD crashes. This gap primarily arises from insufficient data on roadside elements and the challenges involved in gathering this data.

1.2 Problem Statement

The complete analysis of roadside features in relation to RD crashes is crucial for making informed plans and policies aimed at preventing such crashes for Departments of Transportation (DOTs). To achieve this, it is essential to study four key roadside features—clear zones, rigid obstacles, side slopes, and safety barriers—along with their interrelationships in impacting road safety. The primary challenge lies in gathering comprehensive datasets on these roadside features. This can be addressed by utilizing a computer vision model to extract roadside features from images.

In recent years, numerous studies have analyzed the relationship between roadside features and RD crashes. However, these studies often fail to incorporate all significant roadside features. For instance, Peng et al. (2012) investigated the impact of roadside features on RD crashes but focused only on side slopes and lateral clearance, analyzing just 245 miles of road segments. Dissanayake and Roy (2014) focused solely on rigid obstacles. Similarly, Ewan et al. (2016) analyzed roads in Oregon but limited their study to those with Annual Average Daily Traffic (AADT) of 1000 or less and a speed limit of 55 mph. These gaps primarily stem from insufficient data on roadside elements and the challenges involved in collecting this data.

This research addresses the challenge of limited data on roadside features by utilizing a computer vision model developed in the UDOT project, Automated Safety Assessment of Rural Roadways Using Computer Vision (Mashhadi et al., 2023). Previous research has used computer vision techniques for identifying hazards or extracting important information from imagery. This project used the computer vision model to extract four key roadside features along five rural roads in Utah (US-6, SR-10, SR-12, US-40, and SR-150). Building upon this foundation, our study aims to extend the database on roadside features to two additional major roads in Utah, I-15 and I-80.

To facilitate this expansion, the existing computer vision model, which was initially trained with Mandli images from five rural routes, is retrained using Pathway images. Image-based technologies have been crucial in data collection and analysis in the past. The labels that were developed and applied to the Mandli images for the initial five routes are transferred directly to similar Pathway images, and additional images from these routes are also labeled. For the new roads, I-15 and I-80, a fresh set of labels are created and applied to their respective images. This structured approach ensures that the methodology remains consistent while enabling comprehensive data collection and robust analysis across all roads.

After retraining the computer vision model on the new set of Pathway images, it is used to extract the roadside features from all seven routes. These features are then used to assign safety ratings to the roadways in accordance with FHWA roadside rating, utilizing the algorithm developed in the previous study conducted by Mashhadi et al. (2023). By integrating these roadside features and ratings with crash data obtained from UDOT, a comprehensive statistical analysis is performed to uncover patterns and correlations between roadside features and rural RD crashes. Subsequent hotspot identification pinpoints the top 10 most hazardous locations on each route studied, facilitating the proposal of targeted safety measures based on an extensive literature review.

1.3 Objectives

This project aims to assist UDOT in analyzing the impact of roadside features on rural RD crashes and in prioritizing locations and safety measures to mitigate these crashes. The proposed method utilizes two databases: One is the database on roadside features extracted through computer vision techniques for seven roads in Utah (US-6, SR-10, SR-12, I-15, US-40, I-80, and SR-150), and the other is the crash database obtained from UDOT, which includes rural RD crash data recorded over 12 years. These two datasets are merged based on milepoint information to analyze the correlation between roadside features and the occurrence and severity of RD crashes in rural areas. The next step involves prioritizing locations and suggesting safety measures based on the condition of roadways and roadside features identified in the images. This study includes several phases:

1. Extending the Database on Roadside Features
2. Data Fusion
3. Statistical Analysis Quantifying the Impact of Roadside Features on RD Crashes
4. Identification of Hotspot Locations
5. Recommendation of Safety Measures

1.4 Outline of Report

The chapters of this study are outlined as follows:

1. Introduction
2. Literature Review
3. Research Methods
4. Analysis and Results
5. Conclusions
6. Recommendations and Implementation

2.0 LITERATURE REVIEW

Identifying roadside featues and their relationship with RD crashes on rural roadways is essential for the recommendation of safety measures. Among the primary roadside features that demand consideration, four stand out: clear zone width, side slope, rigid obstacles, and the presence or absence of safety barriers, mainly guardrails. This chapter will discuss how these roadside features can impact RD crashes, along with safety measures and prioritization strategies based on findings from literature.

2.1 Roadside Features

2.1.1 Clear Zone

The width of the clear zone is a crucial element in reducing the impact of RD crashes. Defined by the FHWA as a manageable space on the roadside where a driver can safely halt or regain control if they deviate from the roadway, clear zones play a vital role in road safety. Research by Peng et al. (2012) indicates that increasing the width of these zones can significantly lower both the occurrence and the severity of crashes. Factors considered in determining the appropriate width of a clear zone include the presence of side slopes, obstacles in proximity, and the general terrain, according to FHWA guidelines. Jalayer and Zhou (2016b) further explored this topic by employing a probabilistic model to assess roadside hazard ratings (RHR), linking broader clear zones and gentler side slopes with improved roadside safety. Their analysis revealed that higher reliability index scores, derived from these ratings, correspond to fewer RD crashes, thereby emphasizing the essential role that clear zone width plays in maintaining roadway safety. The study indicated that reliability indices can act as proxies for evaluating safety levels, where higher indices correspond to safer roadside conditions and fewer crash incidents. These indices are calculated using a probabilistic approach that considers clear zone width and side slope as continuous variables. This approach measures safety by comparing actual and recommended values, with higher indices suggesting lower chances of non-compliance and, thus, safer roadside settings.

2.1.2 Side Slope

The impact of side slopes on RD crashes is significant. Peng et al. (2012) examined a stretch of road spanning 245.3 miles, employing negative binomial and multinomial logit models to evaluate the frequency and severity of crashes. They assigned ratings to side slopes, with 5 indicating the worst condition and 1 the best. Their findings suggest that enhancements to substandard side slope conditions lead to reductions in both the frequency and severity of crashes. Similarly, Roque et al. (2015) conducted a study in Portugal using multinomial and mixed logit models, which showed that side slopes can significantly elevate the risk of fatal injuries in crashes—by up to 469%. These investigations underscore the crucial importance of side slope conditions in enhancing road safety and preventing crashes.

2.1.3 Rigid Obstacles

Rigid obstacles represent another crucial roadside feature that contributes significantly to RD crashes. Dissanayake and Roy (2014) found that rigid obstacles markedly raise the chances of sustaining various injuries during a crash. Similarly, Daniello and Gabler (2011) pointed out that the risk of a fatal injury is 15 times greater when a vehicle collides with a tree. Lee and Mannering (2002) observed that crashes near road segments lined with clusters of trees tend to result in severe injuries. To reduce such hazards, they suggest strategies like increasing the spacing between light poles, minimizing the presence of isolated trees, and avoiding cut slopes. Properly recognizing and mitigating the risks posed by rigid obstacles is crucial for improving road safety and reducing the severity of RD crashes.

2.1.4 Safety Barriers

The fourth significant roadside feature is the safety barrier, employed to protect vehicles as they depart from the roadway. A study conducted by Li et al. (2018) underscores the critical role of guardrails in reducing fatal and severe injuries by 45% to 50% when compared to incidents where guardrails are not present. Similarly, research conducted on Indiana roads by Zou et al. (2014) revealed a notable 65% reduction in injuries when guardrails were involved. Holdridge et al. (2005) also found that collisions with guardrails lead to fewer suspected serious injuries than collisions with fixed rigid obstacles. Furthermore, a study by Roque et al. (2015)

highlighted the increased risk of RD crashes in the absence of guardrail barriers, particularly in areas with steeper slopes and horizontal curves. An effective safety barrier system, such as guardrails, plays a vital role in mitigating the severity of RD crashes and enhancing overall roadside safety.

Understanding the relationship between roadside features and RD crashes is crucial for enhancing road safety. The studies discussed above reveal that clear zones, rigid obstacles, side slopes, and safety barriers play important roles in determining the frequency and severity of such crashes. These features are not passive elements; they actively influence the safety of road users. Safety barriers, for instance, have been shown to significantly reduce the risk of severe injuries. These findings provide valuable insights for future roadside safety research and the development of effective safety measures.

2.2 Safety Measures for Road Departure Crashes

Countermeasures should be strategically applied to high-risk locations to enhance safety against RD crashes. Selecting appropriate safety measures should be based on a thorough assessment of risk factors associated with specific road segments. Identifying these risk factors and implementing corresponding countermeasures is crucial for minimizing RD crashes. Zhou et al. (2015) proposed several countermeasures in their study, including but not limited to the installation of centerline and shoulder rumble strips.

2.2.1 Signage

Signage stands out as a cost-effective and efficient countermeasure for preventing RD crashes. Signs play a vital role in alerting drivers to changing road conditions, thereby enhancing their preparedness. They are particularly recommended on road sections with horizontal curves as a proactive measure against RD incidents. It's noteworthy that a substantial 83% of fatal crashes on horizontal curves are attributed to RD occurrences (Satterfield et al., 2009). According to Dissanayake & Galgamuwa (2017), chevrons contribute to safety improvements by reducing all RD by 10% to 27%. Therefore, strategically placing signs to forewarn drivers about upcoming curves and guide them safely through these curves is important. Various types of signs, such as chevrons, dynamic curve warning systems, advanced curve warning systems, and advisory signs, can prove highly beneficial. Chevrons, in particular, are considered a cost-effective safety measure for addressing horizontal curves. The Manual on Uniform Traffic Control Devices recommends their use in locations where there is a speed difference of over 15 mph between the posted speed limit and the advisory speed (Zhou et al., 2015). One challenge with signage is finding the right balance between too little and too much information, as both can negatively impact driving safety (Han et al., 2022). To address this, a recommended Traffic Signs Information Volume (TSIV) density of 30 bits per kilometer ensures that drivers receive enough information without being overwhelmed, promoting both safety and comfort.

2.2.2 High-Friction Surface Treatments

Another highly effective safety measure (illustrated by Figure 2.1) is the application of high-friction surface treatments (HFST). This method involves applying high-quality aggregates, such as calcined bauxite, with a polymer binder to enhance and maintain pavement friction, particularly in areas with high crash potential or existing crash hotspots. The implementation of HFST in Kentucky, for instance, resulted in a remarkable 91% decrease in RD crashes in wet conditions and a 78% decrease in dry conditions (Jalayer & Zhou, 2016b). In Delaware, the application of HFST resulted in a decline in RD crashes at 83% of the locations, achieving an average overall reduction of 56% (David Merritt et al., 2021). Although HFST can be costly, ranging from $21 to $26 per square yard (Deef-Allah et al., 2022), its 10-year life cycle makes it a cost-effective investment over time.

Figure 2.1: Example Images of High-Friction Surface Treatment (Merritt et al., 2020)

2.2.3 Raised Pavement Markers

Raised pavement markers (RPMs) represent another valuable safety measure aimed at enhancing visibility, particularly during nighttime conditions (Zhou et al., 2015). This cost-effective strategy improves the visibility of road alignment in low-light situations and has proven highly effective in mitigating RD crashes (ATSSA, 2011). For instance, RPMs were installed on ten rural roadways in Mobile County, Alabama, which had the highest rates of RD crashes. These markers were strategically placed just outside the existing edge line to improve visibility and guide drivers. Their application led to a significant reduction in fatalities and injuries, with injuries (all types of injuries including fatal) from RD crashes decreasing from 177 to just 10 between 2009 and 2012. Furthermore, the state reported an 86% reduction in RD crash frequency and a 94% decrease in RD crash-related injuries compared to the previous year (Jalayer & Zhou, 2016b). An example of RPM is provided in Figure 2.2. While RPMs provide significant safety benefits by enhancing visibility during nighttime and adverse weather conditions, they can deteriorate or become less effective in regions where snowplowing is frequent (Abdel-Rahim et al., 2018). Snowplows can dislodge or damage RPMs when scraping the road surface, which reduces their visibility and functionality over time.

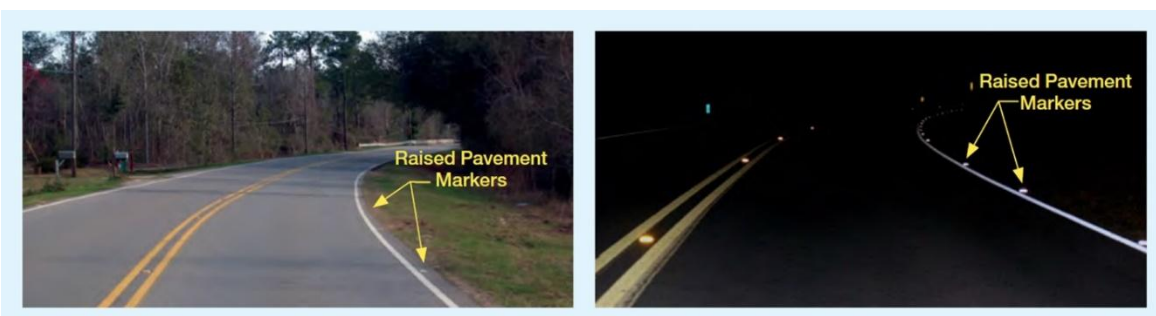

Figure 2.2: Example Images of Raised Pavement Marking (FHWA, 2013)

2.2.4 Roadside Design

Effective roadside design with careful consideration of roadside features is essential for preventing RD crashes (Zhou et al., 2015). Clear zone improvement is one such strategy that enhances road safety by providing a recoverable area before any departure occurs, allowing vehicles that have left the lane to regain control. Clearing hazards alongside roads, such as trees and poles, or, when they can’t be removed, delineating these objects is part of this approach

(Zhou et al., 2015). In Iowa, the implementation of clear zone improvements resulted in a notable 38% decrease in all types of crashes (Sperry et al., 2008). However, widening clear zones can disrupt ecosystems, so a balanced approach is needed to ensure safety improvements while minimizing environmental impacts.

2.2.5 Shoulder Widening

Shoulder widening is another valuable method for enhancing roadside design to prevent RD crashes. It offers room for vehicle recovery and facilitates maneuvering to avoid crashes. In the context of horizontal curves, shoulder widening improves stopping sight distance (Zhou et al., 2015). Studies have shown that widening narrow shoulders can lead to a 79% reduction in RD crashes (Gayah and Donnell, 2014). For instance, Wu et al. (2015) studied 22 shoulder widening projects in Texas and revealed that improving shoulder width led to a decrease in RD crashes by 35.7% and a reduction in fatal injuries by 29.5%.

2.2.6 Rumble Strips

Rumble strips are an effective safety measure for mitigating RD crashes. The sound and vibrations they produce alert drivers when their vehicle drifts off the traveled way. These strips help drivers maintain their lane during distractions or low-light conditions by creating noise and vibrations when tires roll over them. Rumble strips can be installed on the centerline or shoulders of the road. For instance, following the implementation of centerline rumble strips in Georgia, there was a noticeable reduction of 42% in crashes associated with crossing the centerline, as reported by Guin et al. (2018). In a similar study by Himes et al. (2017), the implementation of edge-line rumble strips on rural two-lane curved roads in Kentucky and Ohio was linked to a decrease in crash incidents. This was demonstrated by Crash Modification Factors (CMFs) varying between 0.71 and 0.79 for different types of crashes and injury levels, including single-vehicle run-off-road, occurring both in daylight and nighttime. Although concerns about roadside noise, pavement deterioration, and potential risks to bicyclists exist (Kirk, 2008), these issues are less relevant on rural freeways where bicycles are not typically found, and noise concerns are minimal compared to the significant safety benefits provided by rumble strips.

2.2.7 Safety Barriers

Another crucial safety measure is the installation of barriers, which are designed to safeguard a driver who has veered off the road and minimize the severity of a crash (Avelar et al., 2020). A comprehensive meta-analysis by Elvik (1995) encompassing 32 studies revealed that setting up median barriers and roadside guardrails notably lowers the incidence of fatal and personal injury crashes across all crash types, with reductions of 45% and 50%, respectively. Likewise, in North Carolina, the implementation of guardrails at various sites led to a reduction in the severity index of RD crashes, ranging from 16.6% to 36.7% (Zhou et al., 2015). The majority of the other safety measures we have examined primarily focus on keeping vehicles within their designated lanes. Nevertheless, in cases where a vehicle departs from its lane, barriers are employed to prevent it from colliding with solid objects or overturning on steep embankments. Although safety barriers are effective in reducing severe injuries, they may contribute to an increase in property damage-only (PDO) crashes and some injury crashes (Qawasmeh & Eustace, 2022). These increases can occur due to collisions with the barriers themselves, side impacts, or sideswipe incidents. Despite this, their overall benefit in preventing more serious outcomes makes them an important safety feature.

2.2.8 Wider Longitudinal Road Markings

Wider pavement markings are another safety measure that can significantly enhance road safety. Various studies have demonstrated the effectiveness of wider road markings. For instance, total collisions were reduced by 11.1%, 27.5%, and 1.1% in Alberta, British Columbia, and Quebec, respectively, following the increase in road marking width (Hussein et al., 2020). Wider road markings also create a perception of a narrower lane, which encourages drivers to reduce their speed (Calvo-Poyo et al., 2020). In a study conducted by Calvo-Poyo et al. (2020) a speed reduction effect of approximately 3.1% was observed with wider road markings. Additionally, analysis by Miles et al. (2010) indicated that wider edge lines are particularly beneficial in areas with high rates of RD crashes as they help drivers stay within their lane. While the speed reduction effect may be modest, wider pavement markings have been proven to positively influence driver behavior and reduce fatal and severe RD crashes. In Idaho, for instance, (Mohamed, 2018) reported a 10% reduction in fatal and serious RD crashes across 38 locations following the use of wider markings. The studies conducted on widening the pavement markings suggest increasing edge line widths from 4 inches to 6 inches and from 6 inches to 8 inches.

A comprehensive understanding of these countermeasures provides valuable insights into their effectiveness in preventing RD crashes. Real-world applications of different countermeasures help in selecting appropriate safety measures based on the conditions of high-risk locations. These measures focus on two key approaches: preventing RD crashes through strategies like rumble strips, signs, HFST, and improved pavement markings; and minimizing the impact after a vehicle has experienced RD. Shoulder widening and safety barriers serve this latter purpose, with safety barriers proving effective in reducing the severity of RD crashes.

2.3 Classification of Severity Levels in RD Crashes

The classification of severity into various levels plays a pivotal role in the study and analysis of RD crashes. Severity, in the context of RD crashes, relates to the extent of injury resulting from a crash and is typically categorized on a scale of 1 to 5, ranging from no injury to fatal outcomes. To standardize these severity levels, the FHWA has introduced the KABCO scale (Administrations, 2019).

In the KABCO scale, fatality is represented by 'K,' suspected serious injury is denoted by 'A,' suspected minor injury is referred to as 'B,' possible injury is represented by 'C,' and cases involving no injury but only damage to property are labeled as 'O' (Zou et al., 2014). This standardized scale serves as a common framework adopted by various studies, with some refinements in how each defines and analyzes severity levels within their specific contexts or prediction models.

Islam and Pande (2020) employed distinct categorizations of severity levels when analyzing RD crashes. In their study, the categorization of injuries was divided into three groups. Fatal injuries and suspected serious injuries were combined to form the category of severe injuries, while minor injuries included both suspected minor and possible injuries. Additionally, the category labeled 'no injury' was equated with 'property damage only' incidents. Likewise, Obaid et al. (2023) used the same three-level classification for injury severity in their analysis.

The research by Zou et al. (2014) assigned a coded value of 1 to cases involving injuries, encompassing fatal, suspected serious injuries, and suspected minor injuries, while incidents with no injuries were coded as 0. Cai et al. (2023) used a binary system, assigning a severity value of 1 to cases involving fatal and suspected injuries, while a value of 0 was assigned to all other injury types.

An important aspect of determining severity levels in RD crash analysis is the choice between using the highest severity of any person in the crash or the condition of the driver. Dissanayake and Roy (2014) opted to use the highest injury severity in their study as a measure of severity. In contrast, Roque et al. (2015) employed a dual model approach, considering the driver's severity condition for the initial model and the highest severity of the occupant for the subsequent model. Properly defining and utilizing severity in crash analysis is the foundational and crucial step in the analytical process.

It is worth noting that nearly every study focusing on severity analysis adopts the FHWA injury scale for modeling and analyzing crash data in relation to severity. However, the KABCO scale can be customized to meet the specific requirements of a study. UDOT's approach considers the highest severity level sustained by any person involved in the crash as a key factor in their analysis. In line with this methodology, our analysis also uses the highest injury level sustained in a crash.

2.4 Prioritization of Location for Safety Measures

The process of selecting and prioritizing countermeasures to address RD crashes necessitates a thorough analysis of crash data. This involves identifying specific locations and the contributing factors associated with these incidents. The conventional method typically revolves around identifying "hot spots" by examining the crash frequency and proposing countermeasures focused on these areas. However, this approach predominantly relies on historical crash data, sometimes overlooking considerations such as traffic volume and location-specific features. We address this issue by calculating severity rates that take traffic volume into account.

The first crucial step involves pinpointing the locations that require countermeasure planning. Numerous studies have investigated the identification of crash hot spots, defined as areas with a higher incidence of crashes compared to similar locations (Elvik, 2007). The severity is weighted differently across various studies based on specific needs and requirements. In the following sections, we will discuss some of the weighting systems used for severity index calculation.

2.4.1 Belgium System

This system was utilized by the Belgian government for the purpose of hotspot identification (Choudhary et al., 2015). In this approach, fatal injuries are weighted by 5, suspected serious injuries by 3, and all other injuries by 1. The formula used is as follows:

$$SI = 5 \times F + 3 \times G + R.$$

Here, F represents the total number of fatal injuries, G denotes the total number of suspected serious injuries and R indicates the total number of minor injuries and property-damage-only crashes.

2.4.2 New South Wales System

This approach was used by Alam and Tabassum (2023) for crash severity analysis in Ohio. In this system, fatal injuries are weighted at 3, suspected serious injuries at 1.8, minor injuries including suspected minor injuries and possible injuries at 1.3, and property-damage-only scenarios are weighted at 1. The formula used is as follows:

$$SI = 3 \times F + 1.8 \times G + 1.3 \times M + N.$$

Here, F represents the total number of fatal injuries, G denotes the total number of suspected serious injuries, M indicates the total number of suspected minor and possible injuries, and N corresponds to the total number of incidents involving no injuries or only property damage.

2.4.3 Utah’s Crash Cost (2022)

The crash cost can be a good measure to weight the severity of the crash for the calculation of the severity index. Table 2.1 presents the Utah’s 2022 crash costs in dollars for each crash severity as defined by UDOT. The Equivalent Property-Damage-Only (EPDO) value is calculated from the crash cost by dividing the cost for each severity by the value of “No Injury” (O) or “Property Damage Only.” These values can be used for the calculation of the severity index.

Table 2.1: 2022 Utah's Crash Costs in Dollars

Crash Severity	Crash Cost	EPDO
K (Fatal)	$15,279,600	888
A (Sus. Serious Injury)	$1,612,100	94
B (Sus. Minor Injury)	$383,000	22
C (Possible Injury)	$195,500	11
O (No Injury)	$17,200	1
KA (Severe)	$3,932,300	229
KAB (Injury)	$1,077,800	63
KABC (Anticipated Injury)	$568,300	33
KABCO (Total Crashes)	$180,900	11

2.5 Summary

This literature review examined the influence of key roadside features, such as clear zone width, side slope, rigid obstacles, and safety barriers, on RD crash severity and frequency. Studies emphasized that wider clear zones and flatter side slopes significantly enhance safety, while rigid obstacles increase the risk of severe injuries in RD crashes. Safety barriers, primarily guardrails, are effective in mitigating crash severity. Findings from previous literature informed the development of safety improvement recommendations targeting these critical roadside elements. RD crash severity is typically classified using the FHWA KABCO scale, ranging from no injury to fatal. This review also covers ways to identify high-risk areas, using systems from Belgium, New South Wales, and Utah’s 2022 crash cost data to guide where safety improvements are most needed. These insights support targeted actions to make roads safer and reduce severe crashes.

3.0 RESEARCH METHODS

3.1 Retraining the Computer Vision Model

The roadside features dataset is essential for establishing the relationship between RD crashes and roadside conditions. The more data we collect on roadside features, the more comprehensive and scaled our analysis will be, enabling us to depict this relationship more clearly. Historically, image-based technologies have been instrumental in data collection and analysis (Brilakis et al., 2011; Dai et al., 2013). In this study, we make use of images gathered by Pathway, a company specializing in asset collection, which captures road images with cameras mounted on vehicles traveling along specific routes. These images can be analyzed to extract meaningful roadside feature information using advanced computer vision techniques.

Earlier studies have shown that computer vision techniques are highly effective in identifying hazards and extracting key information from images (Farhadmanesh et al., 2024; Matsumoto et al., 2021; Xie et al., 2019). In order to prepare the dataset on roadside features, this project aims to implement the computer vision model developed in the previous study, Automated Safety Assessment of Rural Roadways Using Computer Vision (Mashhadi et al., 2023). The model was initially trained on images collected by Mandli, focusing on five rural roads in Utah: US-6, SR-10, SR-12, US-40, and SR-150. In this project, we aim to train the model on images made available by Pathway, a different asset collection company assisting UDOT in gathering road image data. Additionally, we will extend the dataset by including images from two major routes within Utah, I-15 and I-80. To achieve this, we will undertake several steps: training the model on the new images, applying it to predict roadside features from unseen images of the seven roads within Utah (US-6, SR-10, SR-12, US-40, SR-150, I-15, and I-80), and expanding the roadside features dataset. These steps will be discussed in detail.

3.1.1 Transfer of Labels

The computer vision model developed in the Automated Safety Assessment of Rural Roadways Using Computer Vision (Mashhadi et al., 2023) project is initially trained on Mandli images. To ensure it performs well on the Pathway images, the model must be retrained on this new dataset so that roadside features can be accurately extracted. The labels from the training set created using Mandli images are transferred to the Pathway images using the milepoints and longitude and latitude information available from both image sets for the initial five routes. After transferring the labels, they are manually checked, and any incorrectly transferred labels are discarded. This transfer of labels helps save time and effort by preventing the need for complete relabeling. Figure 3.1 illustrates an example of the transfer of labels from Mandli to the Pathway Image.

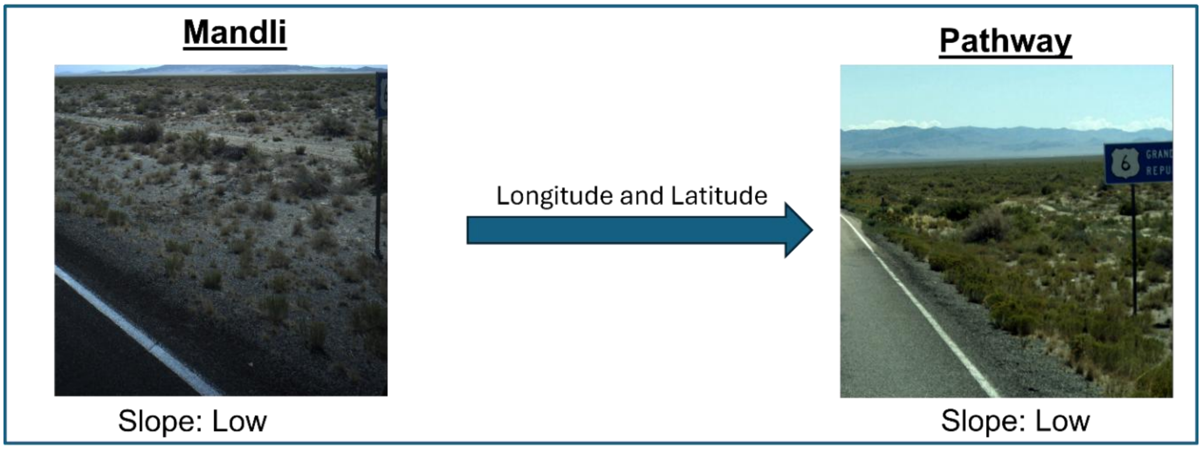

Figure 3.1: Transfer of Labels From Mandli to Pathway Images

3.1.2 Labeling of Images

The Pathway images for the additional two routes within Utah (I-15 and I-80), along with those from the previous five routes, are labeled to train the computer vision model, perform statistical analysis, and establish the correlation between roadside features and RD crashes. The seven roads combined cover a total of 1300 miles, providing UDOT with an extensive dataset for scaling the analysis. The newly labeled images from the seven roads, along with the transferred labels from the initial five routes, are combined to retrain the model on the Pathway images. This retraining enables the model to extract roadside feature information from Pathway images. Figure 3.2 shows examples of the labeling process for the images. The details on the labeling process can be found at Mashhadi et al. (2023).

Figure 3.2: Categories and Examples for Labeling of Roadside Features

3.1.3 Training the Computer Vision Model

After preparing the labels on roadside features from the seven roads in Utah, the next step is to train the computer vision model. This training will enable the model to predict roadside features from other unseen images, saving considerable time. We are using the same computer vision model developed in the previous UDOT project titled, Automated Safety Assessment of Rural Roadways Using Computer Vision (Mashhadi et al., 2023). In the following section, we will briefly discuss the mentioned project and the computer vision model used.

3.1.3.1 Automated Safety Assessment of Rural Roadways Using Computer Vision

This project utilized a computer vision model to extract roadside information from images collected by Mandli Communication Inc. Mandli gathers high-quality images using specialized cameras mounted on vehicles that traverse designated routes. The computer vision technique is used to extract information on clear zones, rigid obstacles, side slopes, and safety barriers from these images. The process begins with training the model on labeled images, which is then used to predict roadside features on new, unseen images. The computer vision model was developed to gather roadside information for five routes in Utah: US-6, SR-10, SR-12, US-40, and SR-150. Once the roadside features are identified, a safety rating is assigned based on an algorithm developed in collaboration with UDOT, following FHWA roadside rating guidelines. Table 3.1 presents the categories for roadside features, and Table 3.2 outlines the algorithm used to assign the roadside rating according to FHWA roadside rating (Mashhadi et al., 2023).

Table 3.1: Categories for the Roadside Features

Clear Zone Width	Distance From Rigid Obstacle	Side Slope	Safety Barriers
a. Greater than 30 ft	a. 0-6.5 ft	a. 1:4 (Low)	a. Yes
b. 20-30 ft	b. 6.5-10 ft	b. 1:3 to 1:4 (Med)	b. No
c. 10-20 ft	c. More than 10 ft	c. 1:2 or steeper (High)	
d. 5-10 ft	d. No Rigid Obstacle	d. Not Applicable	
e. Less than 5 ft			

Table 3.2: Algorithm for the Roadside Rating

Condition	Action
IF Safety Barrier is present	
- **IF** Rigid Obstacle distance is between 6.5 ft and 10 ft (inclusive)	Set Rating to 5
- **ELSE**	Set Rating to 4
ELSE IF Clear Zone is 5 ft or less AND Side Slope is High	Set Rating to 7
ELSE IF Clear Zone is 5 ft or less AND Rigid Obstacle distance is 6.5 ft or less	Set Rating to 7
ELSE IF Side Slope is High AND Rigid Obstacle distance is 6.5 ft or less	Set Rating to 7
ELSE IF Clear Zone is 5 ft or less OR Side Slope is High OR Rigid Obstacle distance is 6.5 ft or less	Set Rating to 6
ELSE IF Rigid Obstacle distance is between 6.5 ft and 10 ft (inclusive)	Set Rating to 5
ELSE IF Rigid Obstacle distance is 10 ft or more OR Clear Zone is between 5 ft and 10 ft (inclusive)	Set Rating to 4
ELSE IF Clear Zone is between 10 ft and 20 ft (inclusive) OR Side Slope is Medium	Set Rating to 3
ELSE IF Clear Zone is between 20 ft and 30 ft (inclusive)	Set Rating to 2
ELSE IF Clear Zone is 30 ft or more	Set Rating to 1
END	

The computer vision model utilized in the project uses VGG16 for feature extraction and eXtreme Gradient Boosting (XGBoost) for the task of classification. The model selection was based on various model evaluations. The details can be found in Mashhadi et al. (2023).

a. VGG16:

Feature extraction is a crucial component in image processing and computer vision, as it converts raw images into meaningful feature representations. These representations capture essential details and characteristics, facilitating tasks such as image classification, object detection, and segmentation. A common method for feature extraction is utilizing models pre-trained on extensive datasets like ImageNet. These pre-trained models can be fine-tuned for specific applications, enabling them to effectively extract useful features from input images. These extracted features can then serve as inputs for various machine learning models.

This project utilized VGG16 and compared its performance with ResNet and Inception v3 pre-trained models for feature extraction. Each model has a unique architecture, offering various advantages and disadvantages. VGG16 features a simpler design and uses fewer parameters compared to other models (Hassandokht Mashhadi et al., 2024), which was a critical factor in its selection for this research. The accuracy achieved in classifying various features with VGG16 was higher than that of the other models. Detailed results and comparisons are available in the study by Mashhadi et al. (2023).

b. eXtreme Gradient Boosting (XGBoost):

XGBoost is a powerful supervised learning algorithm that excels in both classification and regression tasks through its implementation of gradient boosting decision trees (GBDT). Unlike random forests, which use a bagging approach to grow multiple decision trees independently and fully, XGBoost builds its trees sequentially, improving the model iteratively. After the feature extraction process using VGG16, XGBoost is employed for the classification task to identify various roadside features.

3.2 Data Fusion

The research utilizes a database of roadside features obtained by applying the computer vision model to Pathway images, which, in this study, produced a database of roadside features such as clear zones, rigid obstacles, side slopes, and safety barriers. After extracting these features, safety ratings were assigned based on the algorithm presented in Table 3.2. This database is combined with crash data obtained from UDOT, which includes information on Utah’s rural RD crashes from 2010 to 2021, detailing their severity, milepoints, and GPS coordinates. By merging the two databases using the milepoints information, we obtained detailed information on crashes and the associated roadside features. Subsequently, we conducted a statistical analysis to identify the correlation between roadside features and rural RD crashes.

We are going to briefly discuss these two databases to provide a comprehensive understanding of the data used in our research.

3.2.1 Roadside Features Database

The roadside features include information on clear zones, rigid obstacles, side slopes, and safety barriers. For simplification, the safety barriers are further categorized based on their presence or absence. A safety rating from 1 to 7 is assigned according to the algorithm detailed in Table 3.2, which is based on the FHWA roadside rating criteria. The categories for the roadside features can be found in Table 3.1.

3.2.2 Crash Database

UDOT has compiled an extensive crash dataset focusing on rural RD incidents in Utah, detailing each crash's severity level, milepoints, and GPS location. The dataset used in this study spans from 2010 to 2021, covering 12 years of data, and includes variables such as time, weather, speed, age of the driver, and roadway conditions.

The dataset contains 237 columns for each individual crash record. These columns encompass a wide range of factors associated with rural RD crashes, including:

- *Geographical Information*: Longitude and latitude.
- *Crash Severity*: Categorized into Fatal Injury, Suspected Serious Injury, Suspected Minor Injury, Possible Injury, and Non-Injury or Property Damage Only.
- *Environmental Conditions*: Light conditions, weather, etc.
- *Roadway Characteristics*: Milepoint, posted speed, region, functional class of the road, roadway type, shoulder width, lane width, presence or absence of horizontal curvature, grade, cross slope, and AADT.

Initially, the dataset did not include information on roadside features. To address this, roadside information extracted from applying the computer vision model was merged with the crash dataset. The merging process involved the following steps:

- *Location Matching*: Milepoint information from the crash dataset was compared with that information in the roadside features dataset.
- *Proximity Calculation*: The closest roadside features to each crash location were identified based on the shortest distance between the milepoints.

- *Data Integration*: Information about the condition of these nearby roadside features was added to the crash records.
- *Safety Rating Addition*: Safety ratings derived from the condition of roadside features were incorporated into the dataset.

This integration provided a richer dataset, enabling a more comprehensive analysis of the factors contributing to RD crashes in rural areas.

3.3 Statistical Analysis

After compiling the dataset on roadside features and RD crashes, the data is ready to perform the statistical analysis. However, some data pre-processing is needed before analysis can be performed. We are going to briefly discuss the process of normalization of crash data for statistical analysis.

3.3.1 Modeling of Severity

The classification of severity into various levels plays an important role in the study and analysis of RD crashes. Severity, in the context of RD crashes, pertains to the extent of injury resulting from a crash and is typically categorized on a scale of 1 to 5, ranging from non-injury to fatal outcomes. To standardize these severity levels, the FHWA introduced the KABCO scale. In the KABCO scale, a fatality is represented by 'K,' a suspected serious injury is denoted by 'A,' a suspected minor injury is referred to as 'B,' a possible injury is represented by 'C,' and cases involving no injury but only damage to property are labeled as 'O.' In our analysis, we are adopting two approaches. The first approach considers only fatal injuries. The second approach combines fatal and suspected serious injuries into one category, representing them as severe injuries to aid in our analysis.

3.3.2 Normalization of Data

Normalization is an important step in ensuring consistent comparison of crash data across different roadside conditions by adjusting for variations in traffic exposure. For instance, common roadside features, such as a clear zone width greater than 30 feet, can be more prevalent along roadways, resulting in higher Vehicle Miles Traveled (VMT) being associated with those features as compared to other features. As a result, these segments record more crashes simply due to the increased exposure, not necessarily because they are riskier. Conversely, less common roadside features might have fewer recorded crashes, not because they are safer but because they are less prevalent along the roadway. Without normalization, roadside features that are more prevalent could misleadingly appear to be unsafe since they are likely to record higher crash frequencies, while those that are less common might seem safer. To address this imbalance, normalization of the crash records based on the roadside features present on the roads under study is necessary.

The process begins by categorizing the crash data and roadside data according to the various roadside features. We then calculate the VMT for each category of roadside feature. This is done by multiplying the total length of each feature category by the AADT, the number of years of data, and 365 days per year. The total crashes experienced by each feature category are then divided by the VMT to normalize the data. For precision, both the length of the segments represented by each roadside feature and the AADT passing through these segments are considered. Finally, the crash rate for each category of roadside features is calculated in terms of 100 million vehicle miles traveled (MVMT). FHWA provides the formula for the calculation of crash rate per 100 MVMT as:

$$R = \frac{\mathrm{C} \times 100{,}000{,}000}{\mathrm{V} \times 365 \times \mathrm{N} \times \mathrm{L}}.$$

Here, R represents the rate of RD crashes per 100 MVMT on a particular road segment, C denotes the total count of RD crashes over the observation period, V refers to traffic volumes measured by AADT counts, N is the duration of the data collection period in years, and L signifies the measured length of the road segment in miles.

Most studies analyzing factors responsible for RD crashes focus on the frequency of crashes. However, crash records only capture incidents after they occur, excluding non-crash incidents. This focus can introduce biases into the analysis as it does not account for the total number of vehicles passing through a location compared to the number of crashes that occurred in that location. Although data such as AADT and milepoint are recorded for each crash, they are only linked to the crash site and do not help with a comprehensive analysis. To address this, we need the AADT and the length of the segment experiencing certain roadside features to calculate the VMT for that section. This is where the detailed database on roadside features for all roadways under study, segmented at 0.1-mile intervals, becomes useful. By using this detailed database along with crash records, we can normalize crash data and calculate the crash rate per 100 MVMT for each roadside feature. This approach helps eliminate biases and provides a more accurate analysis.

In this study, we are using two different sets of data. The first data is the crash data recorded over the 12 years. The second data is the detail on the roadside features on average for every 0.1-mile segment and the AADT passing through that segment. With this information, the VMT for each segment representing certain roadside features can be calculated and used for the analysis, giving a more detailed analysis with respect to the crash rate and severity rate. This helps to prevent biases in the data. Additionally, our analysis focuses exclusively on rural roads as the crash data relates only to rural RD incidents, with urban areas excluded from the analysis.

3.3.3 Spearman Rank Correlation Coefficient

To facilitate our analysis, we have categorized clear zones, side slopes, rigid obstacles, presence or absence of safety barriers, and safety ratings into several variables, as detailed in Table 3.1. Given that these variables are ordinal, we applied Spearman's rank correlation coefficient (Spearman, 1904) to determine the relationships between roadside features, safety ratings, crash frequency rates, and severity rates. Spearman's method is particularly advantageous due to its robustness against outliers and its ability to minimize bias, making it an ideal choice for this analysis (Alsayed & Manzi, 2019). The formula for calculating Spearman's rank correlation coefficient is as follows:

$$\rho = 1 - \frac{6 \sum d_i^2}{n(n^2 - 1)}.$$

Here, ρ represents Spearman's ranks correlation coefficient, d_i denotes the difference between the two ranks for each paired observation, and n is the number of observations.

The level of significance is calculated using:

$$t = \rho \times \sqrt{\frac{n-2}{1-\rho^2}}.$$

The value of t is used to find the confidence interval or p-value.

3.4 Hotspot Identification

Hotspot identification refers to the process of locating specific areas where crashes tend to occur more frequently or with greater severity. These hotspots are determined using statistical and spatial analysis techniques, which help to identify patterns and concentrations of crashes. By focusing on these areas, safety measures can be recommended and implemented to minimize the occurrence and severity of RD crashes. In this study, we first calculate the severity index and normalize it based on the VMT to rank the top 10 locations along each route.

3.4.1 Severity Index

The severity index measures the severity of a crash or series of crashes. To calculate it, injuries of all severities that occurred in a specific road segment are weighted and summed. There are several ways to weight the severity of crashes to calculate the severity index. For this project, we will examine two approaches: one using the New South Wales formula and another using Utah's crash cost. This comparison will help identify hotspots using both methods. However, the hotspots identified through Utah's crash cost approach will be used to recommend safety measures.

3.4.1.1 Utah's Crash Cost

We utilize the categories KA (for fatal and suspected serious injuries), B, C, and O to define the severity index. With the calculated EPDO values as shown in Table 2.1, we assign weights to different injury levels to refine our severity index calculation. For instance, KA is given the highest weight of 229, reflecting its severity. B is weighted at 22, C at 11, and O at 1. The formula used for calculating the severity index is:

$$SI = 229 \times (F + SS) + 22 \times (SM) + 11 \times (PI) + (NI).$$

Here, F represents the total number of fatal injuries (K), SS denotes the total number of suspected serious injuries (A), SM indicates the total number of suspected minor injuries (B), PI is the total number of possible injuries (C), and NI corresponds to the total number of incidents involving no injuries or only property damage (O).

3.4.1.2 New South Wales Formula

The New South Wales formula offers an alternative method for weighting crash severity. The formula for calculating the severity index using this approach is:

$$SI = 3 \times F + 1.8 \times G + 1.3 \times M + N.$$

Here, F represents the total number of fatal injuries, G denotes the total number of suspected serious injuries, M indicates the total number of suspected minor and possible injuries and N corresponds to the total number of incidents involving no injuries or only property damage.

3.4.2 Severity Rate

The severity rate is calculated to normalize the severity index using the volume of traffic or AADT. The severity index is divided by the VMT and multiplied by 10^8 to calculate the severity rate per 100 MVMT. The formula used for calculating the severity rate (SR) is as follows:

$$SR = \frac{SI}{VMT} \times 10^8.$$

Here, SI is the severity index, and VMT is calculated as follows:

$$VMT = AADT \times L \times 365 \times N.$$

Here, L is the length of the road segment, set at 0.5 miles for this analysis, and N refers to the number of years of data collected, which is 12 years for this study.

3.5 Safety Measures Recommendation

After selecting the hotspot locations, safety improvement measures are recommended for each route's top ten 0.5-mile segments. Each selected segment is visually inspected using the images, and safety measures gathered from the literature review are recommended. The following are the main safety measures for RD crashes:

- Signage
- Safety Barriers
- Rumble Strips
- HFST
- Pavement Marking Widening
- Clear Zone Improvement
- Shoulder Widening

Raised pavement markings are excluded from the recommendations as they are particularly vulnerable to damage during snow removal processes. In Utah, where snowplowing is a routine part of road maintenance during the winter months, these markings can quickly deteriorate or become dislodged. This not only reduces their effectiveness but also increases maintenance costs. Therefore, more durable alternatives are considered in place of raised pavement markings to ensure long-term safety and visibility on roads.

3.6 Summary

This study combined computer vision techniques for feature extraction from roadway images with statistical analysis to assess the relationship between roadside features and rural RD crashes. An existing computer vision model, initially trained on non-interstate roadway images, was extended to include data from interstate highways, resulting in a comprehensive roadside feature database. This database was merged with UDOT's crash data containing information on rural RD crashes, enabling a thorough analysis of crash patterns in relation to roadside conditions. Spearman's rank correlation was used to examine associations between roadside features, safety ratings, and rural RD crashes. In addition, hotspot identification methods based on severity rate were applied to locate high-risk areas along Utah roadways, guiding targeted safety improvement recommendations.

4.0 ANALYSIS AND RESULTS

4.1 Statistical Analysis

This section presents the results obtained from Spearman's correlation analysis conducted using data from seven roads in Utah: US-6, SR-10, SR-12, I-15, US-40, I-80, and SR-150. The analysis focuses exclusively on rural road segments, with urban areas excluded. The analysis is divided into three parts:

1. Non-Interstate Roads Analysis: This part includes only the non-interstate roads: US-6, SR-10, SR-12, US-40, and SR-150.
2. Interstate Roads Analysis: This part includes only the interstate roads: I-15 and I-80.
3. Interstate and Non-Interstate Roads Analysis: This part includes both the interstate routes (I-15 and I-80) and the five non-interstate roads (US-6, SR-10, SR-12, US-40, and SR-150).

Additionally, we analyzed these roads based on the use or non-use of restraints (seat belts). This analysis takes into account the severity of the driver's injuries and their restraint or seat belt usage.

4.1.1 Analysis of Roadside Features

4.1.1.1 Clear Zone

a. Non-Interstate Roads: Spearman's correlation analysis indicates a significant relationship between clear zone width and injury rates on non-interstate roads. Specifically, a decrease in clear zone width correlates with an increase in severe injury rate, evidenced by a correlation coefficient of -0.79 and a p-value of 0.10, which is statistically significant at the 90% confidence interval. Additionally, the correlation between clear zone width and fatal injury rate is notably strong, with a correlation coefficient of -0.89 and a p-value of 0.03, achieving statistical significance at the 95% confidence interval. Figure 4.1 presents the bar plot that demonstrates the linkage between clear zone width and both injury rates on non-interstate roads.

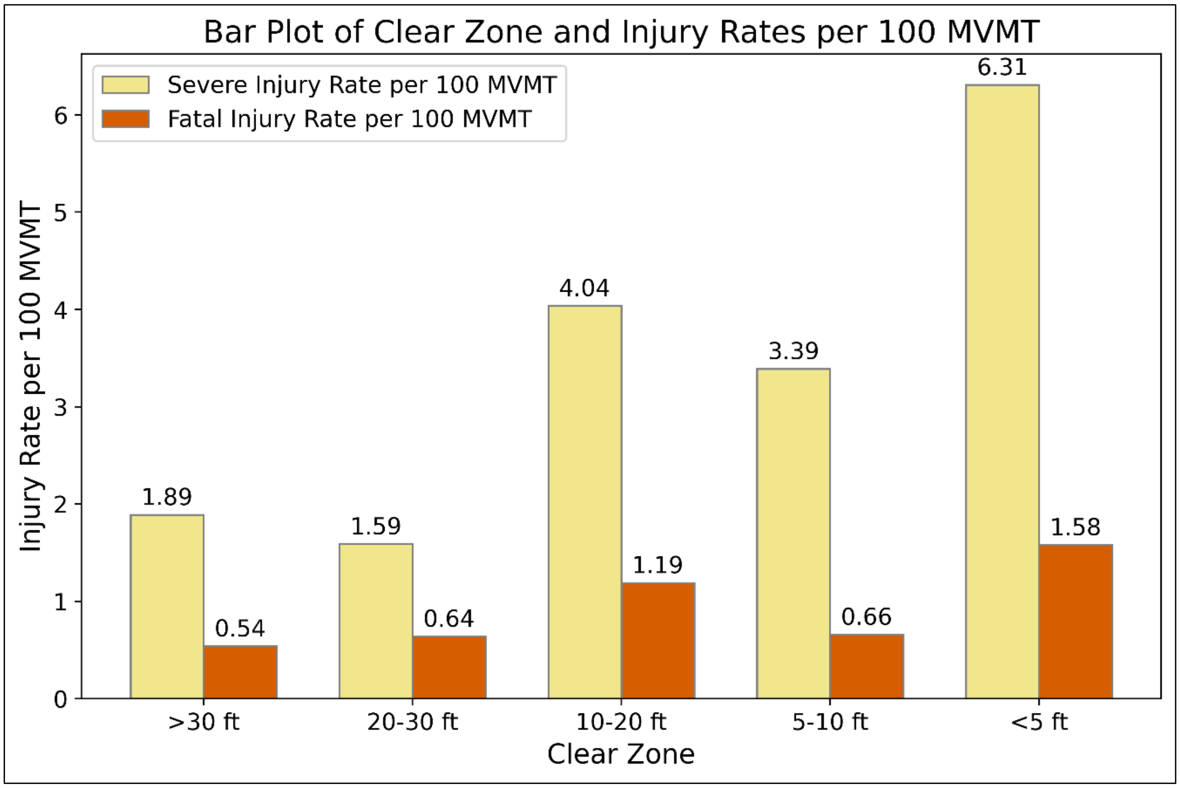

Figure 4.1: Bar Plot of Clear Zone Width and Injury Rates for Non-Interstate Roads

b. Interstate Roads: No significant correlation exists between clear zone width and crash rate, severe injury rate, or fatal injury rate on interstate roads.

c. Combined Interstate and Non-Interstate Roads: In the combined dataset of interstate and non-interstate roads, a strong negative relationship is observed between clear zone width and the rate of severe injuries. The correlation coefficient is -0.90 with a p-value of 0.037, indicating statistical significance within the 95% confidence interval. As the clear zone narrows, the rate of severe injuries rises. Figure 4.2 illustrates this relationship through a bar plot, showing the impact of clear zone width on severe injury rate across both road types.

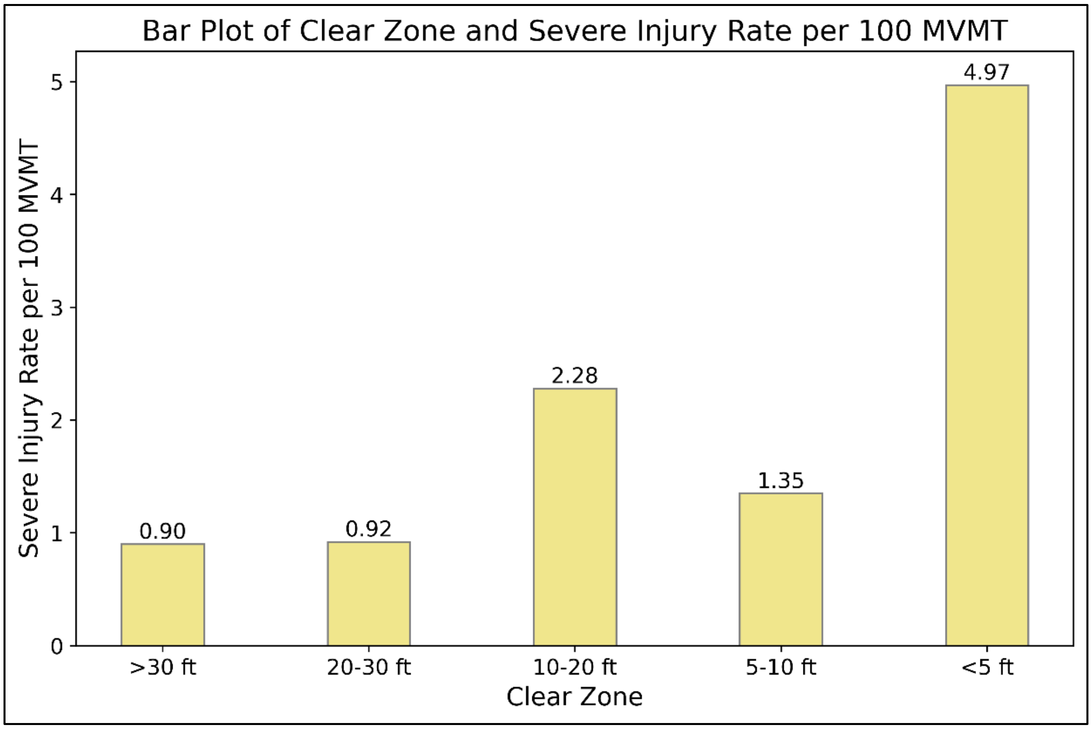

Figure 4.2: Bar Plot of Clear Zone Width and Severe Injury Rate for Combined Roads

4.1.1.2 Rigid Obstacles

a. Non-Interstate Roads: Analysis indicates that the distance from rigid obstacles inversely correlates with the severe injury rate on non-interstate roads. As the distance from rigid obstacles increases, the crash rate decreases. This relationship is statistically significant, with a correlation coefficient of -1 and a p-value of 0, within a 95% confidence interval. Figure 4.3 presents a bar plot showing the relationship between the distance from rigid obstacles and the severe injury rate for non-interstate roads.

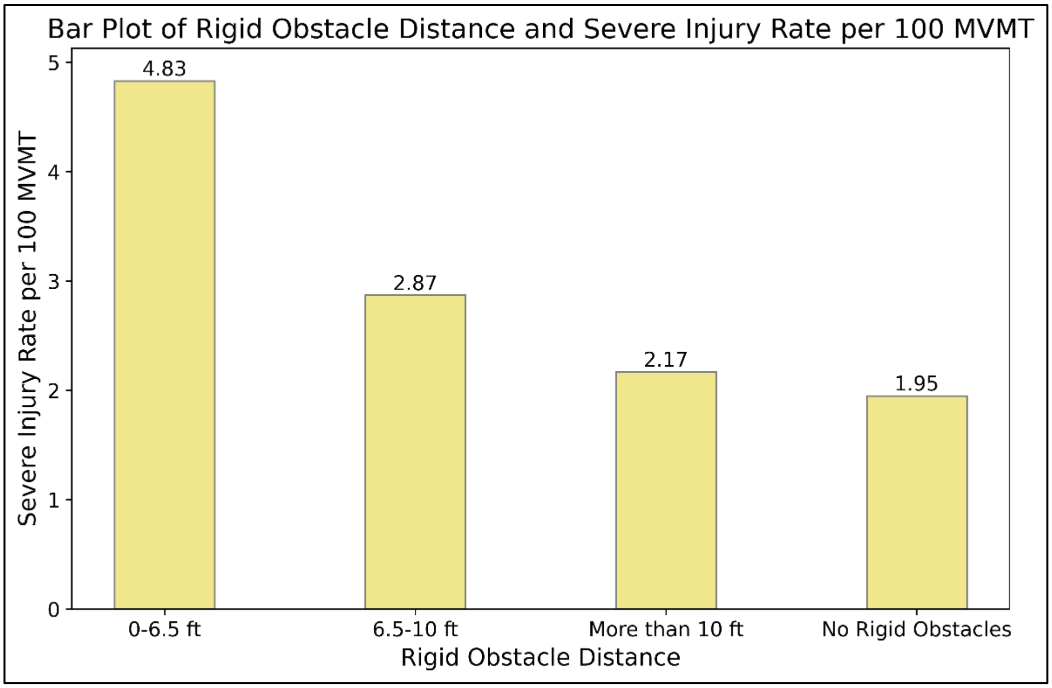

Figure 4.3: Bar Plot of Distance from Rigid Obstacles and Severe Injury Rate for Non-Interstate Roads

b. Interstate Roads: On interstate roads, a strong negative correlation exists between the distance from rigid obstacles and both severe and fatal injury rates. As the distance from rigid obstacles increases, both rates decrease. The correlation coefficient is -1 with a p-value of 0 for both severity rates, indicating a perfect negative relationship within the 95% confidence interval. Figure 4.4 displays a bar plot illustrating the relationship between the distance from rigid obstacles and the rates of severe and fatal injuries on interstate roads.

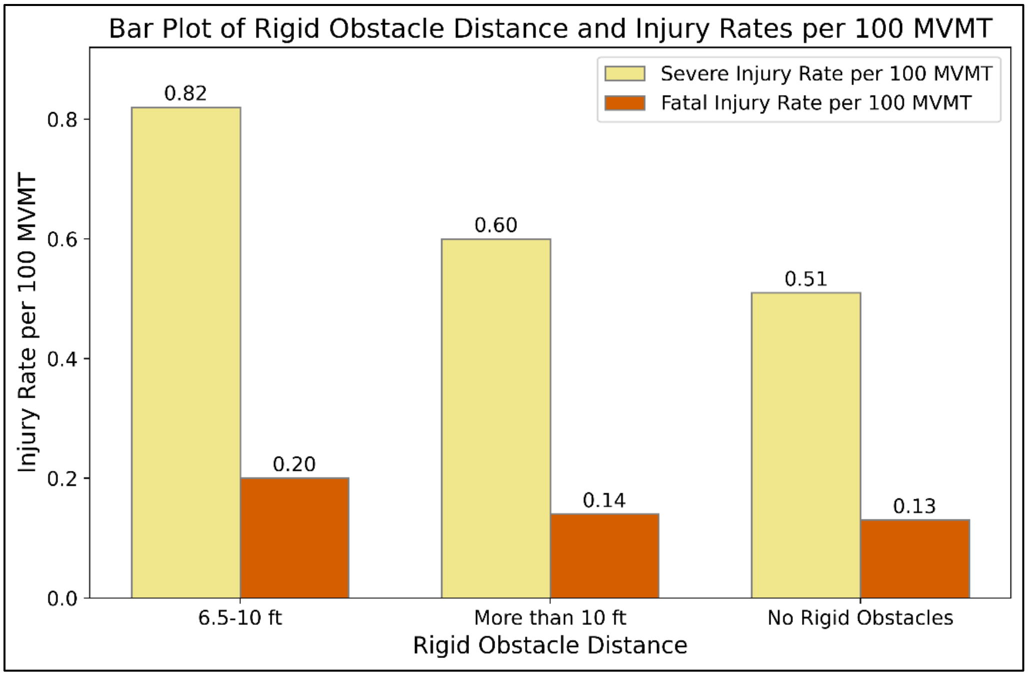

Figure 4.4: Bar Plot of Distance from Rigid Obstacles and Injury Rates for Interstate Roads

c. Combined Interstate and Non-Interstate Roads: For the combined dataset of interstate and non-interstate roads, there is a strong negative correlation between the distance from rigid obstacles and the severe injury rate, with a correlation coefficient of -1 and a p-value of 0. This indicates a perfect negative relationship within the 95% confidence interval. As the distance from rigid obstacles increases, the severe injury rate decreases. Figure 4.5 shows a bar plot depicting the relationship between the distance from rigid obstacles and the severe injury rate across both interstate and non-interstate roads.

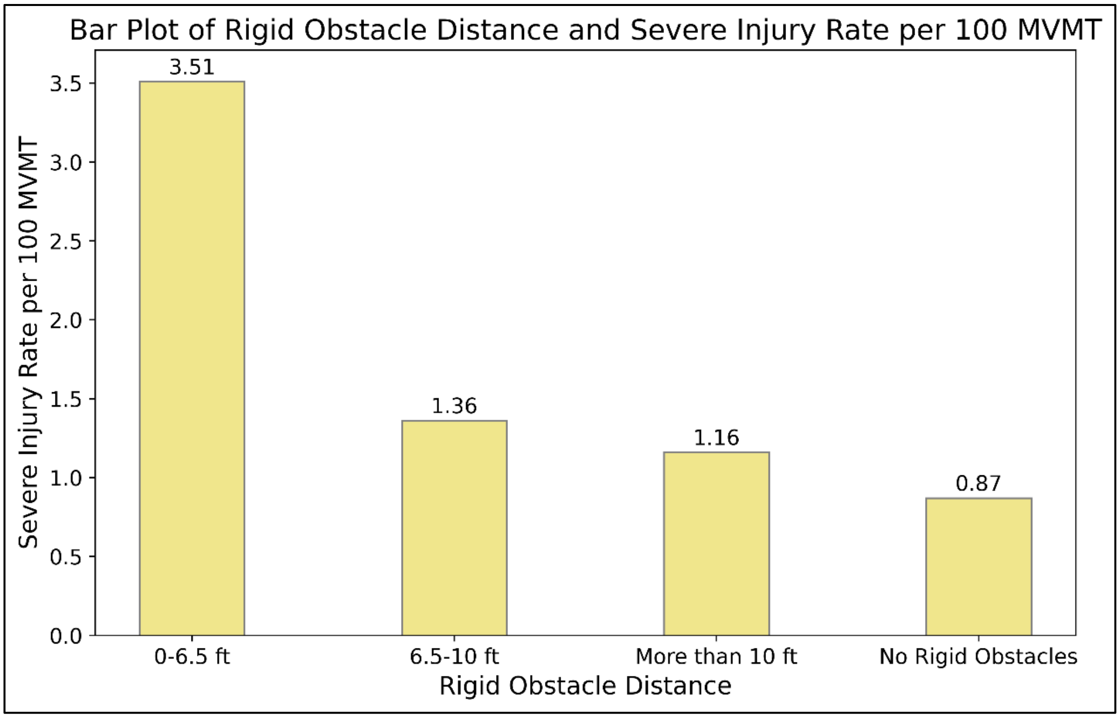

Figure 4.5: Bar Plot of Distance from Rigid Obstacles and Severe Injury Rate for Combined Roads

4.1.1.3 Side Slope

a. Non-Interstate Roads: The condition of side slopes demonstrates a significant positive correlation with crash rate, severe injury rate, and fatal injury rate on non-interstate roads. Specifically, as the steepness of side slopes increases, the crash and severity rates also increase. The analysis shows a correlation coefficient of 1 and a p-value of 0, indicating statistical significance at the 95% confidence interval. Figure 4.6 illustrates the relationship between side slope steepness and crash rate, severe injury rate, and fatal injury rate on non-interstate roads.

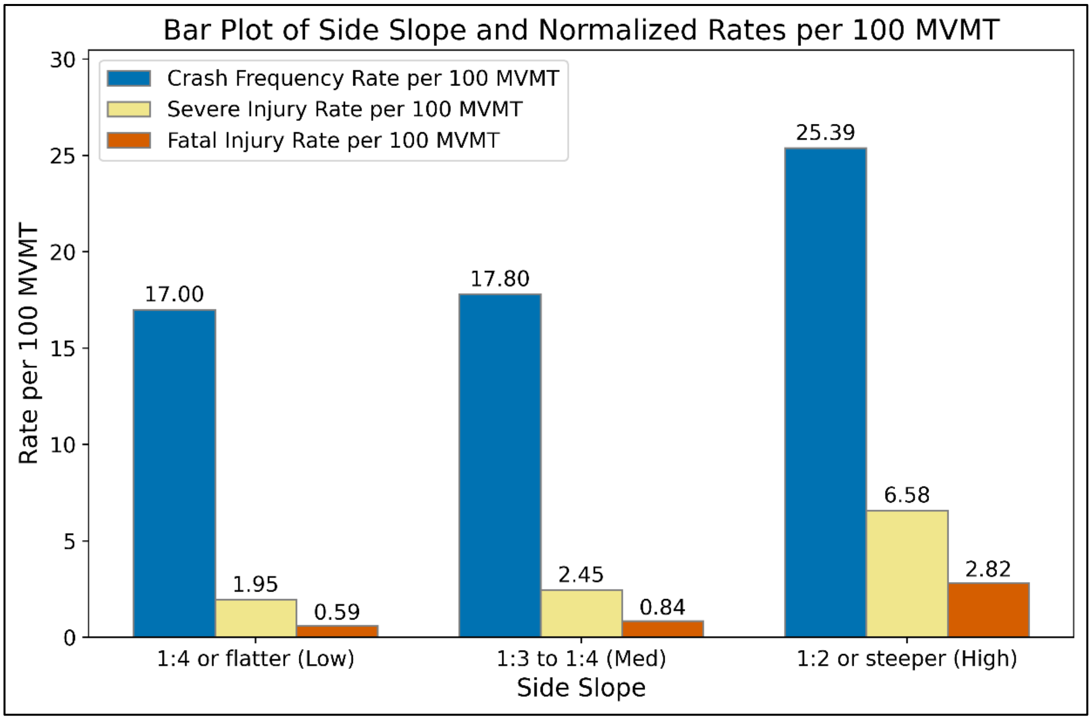

Figure 4.6: Bar Plot of Side Slope and Normalized Rates for Non-Interstate Roads

b. Interstate Roads: Similarly, for interstate roads, there is a significant positive correlation between the steepness of side slopes and both severe and fatal injury rates. The correlation coefficient is 1 with a p-value of 0, indicating a perfect and statistically significant relationship within 95% confidence interval. Figure 4.7 illustrates the relationship between side slope steepness and both severe injury and fatal injury rates on interstate roads.

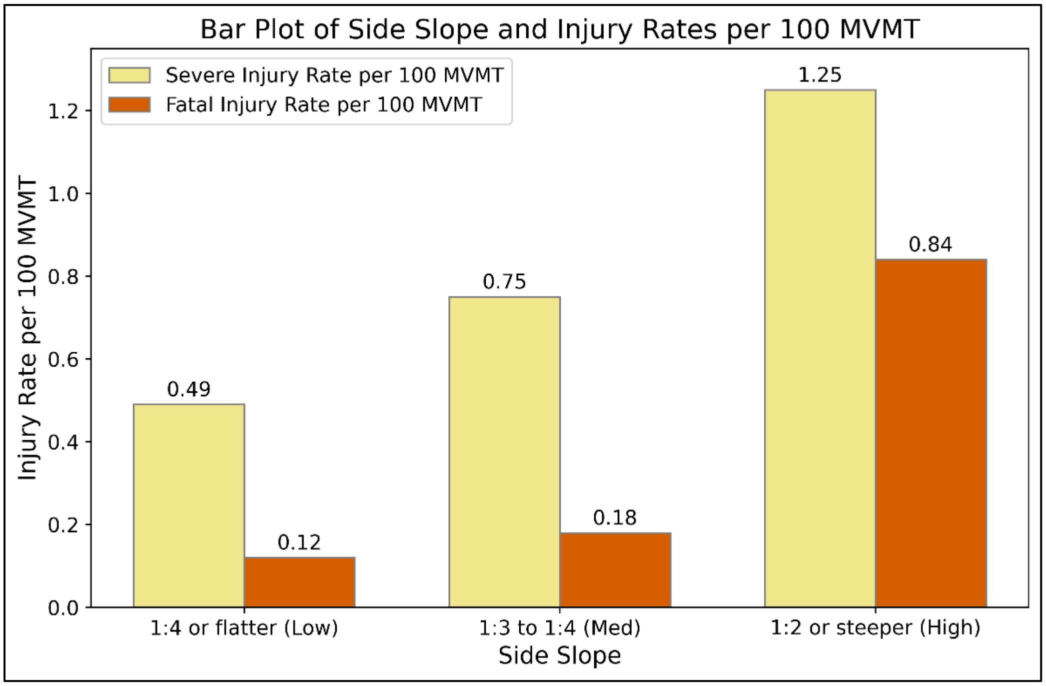

Figure 4.7: Bar Plot of Side Slope and Injury Rates for Interstate Roads

c. Combined Interstate and Non-Interstate Roads: The combined data for interstate and non-interstate roads also indicate a significant positive correlation between side slope steepness and both severe and fatal injury rates. The correlation coefficient remains 1 with a p-value of 0, indicating a perfect and statistically significant relationship within 95% confidence interval. Figure 4.8 illustrates the relationship between side slope steepness and both severe injury rate and fatal injury rate for the combined dataset of interstate and non-interstate roads.

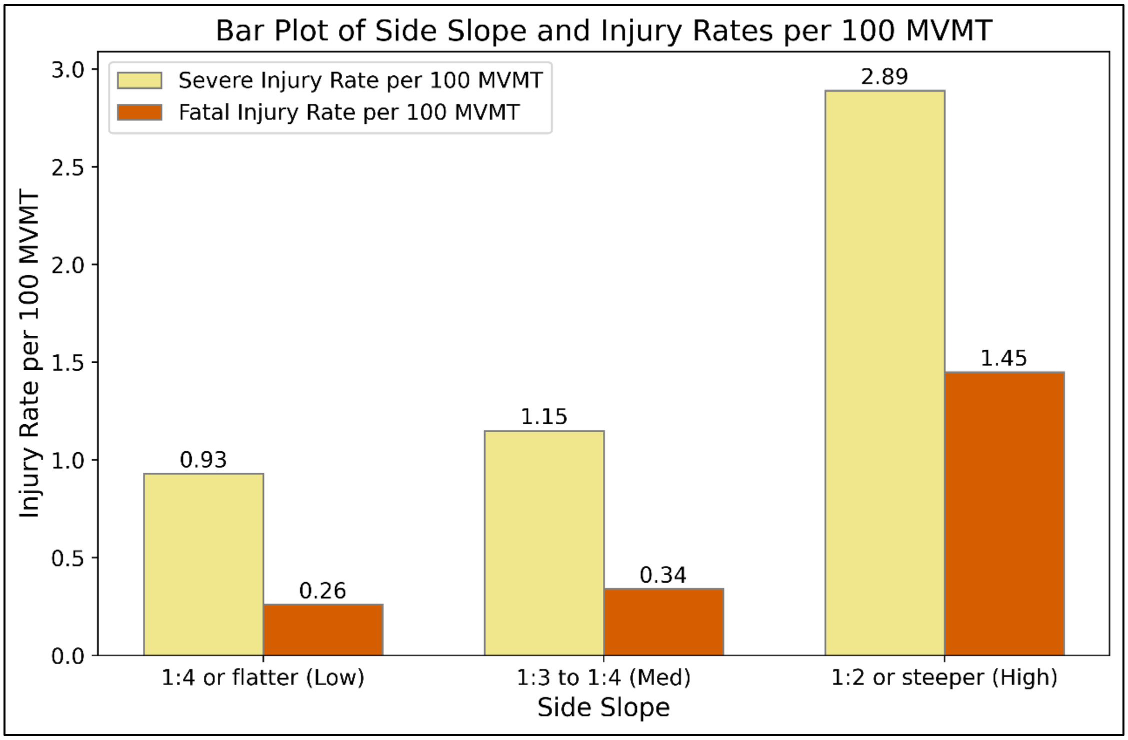

Figure 4.8: Bar Plot of Side Slope and Injury Rates for Combined Roads

4.1.1.4 Safety Rating

a. Non-Interstate Roads: Safety ratings on non-interstate roads show a positive correlation between crash rate and severe injury rate. As the safety rating increases from 1 to 7, both crash rate and severe injury rate rise. The correlation coefficients are 0.89 for the crash rate and 1 for the severe injury rate. These correlations are statistically significant within 95% confidence interval, with p-values of 0.006 for the crash rate and 0 for the severe injury rate. Figure 4.9 presents a bar plot illustrating the relationship between safety ratings and crash rate, as well as severe injury rate, on non-interstate roads.

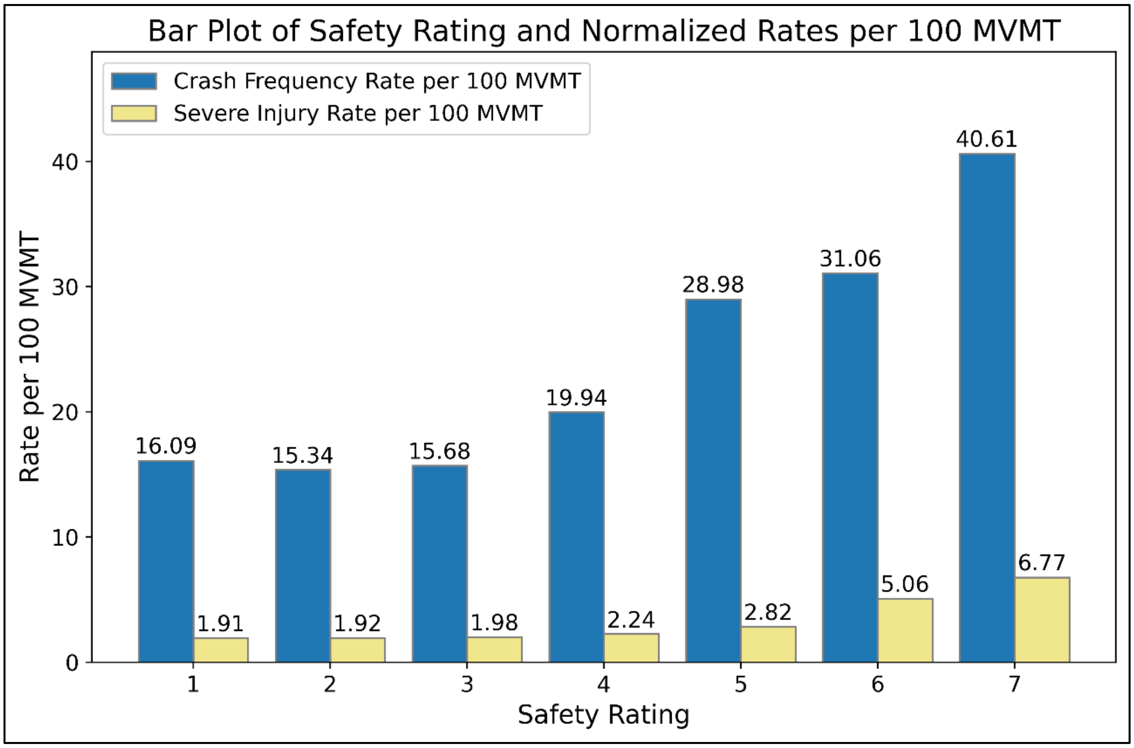

Figure 4.9: Bar Plot of Safety Rating and Normalized Rates for Non-Interstate Roads

b. Interstate Roads: On interstate roads, safety ratings are positively correlated with both severe injury rate and fatal injury rate. As the safety rating increases, both severity rates tend to rise. The correlation coefficient is 0.88 for both severe injury and fatal injury rates, with a p-value of 0.018, indicating statistical significance with the 95% confidence interval. Figure 4.10 illustrates the relationship between safety ratings and both severe injury and fatal injury rates on interstate roads.

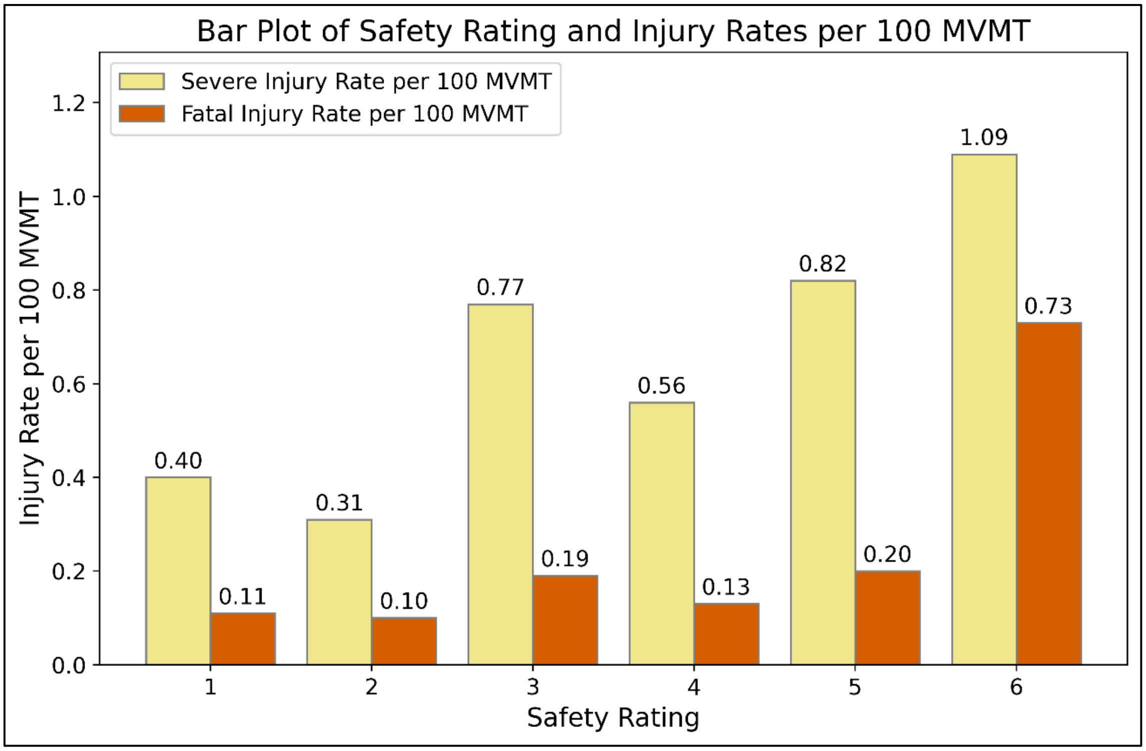

Figure 4.10: Bar Plot of Safety Rating and Injury Rates for Interstate Roads

c. Combined Interstate and Non-Interstate Roads: In the combined dataset of interstate and non-interstate roads, there is a significant positive correlation between safety ratings and both crash and severe injury rates. As safety rating increases, both crash rate and severe injury rate increase. The correlation coefficient for the crash rate is 0.89 with a p-value of 0.006, while for severe injury rate, the correlation is 0.96 with a p-value of 0.0004, reflecting statistical significance within 95% confidence interval. Figure 4.11 visually represents the relationship between safety rating and both crash rate and severe injury rate for combined interstate and non-interstate roads.

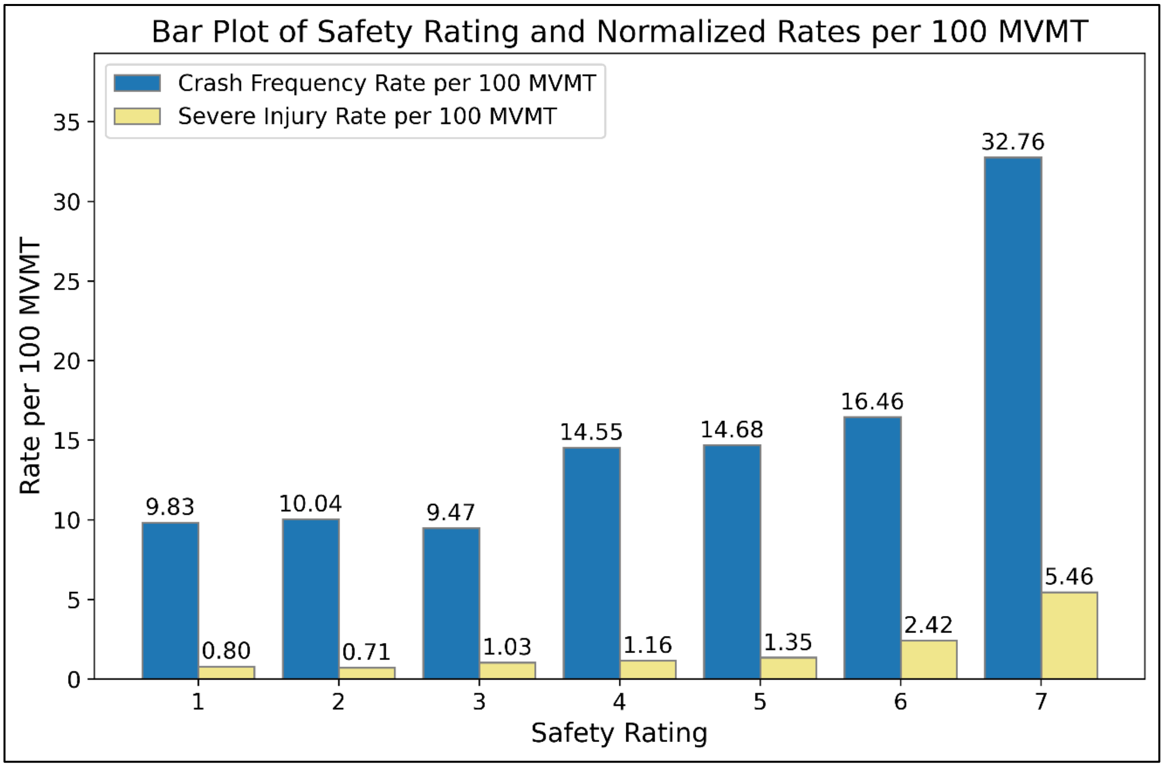

Figure 4.11: Bar Plot of Safety Rating and Normalized Rates for Combined Roads

4.1.1.5 Safety Barriers

In analyzing the impact of safety barriers on RD crashes, we examine whether a vehicle struck a safety barrier and assess the resulting crash severity. A proportional test is used to evaluate how safety barriers influence crash severity outcomes. To determine their effectiveness in reducing injury severity, we compare the severity of two groups of crashes: those where a vehicle struck a safety barrier and those involving no safety barriers, such as crashes with fixed objects or rollovers. This comparison provides insight into how safety barriers may help mitigate the severity of RD crashes.

a. Non-Interstate Roads: In the analysis of non-interstate roads, we examine how hitting a safety barrier during a crash influences injury severity. According to Table 4.1, the likelihood of a fatal injury is significantly lower in crashes where a safety barrier is struck, at 0.7%, compared to 3.7% in crashes without safety barrier impact, resulting in an 81% reduction. Severe injuries also decrease from 12.6% in crashes without safety barrier impact to 4.9% when a safety barrier is hit, showing a 61% reduction. These results highlight the effectiveness of safety barriers in reducing injury severity, confirmed by the proportional test (p-value < 0).

Table 4.1: Conditional Table for Safety Barriers and Severity for Non-Interstate Roads

Safety Barrier	Fatal Injury		Severe Injury	
	No	**Yes**	**No**	**Yes**
No	96.3%	3.7%	87.4%	12.6%
Yes	99.3%	0.7%	95.1%	4.9%
Percent Reduction	81%		61%	
p-value	7.6E-04		2.3E-06	

b. Interstate Roads: For interstate roads, the data in Table 4.2 shows that fatal injuries occur in 0.2% of crashes that hit a safety barrier, compared to 2.4% in crashes without barrier impact, marking a 91% reduction. Similarly, severe injuries drop from 8.9% to 2.2% when a barrier is struck, reflecting a 75% reduction. These reductions are statistically significant, as confirmed by the proportional test (p-value < 0.05).

Table 4.2: Conditional Table for Safety Barriers and Severity for Interstate Roads

Safety Barrier	Fatal Injury		Severe Injury	
	No	**Yes**	**No**	**Yes**
No	97.6%	2.4%	91.1%	8.9%
Yes	99.8%	0.2%	97.8%	2.2%
Percent Reduction	91%		75%	
p-value	3.9E-07		4.3E-15	

c. Combined Interstate and Non-Interstate Roads: When analyzing data from both interstate and non-interstate roads combined, the results show a consistent reduction in injury severity when a crash involves hitting a safety barrier. Table 4.3 shows that fatal injuries are reduced from 3.1% to 0.3%, representing a 90% decrease. Similarly, severe injuries drop from 10.9% to 2.9%, reflecting a 73% reduction. The proportional test confirms that these reductions are statistically significant (p-value < 0).

Table 4.3: Conditional Table for Safety Barriers and Severity for Combined Roads

Safety Barrier	**Fatal Injury**		**Severe Injury**	
	No	**Yes**	**No**	**Yes**
No	96.9%	3.1%	89.1%	10.9%
Yes	99.7%	0.3%	97.1%	2.9%
Percent Reduction	90%		73%	
p-value	3.6E-11		2.5E-24	

4.1.2 Analysis of Roadside Features When Restraints Are Used

4.1.2.1 Clear Zone

a. Non-Interstate Roads: No significant correlation was found between clear zone and crash rate, severe injury rate, or fatal injury rate on non-interstate roads when restraints are used.

b. Interstate Roads: No significant correlation was identified between clear zone width and crash rate, severe injury rate, or fatal injury rate on interstate roads when restraints are used.

c. Combined Interstate and Non-Interstate Roads: In the combined dataset of interstate and non-interstate roads, a significant negative correlation was found between clear zone width and severe injury rates when restraints are used. The correlation coefficient is -0.90, with a p-value of 0.037, indicating statistical significance within 95% confidence interval. As the clear zone width decreases, the severe injury rate increases. Figure 4.12 illustrates this relationship between clear zone width and severe injury rate for both interstate and non-interstate roads when restraints are in use.

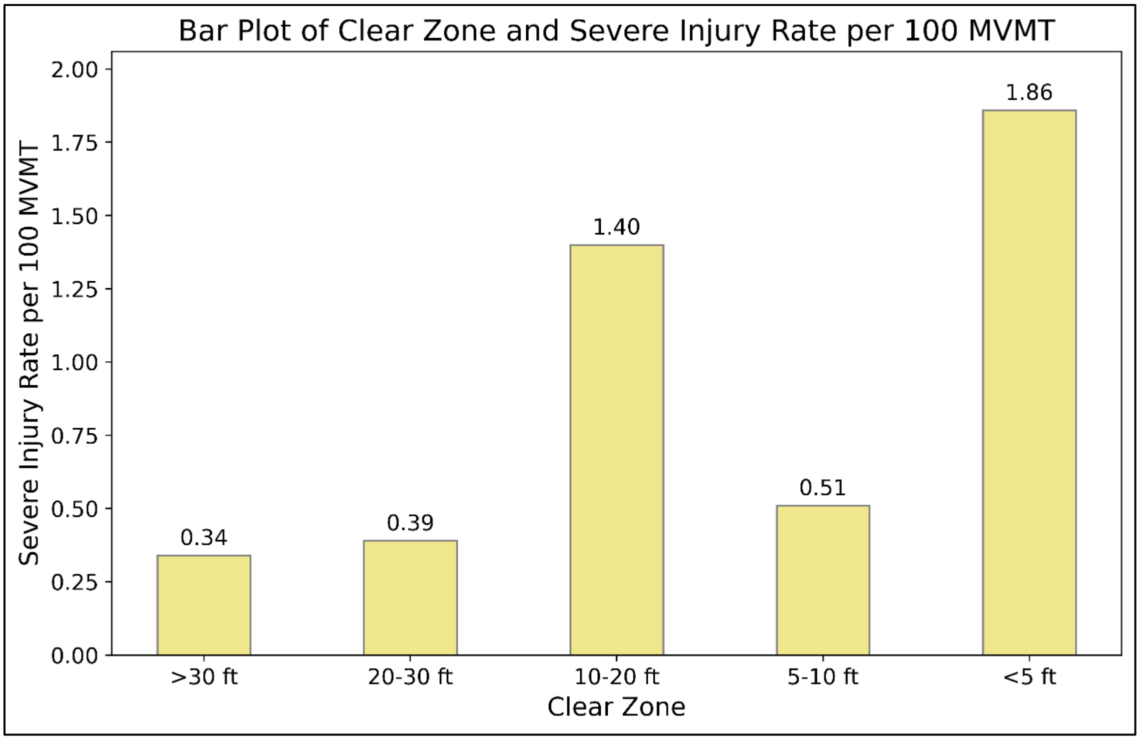

Figure 4.12: Bar Plot of Clear Zone Width and Severe Injury Rate for Combined Roads When Restraints Are Used

4.1.2.2 Rigid Obstacles

a. Non-Interstate Roads: No significant correlation was found between rigid obstacle distance and crash rate, severe injury rate, or fatal injury rate on non-interstate roads when restraints are used.

b. Interstate Roads: For interstate roads, a significant negative correlation exists between the distance from rigid obstacles and both severe injury rates and fatal injury rates. As the distance from rigid obstacles increases, both severe and fatal injury rates decrease. The correlation coefficient for both cases is -1, with a p-value of 0, indicating a perfect negative relationship within 95% confidence interval. Figure 4.13 depicts the relationship between rigid obstacle distance and both severe and fatal injury rates on interstate roads when restraints are used.

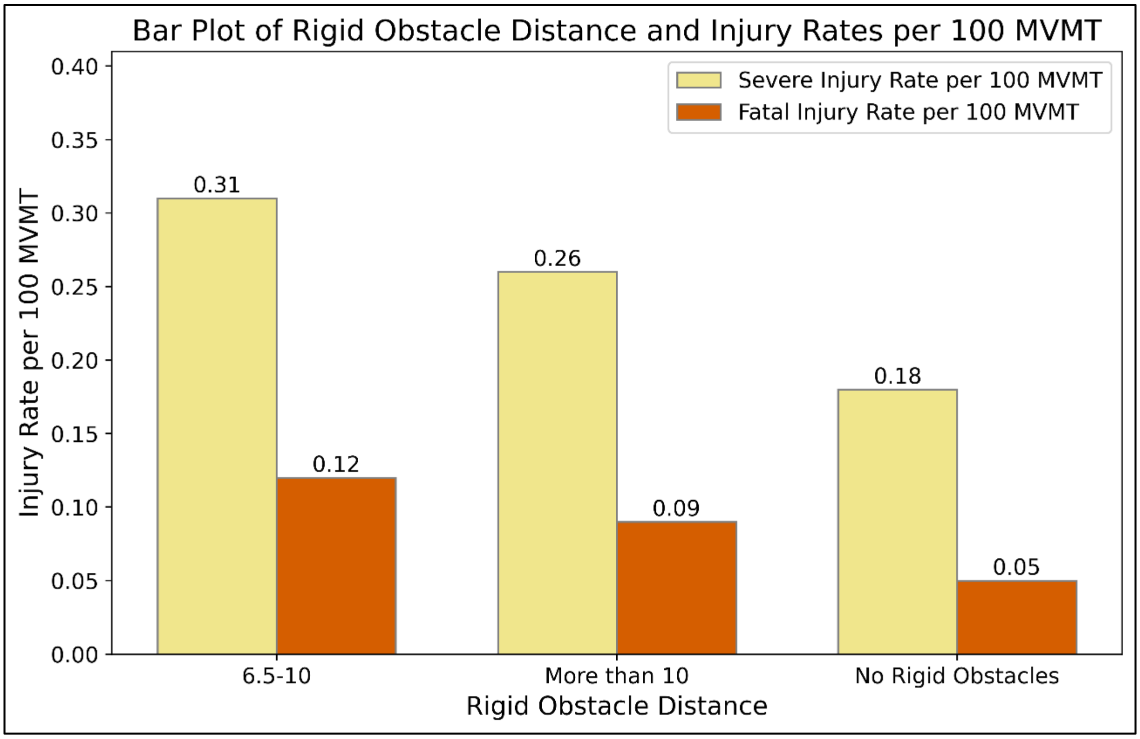

Figure 4.13: Bar Plot of Distance from Rigid Obstacles and Injury Rates for Interstate Roads When Restraints Are Used

c. Combined Interstate and Non-Interstate Roads: When data from both interstate and non-interstate roads were combined, no significant correlation was found between rigid obstacle distance and crash rate, severe injury rate, or fatal injury rate when restraints are used.

4.1.2.3 Side Slope

a. Non-Interstate Roads: The analysis shows that on non-interstate roads, side slope conditions are positively correlated with crash rate, severe injury rate, and fatal injury rate when restraints are used. As the side slope becomes steeper, all three rates: crash rate, severe injury rate, and fatal injury rate increase. This relationship is supported by a correlation coefficient of 1 and a p-value of 0, indicating a perfect and statistically significant correlation within 95% confidence interval. Figure 4.14 illustrates the relationship between side slope condition and crash rate, severe injury rate, and fatal injury rate for non-interstate roads when restraints are used.

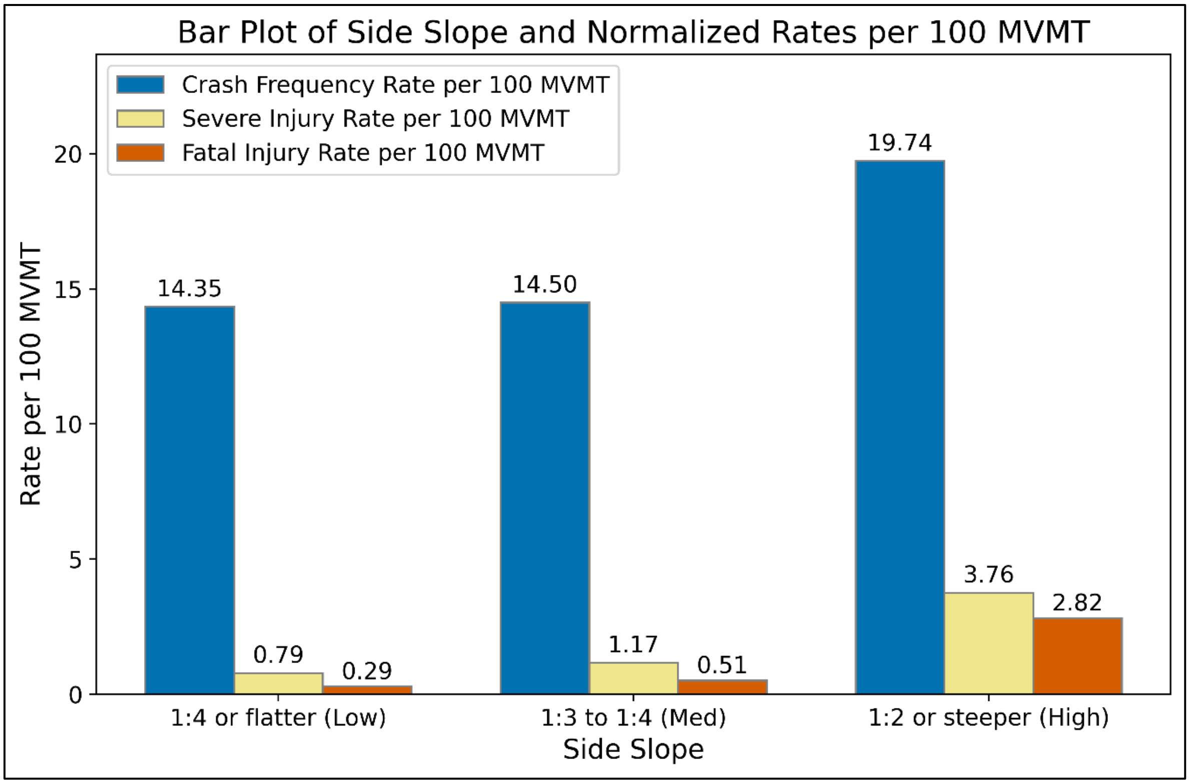

Figure 4.14: Bar Plot of Side Slope and Normalized Rates for Non-Interstate Roads When Restraints Are Used

b. Interstate Roads: Similarly, for interstate roads, there is a positive correlation between side slope conditions and severe injury rate when restraints are used. The correlation coefficient is 1 with a p-value of 0, indicating a perfect and statistically significant correlation within 95% confidence interval. Figure 4.15 illustrates the relationship between side slope and severe injury rate for interstate roads when restraints are used.

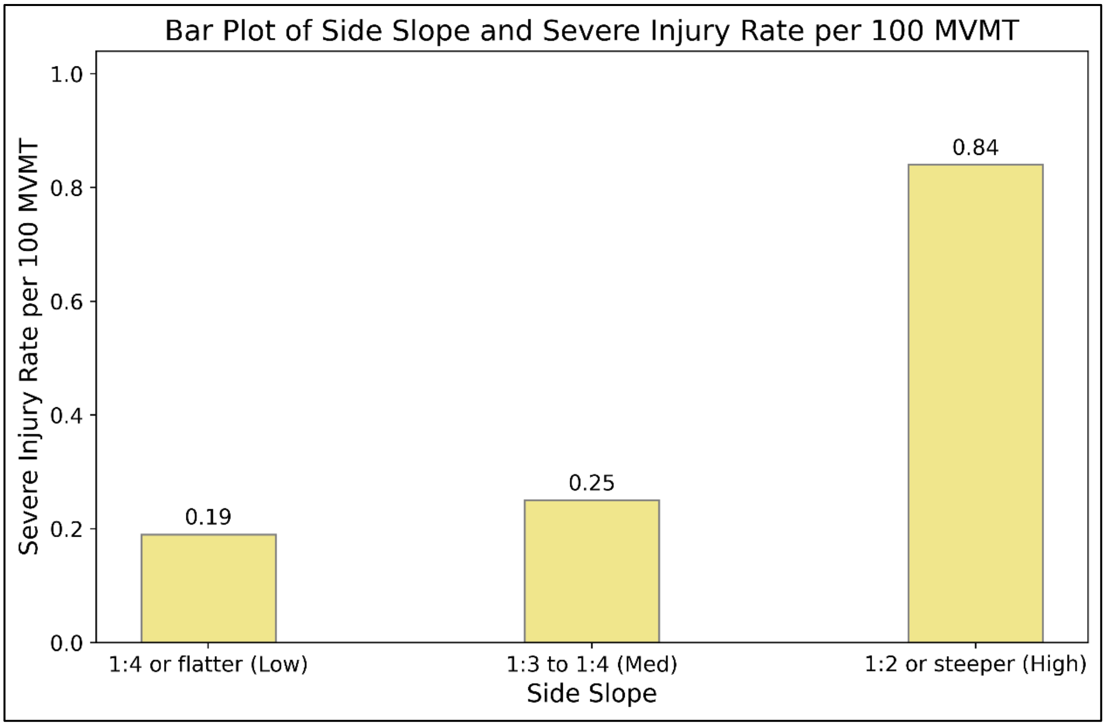

Figure 4.15: Bar Plot of Side Slope and Severe Injury Rate for Interstate Roads When Restraints Are Used

c. Combined Interstate and Non-Interstate Roads: The combined analysis of interstate and non-interstate roads reveals a positive correlation between side slope conditions and both severe injury rate and fatal injury rate when restraints are used. The correlation coefficient is 1, with a p-value of 0, indicating a perfect positive relationship within 95% confidence interval. Figure 4.16 depicts the relationship between side slope steepness and both severe injury and fatal injury rates across the combined dataset of interstate and non-interstate roads when restraints are used.

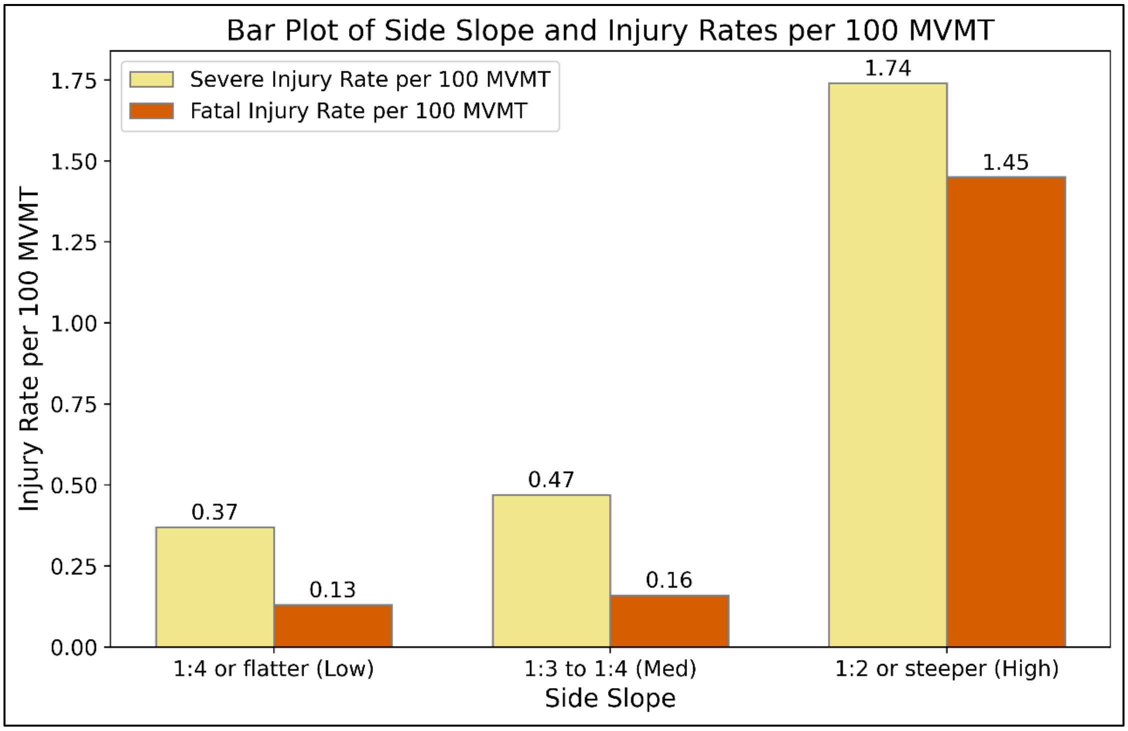

Figure 4.16: Bar Plot of Side Slope and Injury Rates for Combined Roads When Restraints Are Used

4.1.2.4 Safety Rating

a. Non-Interstate Roads: For non-interstate roads, the analysis shows that when restraints are used, there is a positive correlation between safety rating and both crash rate and severe injury rate. Higher safety ratings correspond with the increased crash rate, with a correlation coefficient of 0.86 and a p-value of 0.014. Similarly, for severe injury rate, the correlation coefficient is 0.89, with a p-value of 0.007. Both relationships are statistically significant within the 95% confidence interval. The relationship between safety rating and both crash rate and severe injury rate for non-interstate roads with restraint use is also depicted in Figure 4.17.

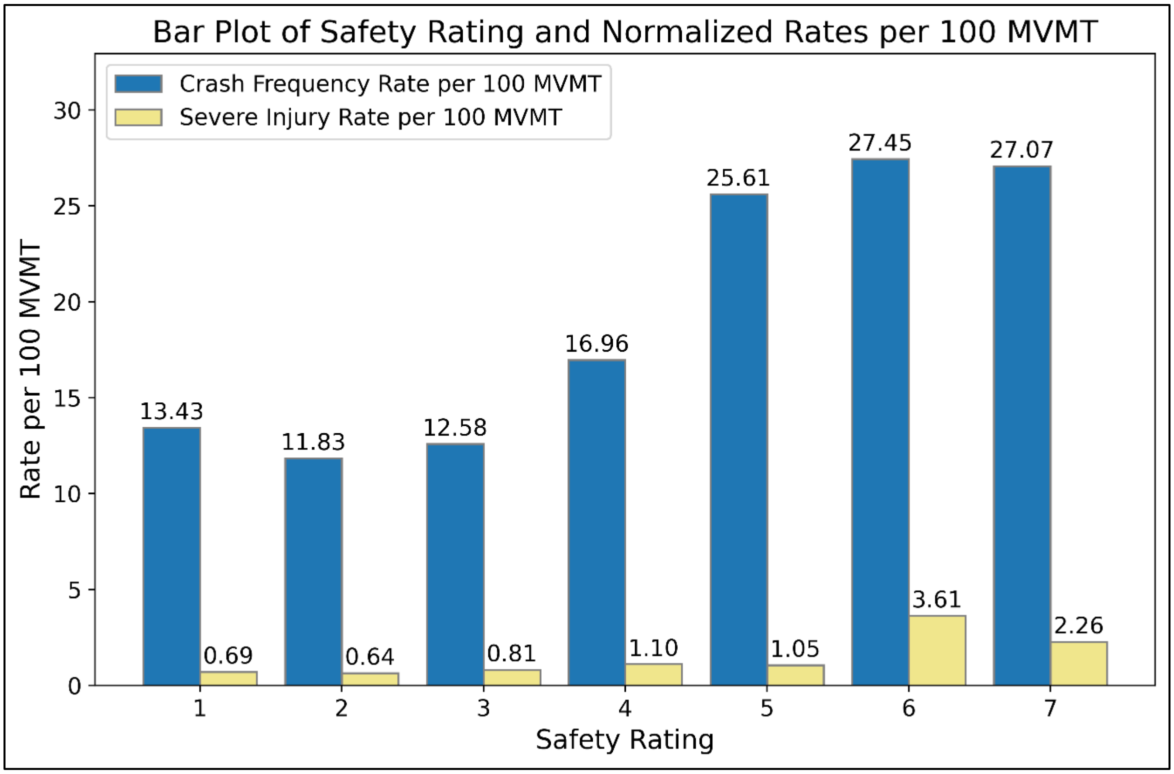

Figure 4.17: Bar Plot of Safety Rating and Normalized Rates for Non-Interstate Roads When Restraints Are Used

b. Interstate Roads: For interstate roads, the analysis shows a positive correlation between safety ratings and both severe and fatal injury rates when restraints are used. The correlation coefficient for severe injury rate is 0.94, with a p-value of 0.05, while for fatal injury rate, the correlation coefficient is 0.83, with a p-value of 0.042. Both relationships are statistically significant within the 95% confidence interval. Figure 4.18 depicts the relationship between safety ratings and both severe and fatal injury rates on interstate roads when restraints are in use.

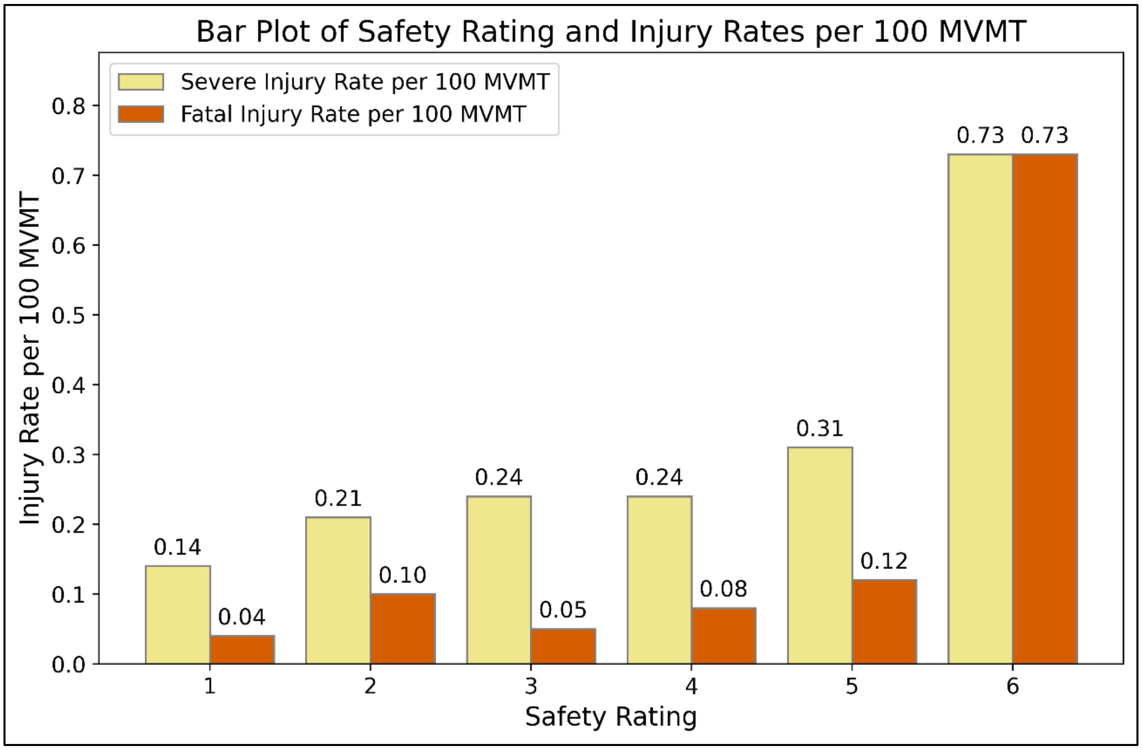

Figure 4.18: Bar Plot of Safety Rating and Injury Rates for Non-Interstate Roads When Restraints Are Used

c. Combined Interstate and Non-Interstate Roads: For the combined analysis of interstate and non-interstate roads, there is a positive correlation between safety rating and both crash rate and severe injury rate. The correlation coefficient for the crash rate is 0.86, with a p-value of 0.0137, while the severe injury rate has a correlation coefficient of 0.96 and a p-value of 0.0004. Both relationships are statistically significant within the 95% confidence interval. Figure 4.19 illustrates the relationship between safety ratings and both crash and severe injury rates for the combined dataset of interstate and non-interstate roads when restraints are in use.

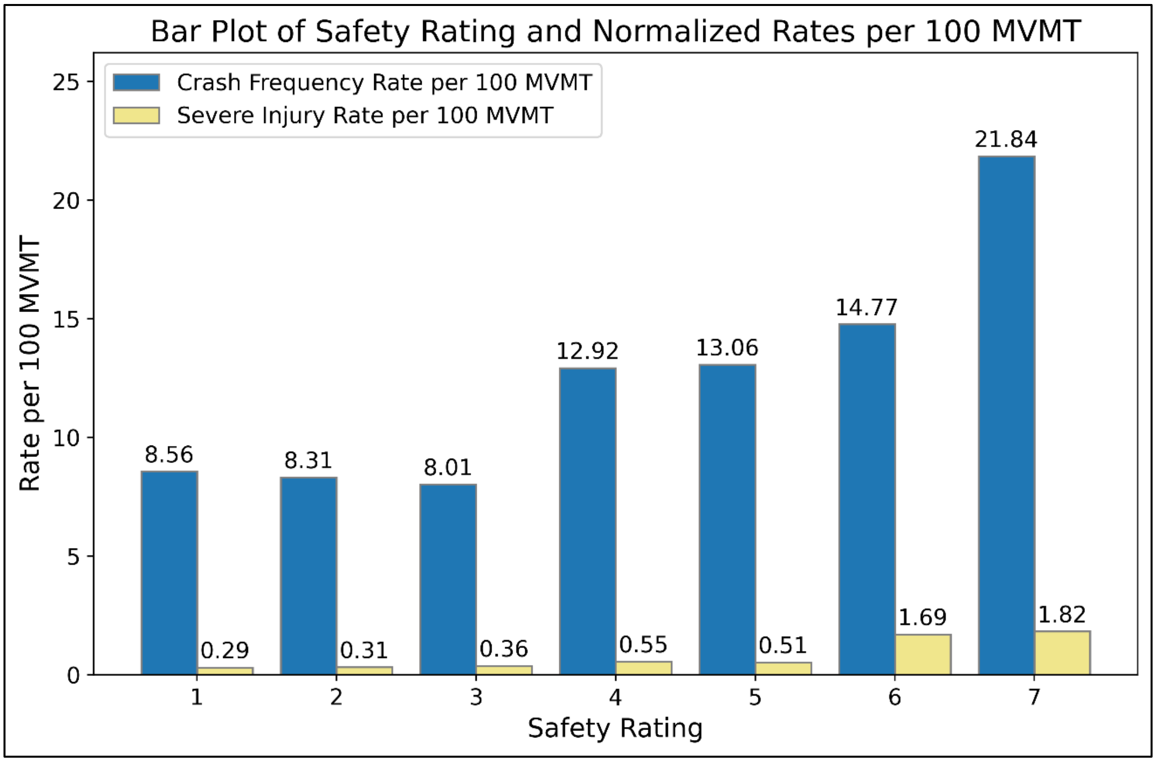

Figure 4.19: Bar Plot of Safety Rating and Normalized Rates for Combined Roads When Restraints Are Used

4.1.3 Analysis of Roadside Features When Restraints Are Not Used

4.1.3.1 Clear Zone

a. Non-Interstate Roads: For non-interstate roads, the analysis reveals a negative correlation between clear zone width and both crash rate and fatal injury rate when restraints are not used. As the clear zone width decreases, the crash rate and the fatal injury rate increase. This relationship is supported by a negative correlation coefficient of -0.90 and a p-value of 0.037 for both metrics, indicating a strong and statistically significant correlation within 95% confidence interval. Figure 4.20 presents a bar plot illustrating the relationship between clear zone width and both crash rate and fatal injury rate on non-interstate roads without restraint use.

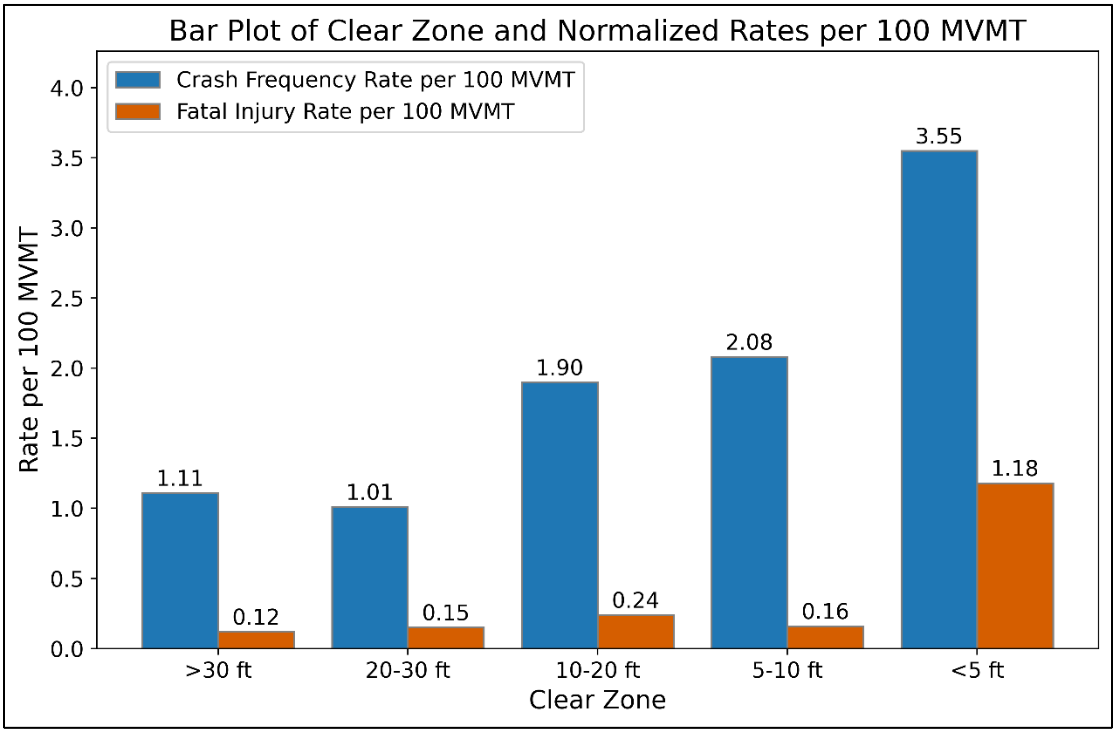

Figure 4.20: Bar Plot of Clear Zone Width and Normalized Rates for Non-Interstate Roads When Restraints Are Not Used

b. Interstate Roads: No significant correlation exists between clear zone width and crash rate, severe injury rate, or fatal injury rate for interstate roads when restraints are not used.

c. Combined Interstate and Non-Interstate Roads: For the combined dataset of interstate and non-interstate roads, when restraints are not used, the analysis reveals a negative correlation between clear zone width and crash rate, severe injury rate, and fatal injury rate. The correlation coefficient for both the crash rate and fatal injury rate is -0.90, with a p-value of 0.037, indicating statistical significance at the 95% confidence level. However, for severe injury rate, the correlation coefficient is -0.80, with a p-value of 0.1, indicating significance at the 90% confidence level but not at the 95% level. Figure 4.21 illustrates the relationship between clear zone width and crash rate, severe injury rate, and fatal injury rate for the combined dataset when restraints are not used.

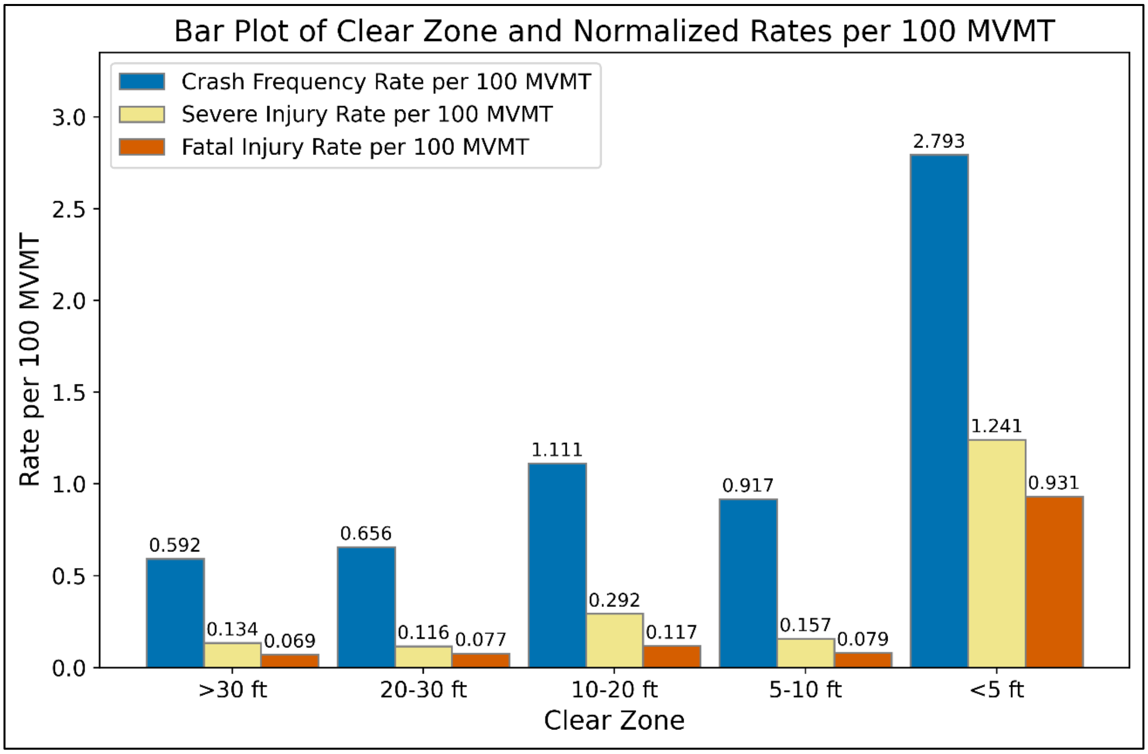

Figure 4.21: Bar Plot of Clear Zone Width and Normalized Rates for Combined Roads When Restraints Are Not Used

4.1.3.2 Rigid Obstacles

a. Non-Interstate Roads: The analysis reveals a strong negative correlation between the distance from rigid obstacles and the crash rate on non-interstate roads when restraints are not used. As the distance from these obstacles increases, the crash rate decreases significantly. This relationship is supported by a perfect correlation coefficient of -1 and a p-value of 0, indicating a highly significant correlation within 95% confidence interval. Figure 4.22 provides a bar plot illustrating the complete relationship between the distance from rigid obstacles and the crash rate for non-interstate roads when restraints are not used.

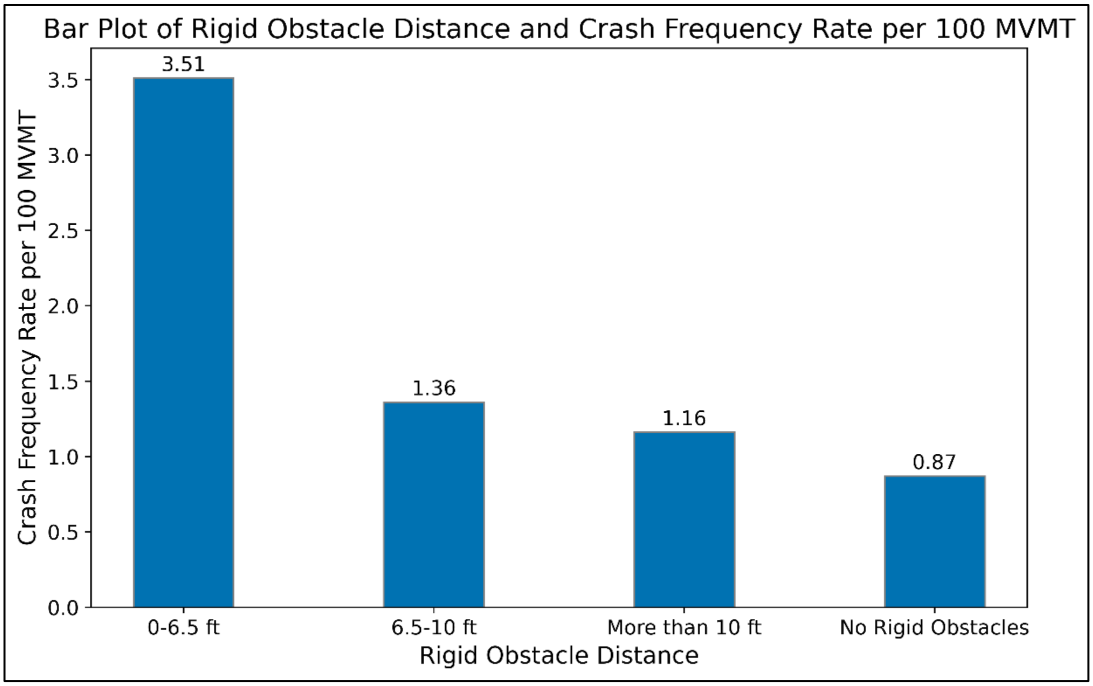

Figure 4.22: Bar Plot of Distance from Rigid Obstacles and Crash Rate for Non-Interstate Roads When Restraints Are Not Used

b. Interstate Roads: No significant correlation exists between distance from rigid obstacles and crash rate, severe injury rate, or fatal injury rate for interstate roads when restraints are not used.

c. Combined Interstate and Non-Interstate Roads: For the combined dataset of interstate and non-interstate roads, when restraints are not used, there is a perfect negative correlation between the distance from rigid obstacles and crash rate. The correlation coefficient is -1, with a p-value of 0, indicating statistical significance within 95% confidence interval and perfect inverse relationship. As the distance from rigid obstacles increases, the crash rate decreases. Figure 4.23 illustrates the relationship between rigid obstacle distance and crash rate on combined interstate and non-interstate roads when restraints are not used.

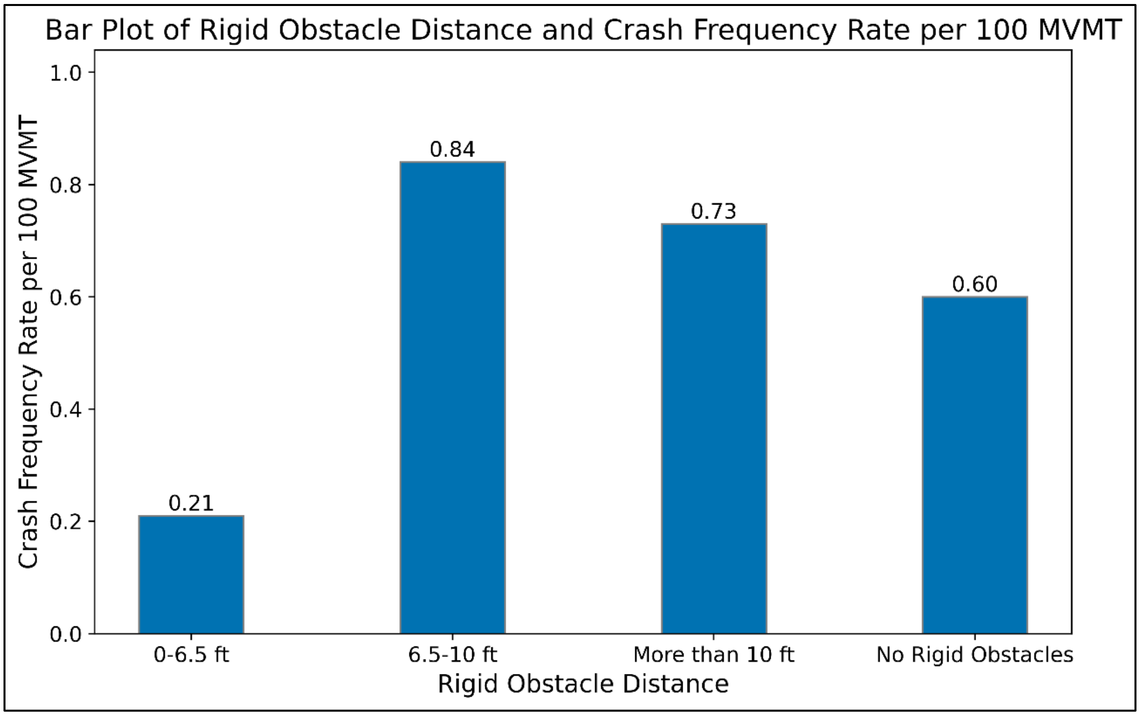

Figure 4.23: Bar Plot of Distance from Rigid Obstacles and Crash Rate for Combined Roads When Restraints Are Not Used

4.1.3.3 Side Slope:

a. Non-Interstate Roads: When restraints are not used on non-interstate roads, the data analysis indicates a strong positive correlation between the steepness of the side slope and the crash rate. As the side slope becomes steeper, the crash rate increases. This relationship is characterized by a correlation coefficient of 1 and a p-value of 0, underscoring a highly significant correlation within 95% confidence interval. Figure 4.24 provides a bar plot illustrating the relationship between side slope and crash rate on non-interstate roads when restraints are not used.

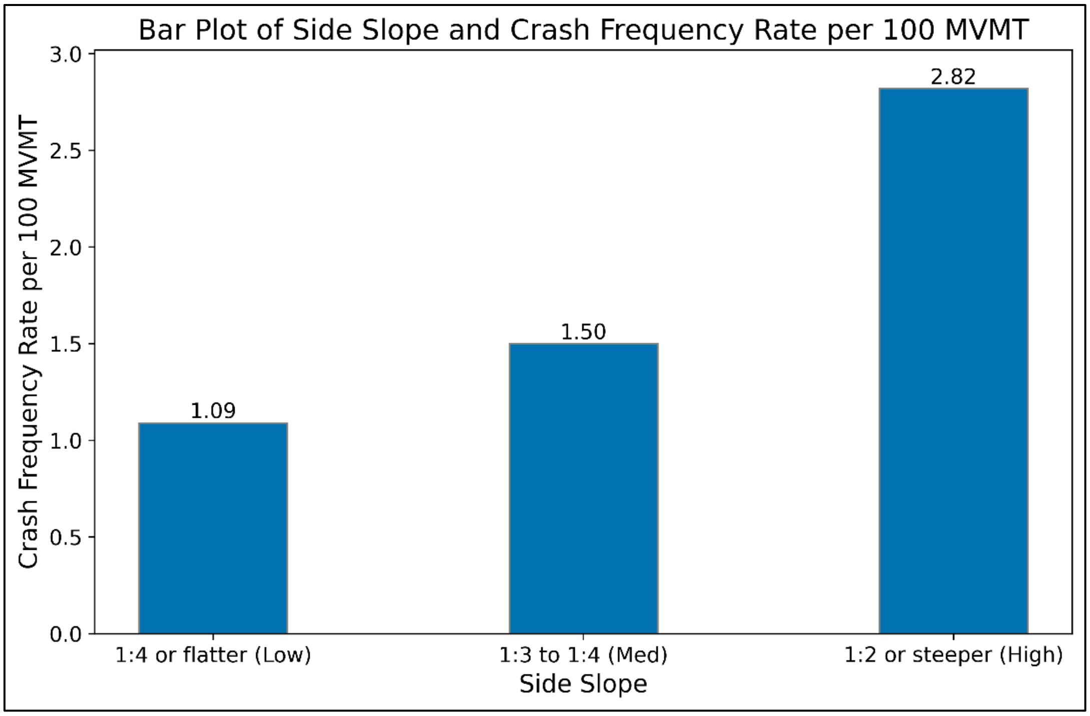

Figure 4.24: Bar Plot of Side Slope and Crash Rate for Non-Interstate Roads When Restraints Are Not Used

b. Interstate Roads: No significant correlation exists between side slope and crash rate, severe injury rate, or fatal injury rate for interstate roads when restraints are not used.

c. Combined Interstate and Non-Interstate Roads: For combined interstate and non-interstate roads, the analysis also indicates a strong positive correlation between the steepness of the side slope and the crash rate when restraints are not used. The correlation coefficient remains 1 with a p-value of 0, indicating perfect correlation within 95% confidence interval. Figure 4.25 shows the bar plot for the relationship between side slope steepness and crash rate on combined interstate and non-interstate roads when restraints are not used.

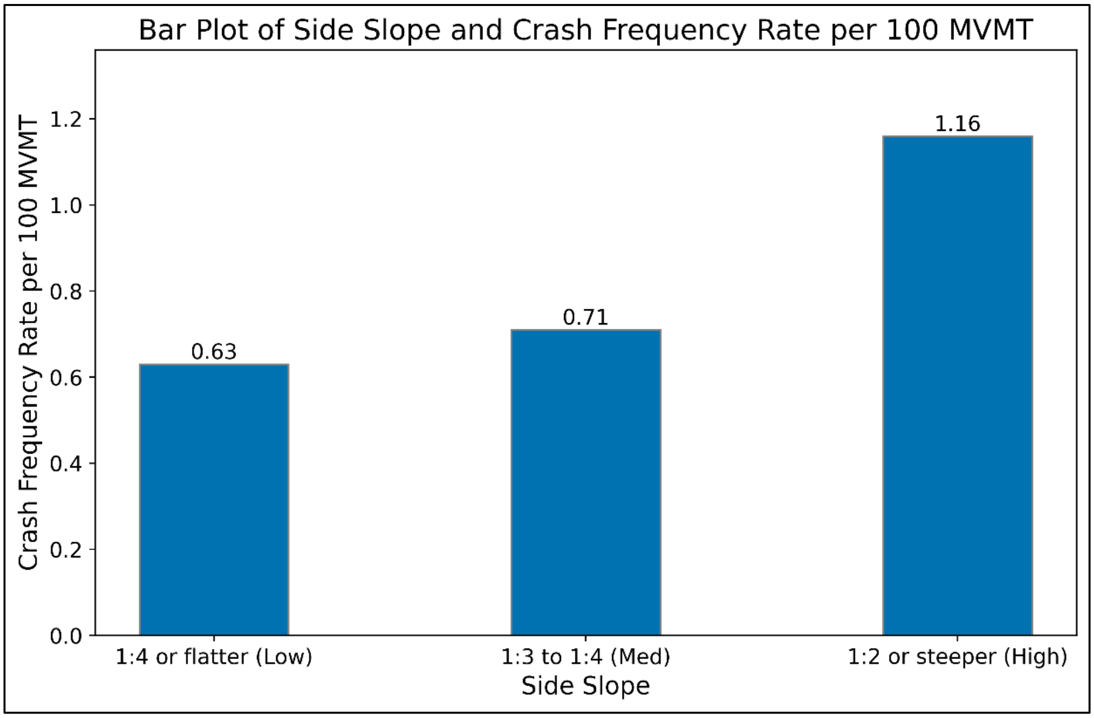

Figure 4.25: Bar Plot of Side Slope and Crash Rate for Combined Roads When Restraints Are Not Used

4.1.3.4 Safety Rating

a. Non-Interstate Roads: No significant correlation exists between safety rating and crash rate, severe injury rate, or fatal injury rate for non-interstate roads when restraints are not used.

b. Interstate Roads: No significant correlation exists between safety rating and crash rate, severe injury rate, or fatal injury rate for interstate roads when restraints are not used.

b. Combined Interstate and Non-Interstate Roads: When data from both interstate and non-interstate roads were combined, no significant correlation was found between safety rating and crash rate, severe injury rate, or fatal injury rate when restraints are used.

4.1.4 Relation Between Restraint and Non-Restraint Cases with Crash Severity on Combined Interstate and Non-Interstate Roads Using t-Test

An analysis using a t-test was conducted to compare the mean crash severity between incidents involving restraint (seat belt use) and non-restraint (no seat belt use) on combined interstate and non-interstate roads. The results demonstrate significant differences in the mean values of fatal, severe, and no-injury crash rates between the two groups, with all p-values indicating statistical significance within 95% confidence interval (p-value less than 0.05). The detailed results are presented in the Table 4.4.

Table 4.4: Mean Table for Restraint and Not Restraint Condition

Condition	Restraint (Mean)	Not Restraint (Mean)	p-value	Comment
Fatal	0.01	0.11	1.81E-42	p-value <0.05
Severe	0.04	0.21	8.08E-52	p-value <0.05
No Injury	0.75	0.51	1.16E-25	p-value <0.05

For fatal incidents, the mean severity is significantly higher for non-restraint cases, at 0.11, compared to 0.01 for restraint cases, with a p-value less than 0.05, indicating statistical significance. Similarly, the mean severity of severe injury incidents is higher for non-restraint cases, at 0.21, compared to 0.04 for restraint cases, with a highly significant p-value. Conversely, the mean proportion of incidents with no injury is higher for restraint cases, at 0.75, compared to 0.51 for non-restraint cases, with a significant p-value of less than 0.05. These findings clearly indicate that the use of restraints significantly reduces the severity of crash outcomes, emphasizing the critical importance of restraint or seat belt usage for enhancing road safety.

4.2 Hotspot Identification

Hotspots are identified for each route based on the ranking of severity rates, with the top ten locations ranked accordingly. This section presents the hotspot locations for the seven study routes: US-6, SR-10, I-15, SR-12, US-40, I-80, and SR-150, using both Utah’s crash cost and the New South Wales approach.

4.2.1 Utah's Crash Cost Approach

4.2.1.1 US-6

Table 4.5: Hotspot Ranking for US-6 Based on Utah's Crash Cost

Rank	Milepoints	Severity Rate
1	26.5-27.0	48552.1
2	52.0-52.5	27031.1
3	54.0-54.5	25846.5
4	77.0-77.5	24769.5
5	56.5-57.0	24661.8
6	25.5-26.0	24276.1
7	5.0-5.5	24179.7
8	13.5-14.0	22060.4
9	143.5-144.0	21637.6
10	143.0-143.5	20132.8

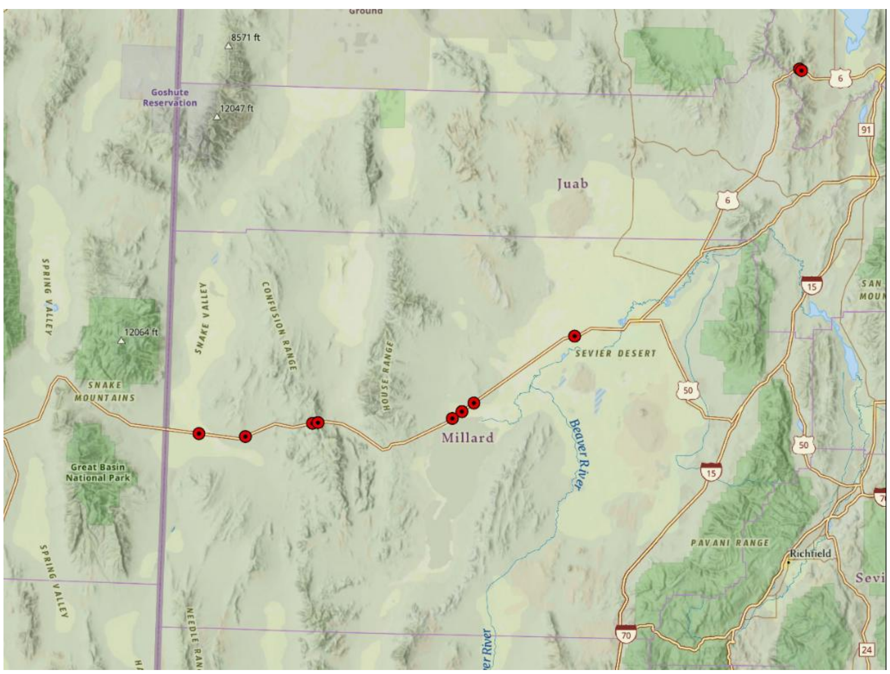

Figure 4.26: Hotspot Map for US-6 Using Utah's Crash Cost

4.2.1.2 SR-10

Table 4.6: Hotspot Ranking for SR-10 Based on Utah's Crash Cost

Rank	Milepoints	Severity Rate
1	11.5-12.0	4271.5
2	38.5-39.0	4248.6
3	3.0-3.5	2510.1
4	17.5-18.0	2405.9
5	55.0-55.5	2402.3
6	0.0-0.5	2395.0
7	54.0-54.5	2345.1
8	30.0-30.5	2029.6
9	34.0-34.5	1507.8
10	45.5-46.0	1394.2

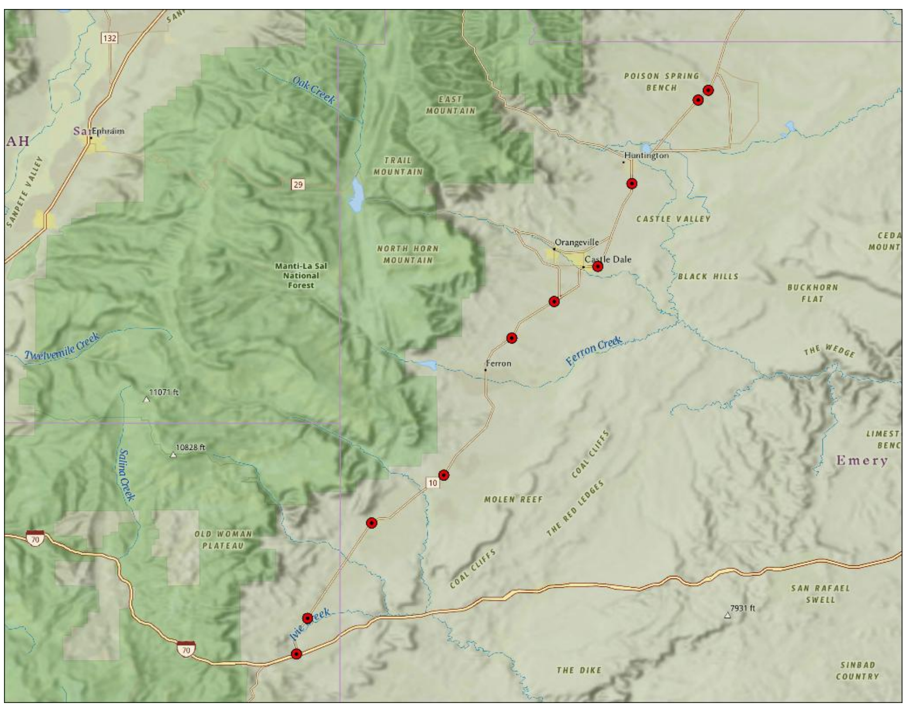

Figure 4.27: Hotspot Map for SR-10 Using Utah's Crash Cost

4.2.1.3 SR-12

Table 4.7: Hotspot Ranking for SR-12 Based on Utah's Crash Cost

Rank	Milepoints	Severity Rate
1	111.0-111.5	71921.5
2	40.5-41.0	45946.0
3	69.5-70.0	45071.6
4	113.0-113.5	33407.7
5	83.5-84.0	31928.6
6	109.0-109.5	27160.1
6	110.0-110.5	27160.1
8	84.5-85.0	15964.3
9	102.0-102.5	15512.0
10	122.0-122.5	15416.8

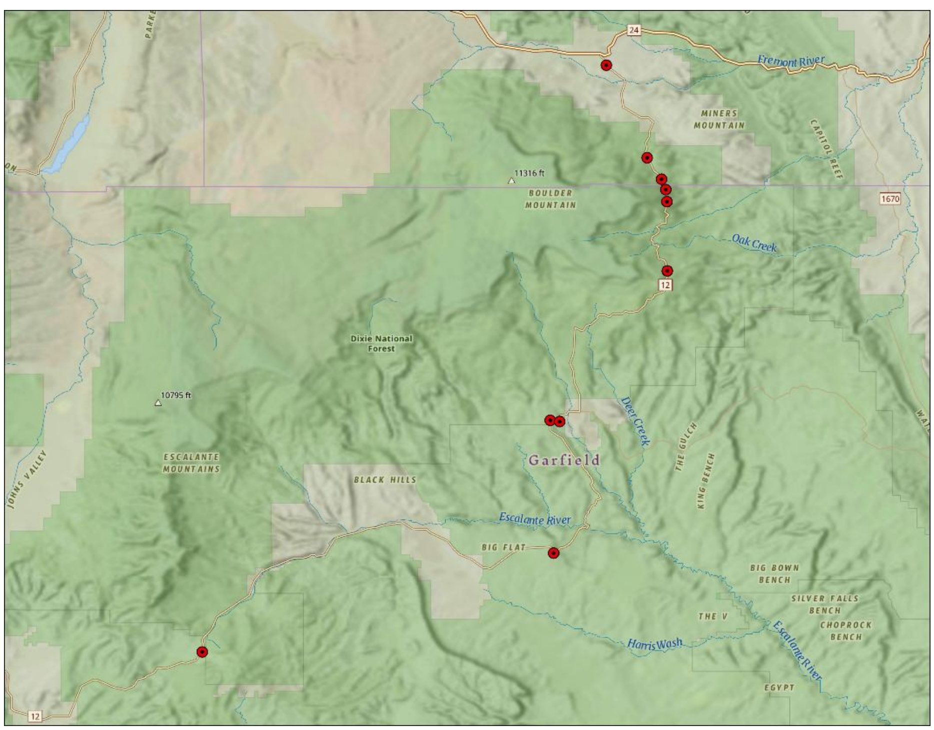

Figure 4.28: Hotspot Map for SR-12 Using Utah's Crash Cost

4.2.1.4 US-40

Table 4.8: Hotspot Ranking for US-40 Based on Utah's Crash Cost

Rank	**Milepoints**	**Severity Rate**
1	33.5-34.0	5709.6
2	32.5-33.0	5577.5
3	152.5-153.0	5407.1
4	56.0-56.5	5183.2
5	65.0-65.5	5103.6
6	164.0-164.5	5002.3
7	54.0-54.5	4719.0
8	29.5-30.0	4007.0
9	42.5-43.0	3964.7
10	40.0-40.5	3649.1

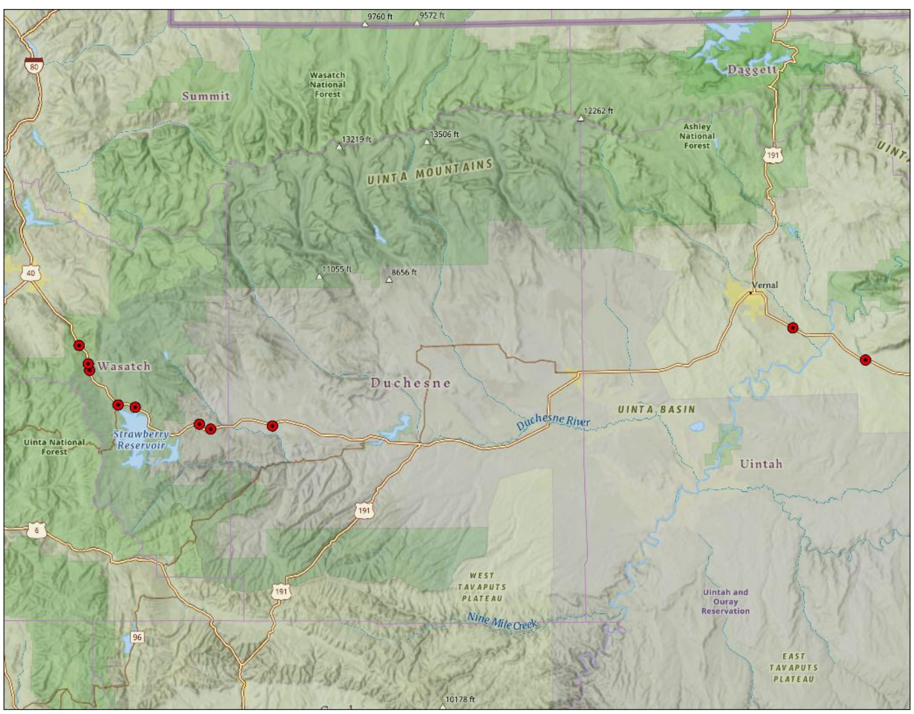

Figure 4.29: Hotspot Map for US-40 Using Utah's Crash Cost

4.2.1.5 SR-150

Table 4.9: Hotspot Ranking for SR-150 Based on Utah's Crash Cost

Rank	Milepoints	Severity Rate
1	33.0-33.5	60936.0
2	42.5-43.0	42765.6
3	44.5-45.0	39017.2
4	0.5-1.0	25120.7
5	27.0-27.5	16048.6
6	5.0-5.5	15285.7
7	15.0-15.5	14583.9
7	17.5-18.0	14583.9
9	14.5-15.0	11597.9
10	29.5-30.0	11188.3

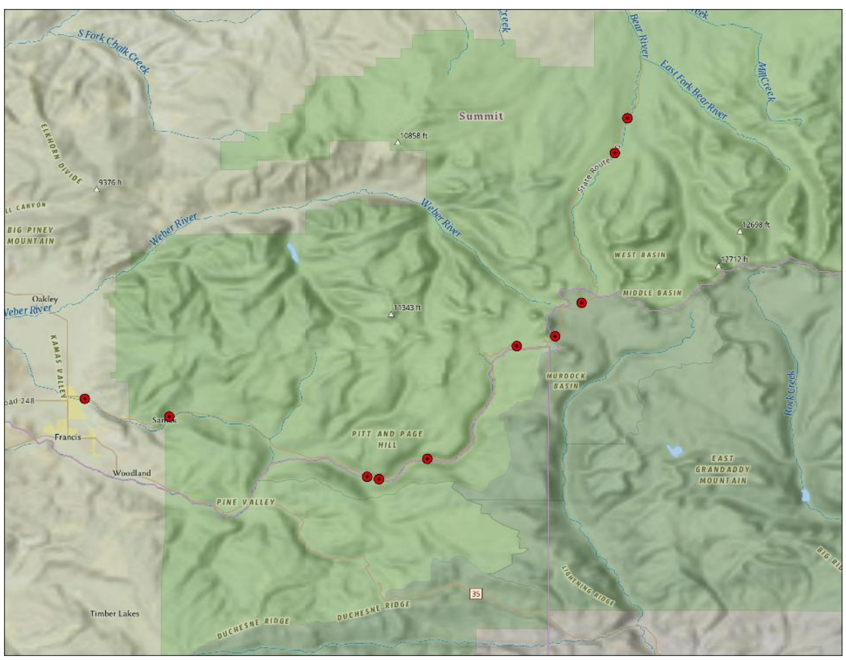

Figure 4.30: Hotspot Map for SR-150 Using Utah's Crash Cost

4.2.1.6 I-15

Table 4.10: Hotspot Ranking for I-15 Based on Utah's Crash Cost

Rank	Milepoints	Severity Rate
1	140.0-140.5	2004.7
2	185.0-185.5	1901.3
3	194.5-195.0	1790.2
4	394.0-394.5	1728.9
5	195.0-195.5	1716.3
6	198.5-199.0	1615.6
7	196.5-197.0	1558.5
8	142.5-143.0	1427.7
9	398.5-399.0	1345.1
10	182.0-182.5	1237.0

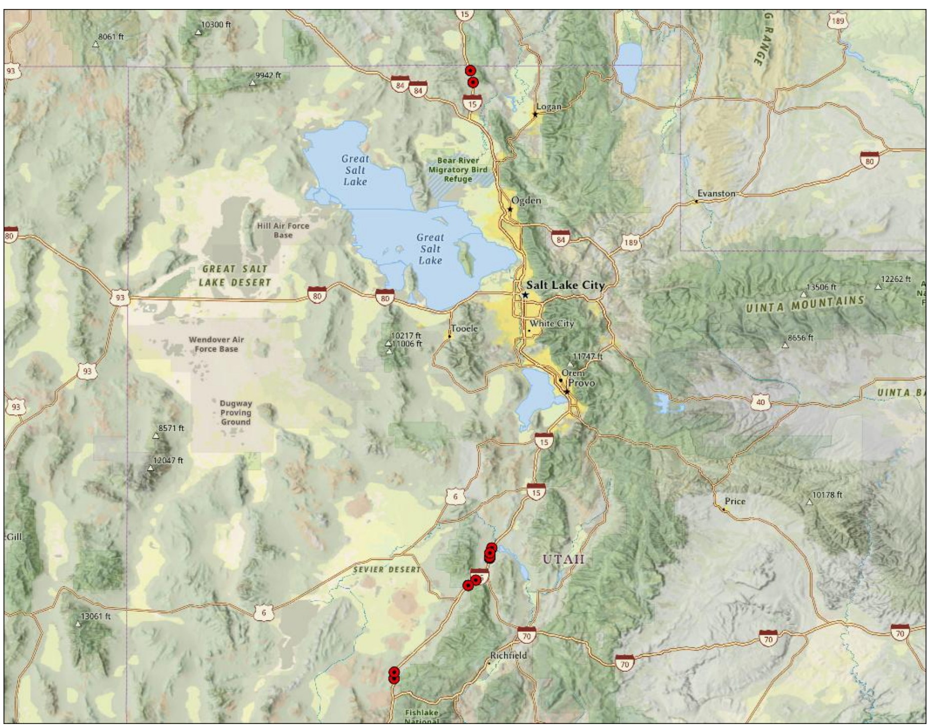

Figure 4.31: Hotspot Map for I-15 Using Utah's Crash Cost

4.2.1.7 I-80

Table 4.11: Hotspot Ranking for I-80 Based on Utah's Crash Cost

Rank	Milepoints	Severity Rate
1	47.0-47.5	3591.1
2	191.5-191.9	2693.1
3	34.5-35.0	2315.2
4	37.0-37.5	2209.8
5	28.5-29.0	2150.2
6	70.0-70.5	1948.2
7	82.0-82.5	1615.6
8	78.0-78.5	1558.5
9	167.5-168.0	1427.7
10	149.5-150.0	1345.1

Figure 4.32: Hotspot Map for I-80 Using Utah's Crash Cost

4.2.2 New South Wales Approach

4.2.2.1 US-6

Table 4.12: Hotspot Ranking for US-6 Based on New South Wales Approach

Rank	Milepoints	Severity Rate
1	26.5-27.0	905.5
2	143.0-143.5	892.5
3	27.0-27.5	635.8
4	143.5-144.0	513.7
5	25.5-26.0	510.6
6	32.5-33.0	472.0
7	54.0-54.5	463.1
7	52.0-52.5	463.1
9	77.0-77.5	430.8
10	69.5-70.0	387.7

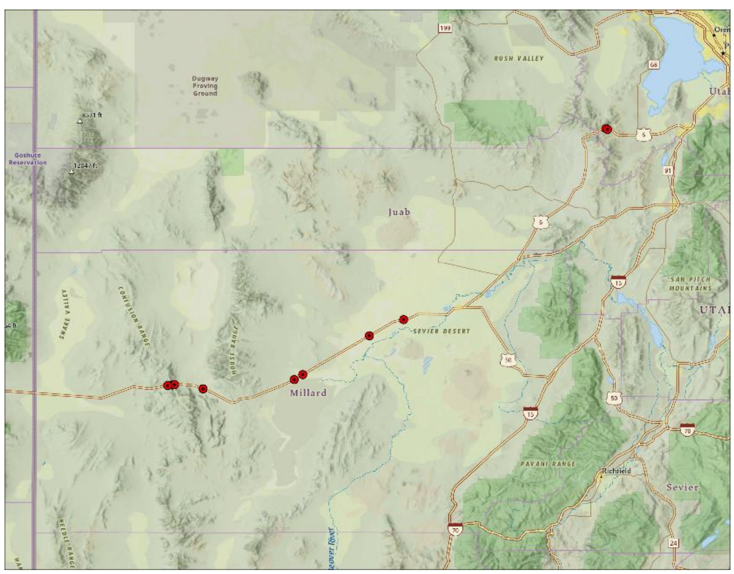

Figure 4.33: Hotspot Map for US-6 Using New South Wales Approach

4.2.2.2 SR-10

Table 4.13: Hotspot Ranking for SR-10 Based on New South Wales Approach

Rank	Milepoints	Severity Rate
1	54.5-55.0	165.9
2	54.0-54.5	86.7
3	10.5-11.0	67.2
4	11.0-11.5	61.6
5	38.5-39.0	58.0
6	50.5-51.0	56.2
7	55.0-55.5	51.5
8	53.0-53.5	46.7
9	16.0-16.5	46.1
10	50.0-50.5	43.9

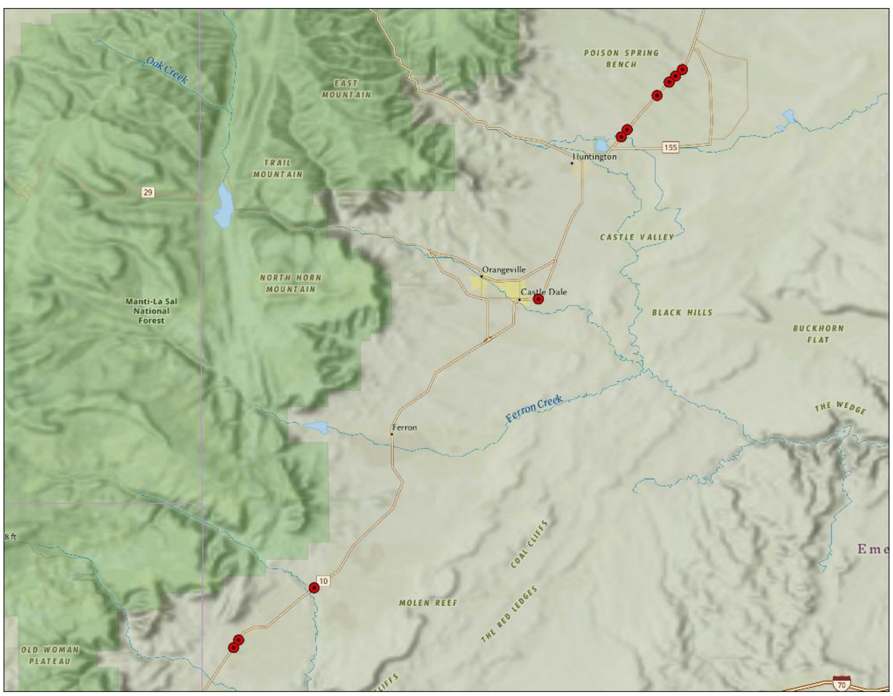

Figure 4.34: Hotspot Map for SR-10 Using New South Wales Approach

4.2.2.3 SR-12

Table 4.14: Hotspot Ranking for SR-12 Based on New South Wales Approach

Rank	Milepoints	Severity Rate
1	111.0-111.5	1196.3
2	40.5-41.0	525.2
3	71.0-71.5	472.4
4	69.5-70.0	433.0
5	111.5-112.0	379.3
6	83.5-84.0	334.6
7	102.0-102.5	311.3
8	105.5-106.0	294.9
9	113.5-114.0	291.8
10	113.0-113.5	262.6

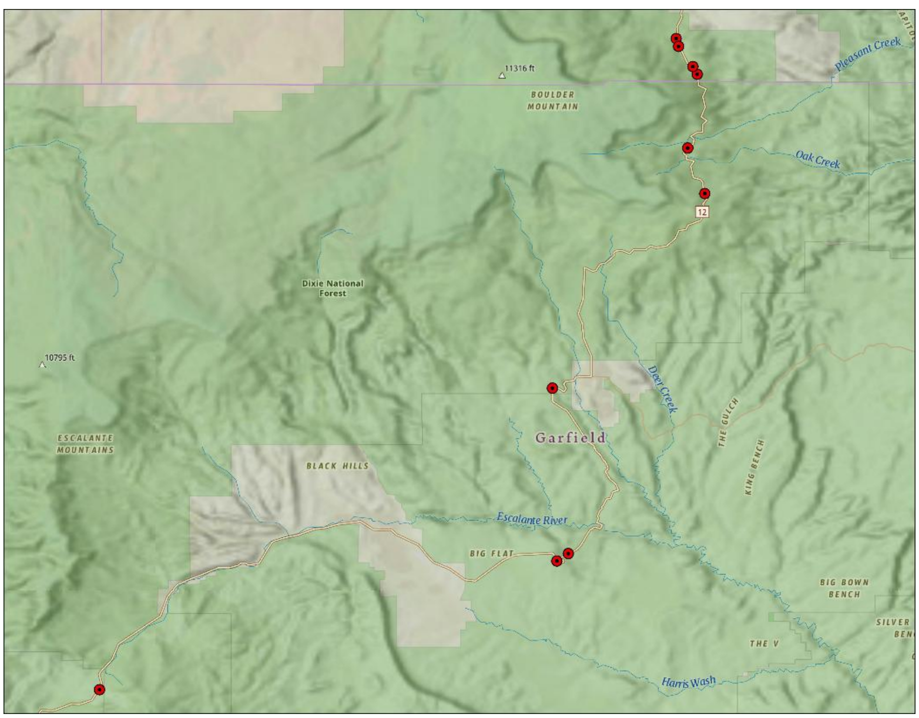

Figure 4.35: Hotspot Map for SR-12 Using New South Wales Approach

4.2.2.4 US-40

Table 4.15: Hotspot Ranking for US-40 Based on New South Wales Approach

Rank	Milepoints	Severity Rate
1	29.5-30.0	163.7
2	139.0-139.5	134.4
3	42.5-43.0	134.1
4	56.0-56.5	130.2
5	32.5-33.0	129.2
6	25.0-25.5	123.3
7	33.5-34.0	118.9
8	36.0-36.5	110.8
9	40.0-40.5	108.5
10	32.0-32.5	107.9

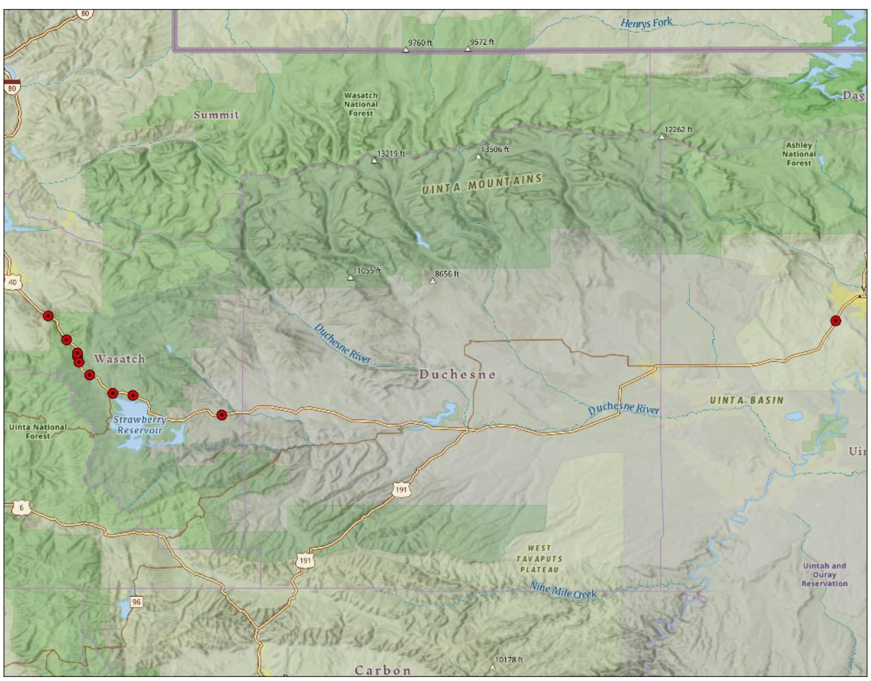

Figure 4.36: Hotspot Map for US-40 Using New South Wales Approach

4.2.2.5 SR-150

Table 4.16: Hotspot Ranking for SR-150 Based on New South Wales Approach

Rank	Milepoints	Severity Rate
1	44.0-44.5	562.3
2	42.5-43.0	528.2
3	33.0-33.5	479.0
4	0.5-1.0	477.6
5	33.5-34.0	443.0
6	27.0-27.5	420.3
7	5.0-5.5	328.5
8	44.5-45.0	306.7
9	5.5-6.0	247.8
10	40.0-40.5	221.5

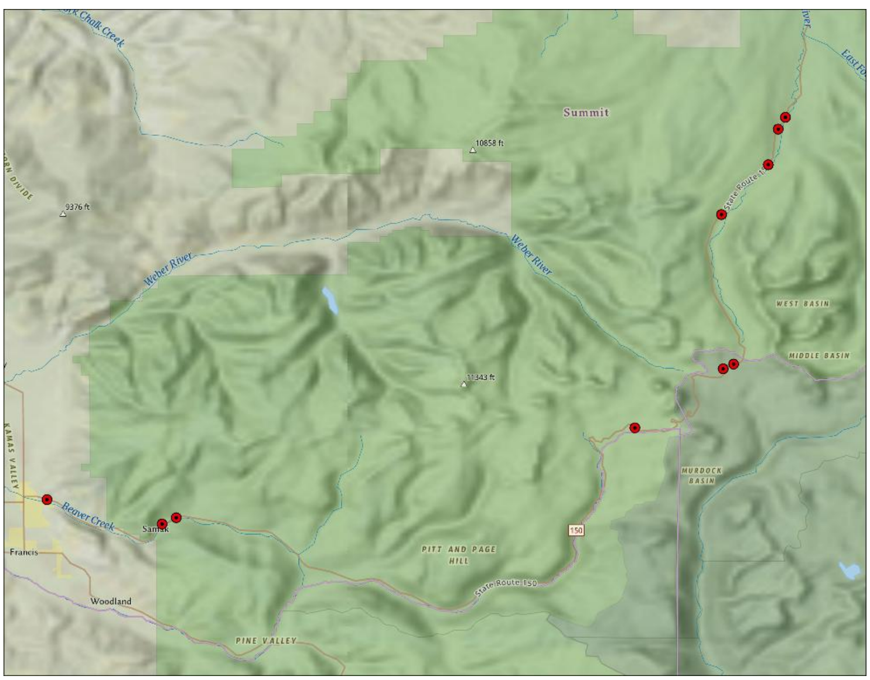

Figure 4.37: Hotspot Map for SR-150 Using New South Wales Approach

4.2.2.6 I-15

Table 4.17: Hotspot Ranking for I-15 Based on New South Wales Approach

Rank	Milepoints	Severity Rate
1	398.5-399.0	155.6
2	185.0-185.5	76.6
3	140.0-140.5	65.0
4	194.5-195.0	63.8
5	123.0-123.5	61.8
6	136.0-136.5	58.7
7	195.0-195.5	55.4
8	398.0-398.5	52.8
9	115.0-115.5	44.7
10	400.0-400.5	42.7

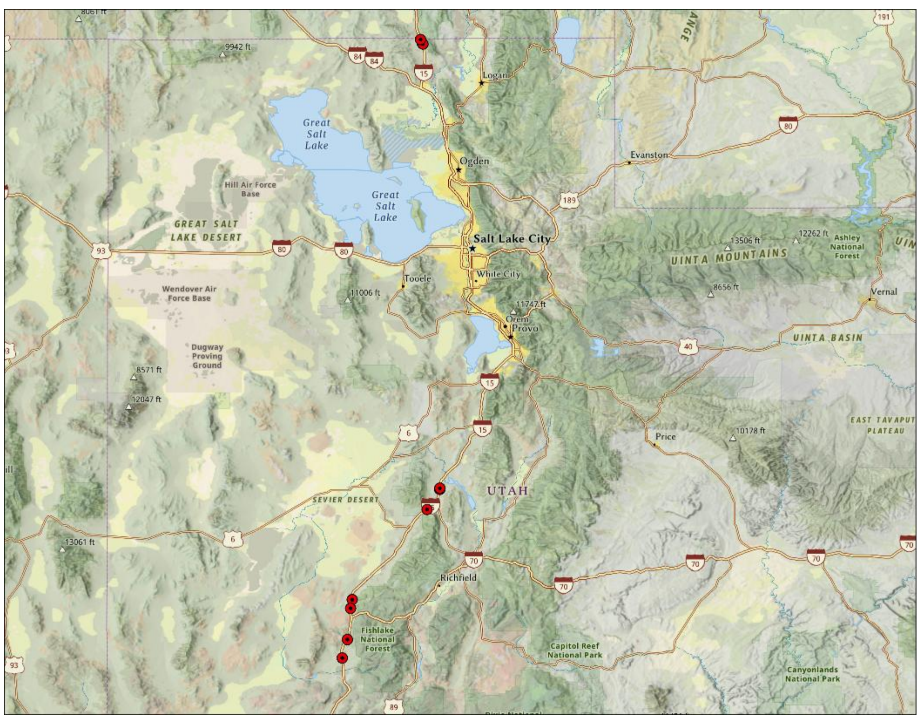

Figure 4.38: Hotspot Map for I-15 Using New South Wales Approach

4.2.2.7 I-80

Table 4.18: Hotspot Ranking for I-80 Based on New South Wales Approach

Rank	Milepoints	Severity Rate
1	191.5-191.9	116.5
2	47.0-47.5	83.3
3	34.5-35.0	53.6
4	150.0-150.5	53.4
5	149.5-150.0	53.2
6	60.0-60.5	49.7
7	88.0-88.5	43.7
8	167.0-167.5	42.0
9	43.0-43.5	41.4
10	82.0-82.5	38.8

Figure 4.39: Hotspot Map for I-80 Using New South Wales Approach

4.2.3 Comparison Between Utah’s Crash Cost and New South Wales Approach

The safety measures in this study are based on hotspots identified using Utah’s 2022 crash cost. However, the two approaches used are compared in this section to evaluate their similarity in terms of hotspot identification. The common hotspots identified along each route using both approaches are presented in Table 4.19.

Table 4.19: Common Hotspots Identified Using Utah's Crash Cost and New South Wales Approach

US-6	SR-10	SR-12	US-40	SR-150	I-15	I-80
26.5-27.0	38.5-39.0	111.0-111.5	33.5-34.0	33.0-33.5	140.0-140.5	47.0-47.5
52.0-52.5	55.0-55.5	40.5-41.0	32.5-33.0	42.5-43.0	185.0-185.5	191.5-191.9
54.0-54.5	54.0-54.5	69.5-70.0	56.0-56.5	44.5-45.0	194.5-195.0	34.5-35.0
77.0-77.5		113.0-113.5	29.5-30.0	0.5-1.0	195.0-195.5	149.5-150.0
25.5-26.0		83.5-84.0	42.5-43.0	27.0-27.5	398.5-399.0	82.0-82.5
143.5-144.0		102.0-102.5	40.0-40.5	5.0-5.5		
143.0-143.5						

The comparison of hotspot identification using Utah’s crash cost and the New South Wales’ approach reveals varying degrees of similarity across different routes. For US-6, there are seven common hotspots identified by both approaches. SR-10 shows three common hotspots, while the analyses for SR-12, US-40, and SR-150 identify six common hotspots each. I-15 and I-80 show five common hotspots. This comparison highlights the effectiveness of both approaches in identifying critical safety hotspots across different routes.

4.3 Safety Measures Recommendation

Following the process of hotspot identification, safety measures are recommended for the top ten locations identified along each route. This section details the safety measures recommended for hotspot locations.

4.3.1 US-6

4.3.1.1 Milepoint: 26.5-27.0

Figure 4.40: US-6 From Milepost 26.5-27.0

Description:

- AADT: 474
- Speed Limit: 35
- Total Crashes: 6 (Fatal:1, Suspected Serious Injury:1)
- Total Crashes Exceeded the Speed Limit: 6

Recommendations:

a. Speed limit signs and speed radars, since all crashes have exceeded the speed limit.
b. Clear zone improvement due to rigid obstacles on the side.
c. Safety barriers after clear zone improvements.
d. Chevrons for the curves.
e. HFST before the curve.

4.3.1.2 Milepoint: 52.0-52.5

Figure 4.41: US-6 From Milepost 52.0-52.5

Description:

- AADT: 424
- Speed Limit: 65
- Total Crashes: 2 (Fatal:1)
- Total Crashes Exceeded Speed Limit: 0

Recommendations

a. Cautionary signs indicating “Risk Ahead,” before entering the zone.
b. Increased width of pavement markings due to narrow shoulders.
c. Paved shoulder widening.

4.3.1.3 Milepoint: 54.0-54.5

Figure 4.42: US-6 From Milepost 54.0-54.5

<u>Description:</u>

- AADT: 424
- Speed Limit: 65
- Total Crashes: 2 (Fatal: 1)
- Total Crashes Exceeded the Speed Limit: 0

<u>Recommendations:</u>

a. Cautionary signs indicating "Risk Ahead," before entering the zone.
b. Increased width of pavement markings due to narrow shoulders.
c. Paved shoulder widening.

4.3.1.4 Milepoint: 77.0-77.5

Figure 4.43: US-6 From Milepost 77.0-77.5

Description:

- AADT: 424
- Speed Limit: 65
- Total Crashes: 2 (Fatal: 1)
- Total Crashes Exceeded the Speed Limit: 0

Recommendations:

a. Cautionary signs indicating "Risk Ahead," before entering the zone.
b. Increased width of pavement markings due to narrow shoulders.
c. Paved shoulder widening.

4.3.1.5 Milepoint: 56.5-57.0

Figure 4.44: US-6 From Milepost 56.5-57.0

Description:

- AADT: 424
- Speed Limit: 65
- Total Crashes: 1 (Suspected Serious Injury: 1)
- Total Crashes Exceeded the Speed Limit: 0

Recommendations:

a. Cautionary signs indicating “Risk Ahead,” before entering the zone.
b. Increased width of pavement markings due to narrow shoulders.
c. Paved shoulder widening.

4.3.1.6 Milepoint: 25.5-26.0

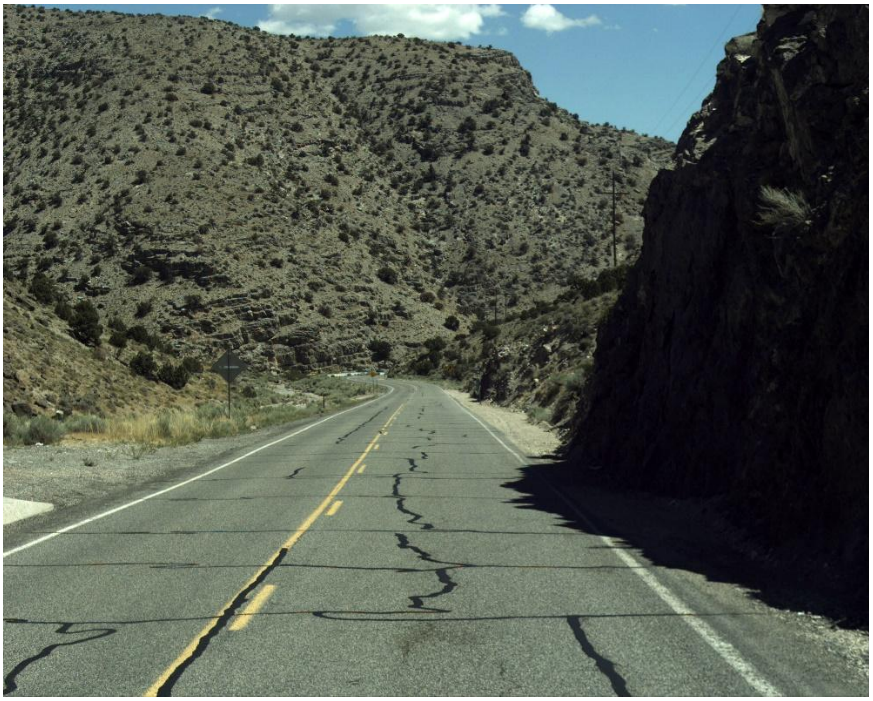

Figure 4.45: US-6 From Milepost 25.5-26.0

<u>Description</u>

- AADT: 474
- Speed Limit: 35
- Total Crashes: 3 (Fatal: 1)
- Total Crashes Exceeded the Speed Limit: 1

<u>Recommendations:</u>

a. Speed limit signs and speed radars, since some crashes have exceeded the speed limit.
b. Clear zone improvement due to rigid obstacles on the side.
c. Safety barriers after clear zone improvements.
d. Chevrons for the curves.
e. HFST before the curve.

4.3.1.7 Milepoint: 5.0-5.5

Figure 4.46: US-6 From Milepost 5.0-5.5

<u>Description</u>

- AADT: 474
- Speed Limit: 65
- Total Crashes: 2 (Suspected Serious Injury: 1)
- Total Crashes Exceeded the Speed Limit: 1

<u>Recommendations:</u>

a. Cautionary signs indicating “Risk Ahead,” before entering the zone.
b. Increased width of pavement markings due to narrow shoulders.
c. Paved shoulder widening.

4.3.1.8 Milepoint: 13.5-14.0

Figure 4.47: US-6 From Milepost 13.5-14.0

<u>Description</u>

- AADT: 474
- Speed Limit: 65
- Total Crashes: 1 (Suspected Serious Injury: 1)
- Total Crashes Exceeded the Speed Limit: 0

<u>Recommendations:</u>

a. Cautionary signs indicating "Risk Ahead," before entering the zone.
b. Increased width of pavement markings due to narrow shoulders.
c. Paved shoulder widening.

4.3.1.9 Milepoint: 143.5-144.0

Figure 4.48: US-6 From Milepost 143.5-144.0

<u>Description:</u>

- AADT: 1760
- Speed Limit: 60
- Total Crashes: 15 (Suspected Serious Injury: 3)
- Total Crashes Exceeded the Speed Limit: 2

<u>Recommendations:</u>

a. Speed limit signs and speed radars, since some crashes have exceeded the speed limit.
b. Clear zone improvement due to rigid obstacles on the side.
c. Safety barriers after clear zone improvements.
d. Chevrons for the curves.
e. HFST before the curve.
f. Increased width of pavement markings due to narrow shoulders and a high number of crashes.

4.3.1.10 Milepoint: 143.0-143.5

Figure 4.49: US-6 From Milepost 143.0-143.5

<u>Description:</u>

- AADT: 1760
- Speed Limit: 60
- Total Crashes: 28 (Suspected Serious Injury: 2)
- Total Crashes Exceeded the Speed Limit: 2

<u>Recommendations:</u>

a. Speed limit signs and speed radars, since some crashes have exceeded the speed limit.
b. Clear zone improvement due to rigid obstacles on the side.
c. Safety barriers after clear zone improvements.
d. Chevrons for the curves.
e. HFST before the curve.
f. Increased width of pavement markings due to narrow shoulders and a high number of crashes.

4.3.2 SR-10

4.3.2.1 Milepoint: 11.5-12.0

Figure 4.50: SR-10 From Milepost 11.5-12.0

Description:

- AADT: 2448
- Speed Limit: 65
- Total Crashes: 1 (Suspected Serious Injury: 1)
- Total Crashes Exceeded the Speed Limit: 1

Recommendations:

a. Speed limit signs and speed radars, since some crashes have exceeded the speed limit.
b. Safety barriers due to rigid obstacles on the side.
c. Chevrons for the curves.
d. HFST before the curve.

4.3.2.2 Milepoint: 38.5-39.0

Figure 4.51: SR-10 From Milepost 38.5-39.0

<u>Description:</u>

- AADT: 7878
- Speed Limit: 55
- Total Crashes: 7 (Suspected Serious Injury: 3)
- Total Crashes Exceeded the Speed Limit: 2

<u>Recommendations:</u>

a. Speed limit signs and speed radars, since some crashes have exceeded the speed limit.
b. Safety barriers due to unrecoverable slope.
c. Chevrons for the curves.
d. HFST before the curve.

4.3.2.3 Milepoint: 3.0-3.5

Figure 4.52: SR-10 From Milepost 3.0-3.5

Description:

- AADT: 4366
- Speed Limit: 65
- Total Crashes: 2 (Suspected Serious Injury: 1)
- Total Crashes Exceeded the Speed Limit: 0

Recommendations:

a. Clear zone improvement due to rigid obstacles on the side.
b. Cautionary signs indicating "Risk Ahead," before entering the zone.
c. Increased width of pavement markings due to narrow shoulders.
d. Paved shoulder widening.

4.3.2.4 Milepoint: 17.5-18.0

Figure 4.53: SR-10 From Milepost 17.5-18.0

Description:

- AADT: 4555
- Speed Limit: 65
- Total Crashes: 2 (Fatal Injury: 1)
- Total Crashes Exceeded the Speed Limit: 0

Recommendations:

a. Chevrons for the curves.
b. HFST before the curve.
c. Safety barriers due to unrecoverable slope.

4.3.2.5 Milepoint: 55.0-55.5

Figure 4.54: SR-10 From Milepost 55.0-55.5

<u>Description:</u>

- AADT: 4790
- Speed Limit: 65
- Total Crashes: 4 (Suspected serious injury: 1)
- Total Crashes Exceeded the Speed Limit: 2

<u>Recommendations:</u>

a. Speed limit signs and speed radars, since some crashes have exceeded the speed limit.
b. Chevrons for the curves.
c. HFST before the curve.

4.3.2.6 Milepoint: 0-0.5

Figure 4.55: SR-10 From Milepost 0-0.5

Description:

- AADT: 4366
- Speed Limit: 65
- Total Crashes: 1 (Suspected Serious Injury: 1)
- Total Crashes Exceeded the Speed Limit: 0

Recommendations:

a. Chevrons for the curves.
b. HFST before the curve.
c. Increased width of pavement markings due to narrow shoulders.
d. Paved shoulder widening due to narrow shoulders.

4.3.2.7 Milepoint: 54.0-54.5

Figure 4.56: SR-10 From Milepost 54.0-54.5

<u>Description:</u>

- AADT: 4790
- Speed Limit: 65
- Total Crashes: 8 (Suspected Serious Injury: 1)
- Total Crashes Exceeded the Speed Limit: 1

<u>Recommendations:</u>

a. Speed limit signs and speed radars, since some crashes have exceeded the speed limit.
b. Paved shoulder widening due to narrow shoulders.

4.3.2.8 Milepoint: 30.0-30.5

Figure 4.57: SR-10 From Milepost 30.0-30.5

<u>Description:</u>

- AADT: 6116
- Speed Limit: 65
- Total Crashes: 3 (Suspected Serious Injury: 1)
- Total Crashes Exceeded the Speed Limit: 0

<u>Recommendations:</u>

a. Safety barriers due to unrecoverable slope.
b. Increased width of pavement markings due to narrow shoulders.

4.3.2.9 Milepoint: 34.0-34.5

Figure 4.58: SR-10 From Milepost 34.0-34.5

<u>Description:</u>

- AADT: 6485
- Speed Limit: 65
- Total Crashes: 5 (Suspected Serious Injury: 1)
- Total Crashes Exceeded the Speed Limit: 0

<u>Recommendations:</u>

a. Cautionary signs indicating “Risk Ahead,” before entering the zone.

4.3.2.10 Milepoint: 45.5-46.0

Figure 4.59: SR-10 From Milepost 45.5-46.0

Description

- AADT: 7533
- Speed Limit: 65
- Total Crashes: 2 (Fatal Injury: 1)
- Total Crashes Exceeded the Speed Limit: 0

Recommendations:

a. Safety barriers due to unrecoverable slope.
b. Increased width of pavement markings due to paved narrow shoulders.

4.3.3 SR-12

4.3.3.1 Milepoint: 111.0-111.5

Figure 4.60: SR-12 From Milepost 111.0-111.5

Description:

- AADT: 313
- Speed Limit: 40
- Total Crashes: 6 (Suspected Serious Injury: 2)
- Total Crashes Exceeded the Speed Limit: 3

Recommendations:

a. Speed limit signs and speed radars, since some crashes have exceeded the speed limit.
b. Clear zone improvement due to rigid obstacles on the side.
c. Chevrons for the curves.
d. HFST before the curve.

4.3.3.2 Milepoint: 40.5-41.0

Figure 4.61: SR-12 From Milepost 40.5-41.0

<u>Description:</u>

- AADT: 965
- Speed Limit: 30
- Total Crashes: 7 (Suspected Serious Injury: 4)
- Total Crashes Exceeded the Speed Limit: 2

<u>Recommendations:</u>

a. Speed limit signs and speed radars, since some crashes have exceeded the speed limit.
b. Clear zone improvement due to rigid obstacles on the side.
c. Safety barriers after clear zone improvement.
d. Chevrons for the curves.
e. HFST before the curve.

4.3.3.3 Milepoint: 69.5-70.0

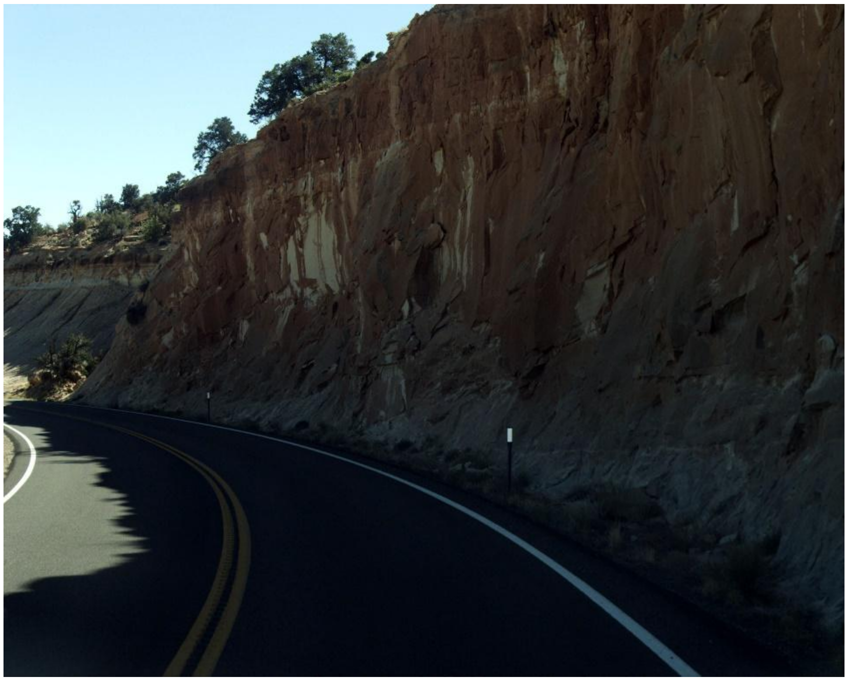

Figure 4.62: SR-12 From Milepost 69.5-70.0

Description:

- AADT: 696
- Speed Limit: 30
- Total Crashes: 3 (Fatal: 1, Suspected Serious Injury: 2)
- Total Crashes Exceeded the Speed Limit: 1

Recommendations:

a. Speed limit signs and speed radars, since some crashes have exceeded the speed limit.
b. Clear zone improvement due to rigid obstacles on the side.
c. Safety barriers after clear zone improvement.
d. Chevrons for the curves.
e. HFST before the curve.
f. Increased width of pavement markings due to paved narrow shoulders.

4.3.3.4 Milepoint: 113.0-113.5

Figure 4.63: SR-12 From Milepost 113.0-113.5

<u>Description:</u>

- AADT: 313
- Speed Limit: 40
- Total Crashes: 1 (Suspected Serious Injury: 1)
- Total Crashes Exceeded the Speed Limit: 0

<u>Recommendations:</u>

a. Clear zone improvement due to rigid obstacles on the roadside.
b. Safety barriers due to rigid obstacles on the roadside.
c. Chevrons for the curves.
d. HFST before the curve.

4.3.3.5 Milepoint: 83.5-84.0

Figure 4.64: SR-12 From Milepost 83.5-84

Description:

- AADT: 655
- Speed Limit: 35
- Total Crashes: 2 (Fatal: 1, Suspected Serious Injury: 1)
- Total Crashes Exceeded the Speed Limit: 2

Recommendations:

a. Speed limit signs and speed radars, since some crashes have exceeded the speed limit.
b. Clear zone improvement due to rigid obstacles on the roadside.
c. Safety barriers due to rigid obstacles on the roadside.
d. Chevrons for the curves.
e. HFST before the curve.

4.3.3.6 Milepoint: 109.0-109.5

Figure 4.65: SR-12 From Milepost 109-109.5

<u>Description:</u>

- AADT: 385
- Speed Limit: 40
- Total Crashes: 1 (Suspected Serious Injury: 1)
- Total Crashes Exceeded the Speed Limit: 1

<u>Recommendations:</u>

a. Speed limit signs and speed radars, since some crashes have exceeded the speed limit.
b. Clear zone improvement due to rigid obstacles on the roadside.
c. Safety barriers due to rigid obstacles on the roadside.
d. Increased width of pavement markings due to paved narrow shoulders.

4.3.3.7 Milepoint: 110.0-110.5

Figure 4.66: SR-12 From Milepost 110.0-110.5

Description:

- AADT: 385
- Speed Limit: 40
- Total Crashes: 1 (Suspected Serious Injury: 1)
- Total Crashes Exceeded the Speed Limit: 0

Recommendations:

a. Clear zone improvement due to rigid obstacles on the roadside.
b. Safety barriers due to rigid obstacles on the roadside.
c. Chevrons for the curves.
d. HFST before the curve.

4.3.3.8 Milepoint: 84.5-85.0

Figure 4.67: SR-12 From Milepost 84.5-85.0

<u>Description:</u>

- AADT: 655
- Speed Limit: 35
- Total Crashes: 1 (Suspected Serious Injury: 1)
- Total Crashes Exceeded the Speed Limit: 0

<u>Recommendations:</u>

a. Safety barriers due to unrecoverable slope.
b. Chevrons for the curves.
c. HFST before the curve.

4.3.3.9 Milepoint: 102.0-102.5

Figure 4.68: SR-12 From Milepost 102-102.5

<u>Description:</u>

- AADT: 836
- Speed Limit: 40
- Total Crashes: 4 (Suspected Serious Injury: 1)
- Total Crashes Exceeded the Speed Limit: 1

<u>Recommendations:</u>

a. Safety barriers due to unrecoverable slope.
b. Chevrons for the curves.
c. HFST before the curve.

4.3.3.10 Milepoint: 122.0-122.5

Figure 4.69: SR-12 From Milepost 122.0-122.5

<u>Description:</u>

- AADT: 776
- Speed Limit: 40
- Total Crashes: 3 (Suspected Serious Injury: 1)
- Total Crashes Exceeded the Speed Limit: 0

<u>Recommendations:</u>

a. Safety barriers due to unrecoverable slope.
b. HFST before the curve.

4.3.4 US-40

4.3.4.1 Milepoint: 33.5-34.0

Figure 4.70: US-40 From Milepost 33.5-34.0

Description:

- AADT: 6222
- Speed Limit: 60
- Total Crashes: 12 (Suspected Serious Injury: 3)
- Total Crashes Exceeded the Speed Limit: 1

Recommendations:

a. Speed limit signs and speed radars, since some crashes have exceeded the speed limit.
b. Improved pavement markings.
c. Chevrons for the curve.
d. HFST before the curve.

4.3.4.2 Milepoint: 32.5-33.0

Figure 4.71: US-40 From Milepost 32.5-33.0

<u>Description:</u>

- AADT: 6222
- Speed Limit: 60
- Total Crashes: 17 (Suspected Serious Injury: 3)
- Total Crashes Exceeded the Speed Limit: 6

<u>Recommendations:</u>

a. Speed limit signs and speed radars, since some crashes have exceeded the speed limit.
b. Improved pavement markings.
c. Chevrons for the curve.
d. HFST before the curve.

4.3.4.3 Milepoint: 152.5-153.0

Figure 4.72: US-40 From Milepost 152.5-153.0

Description:

- AADT: 4062
- Speed Limit: 65
- Total Crashes: 5 (Suspected Serious Injury: 2)
- Total Crashes Exceeded the Speed Limit: 0

Recommendations:

a. Cautionary signs indicating “Risk Ahead,” before entering the zone.
b. Increased width of pavement markings due to narrow shoulders.
c. Paved shoulder widening due to narrow shoulders.

4.3.4.4 Milepoint: 56.0-56.5

Figure 4.73: US-40 From Milepost 56.0-56.5

<u>Description:</u>

- AADT: 7083
- Speed Limit: 65
- Total Crashes: 13 (Suspected Serious Injury: 3)
- Total Crashes Exceeded the Speed Limit: 1

<u>Recommendations:</u>

a. Speed limit signs and speed radars, since some crashes have exceeded the speed limit.
b. Improved pavement markings.
c. Chevrons for the curve.
d. HFST before the curve.

4.3.4.5 Milepoint: 65.0-65.5

Figure 4.74: US-40 From Milepost 65.0-65.5

<u>Description:</u>

- AADT: 6764
- Speed Limit: 65
- Total Crashes: 10 (Suspected Serious Injury: 3)
- Total Crashes Exceeded the Speed Limit: 2

<u>Recommendations:</u>

a. Speed limit signs and speed radars, since some crashes have exceeded the speed limit.
b. Safety barriers due to rigid obstacles on the roadside.
c. HFST before the curve.
d. Increased width of pavement markings due to narrow shoulders.
e. Paved shoulder widening due to narrow shoulders.

4.3.4.6 Milepoint: 164.0-164.5

Figure 4.75: US-40 From Milepost 164-164.5

<u>Description:</u>

- AADT: 4199
- Speed Limit: 65
- Total Crashes: 4 (Fatal Injury: 1, Suspected Serious Injury: 1)
- Total Crashes Exceeded the Speed Limit: 0

<u>Recommendations:</u>

a. Cautionary signs indicating “Risk Ahead,” before entering the zone.

4.3.4.7 Milepoint: 54.0-54.5

Figure 4.76: US-40 From Milepost 54-54.5

<u>Description:</u>

- AADT: 7083
- Speed Limit: 55
- Total Crashes: 6 (Suspected Serious Injury: 3)
- Total Crashes Exceeded the Speed Limit: 3

<u>Recommendations:</u>

a. Speed limit signs and speed radars, since some crashes have exceeded the speed limit.
b. Safety barriers due to rigid obstacles on the roadside.
c. Chevrons for the curve.
d. HFST before the curve.

4.3.4.8 Milepoint: 29.5-30.0

Figure 4.77: US-40 From Milepost 29.5-30.0

Description:

- AADT: 6222
- Speed Limit: 60
- Total Crashes: 18 (Fatal Injury: 1, Suspected Serious Injury: 1)
- Total Crashes Exceeded the Speed Limit: 5

Recommendations:

a. Speed limit signs and speed radars, since some crashes have exceeded the speed limit.
b. Safety barriers due to rigid obstacles and unrecoverable slopes on the roadside.
c. Chevrons for the curve.
d. HFST before the curve.
e. Increased width of pavement markings due to a high number of crashes.

4.3.4.9 Milepoint: 42.5-43.0

Figure 4.78: US-40 From Milepost 42.5-43.0

Description:

- AADT: 7083
- Speed Limit: 65
- Total Crashes: 15 (Fatal Injury: 1, Suspected Serious Injury: 1)
- Total Crashes Exceeded the Speed Limit: 1

Recommendations:

a. Speed limit signs and speed radars, since some crashes have exceeded the speed limit.
b. Safety barriers due to unrecoverable slope on the roadside.
c. Chevrons for the curve.
d. HFST before the curve.
e. Increased width of pavement markings due to a high number of crashes.

4.3.4.10 Milepoint: 40.0-40.5

Figure 4.79: US-40 From Milepost 40.0-40.5

Description:

- AADT: 6394
- Speed Limit: 65
- Total Crashes: 13 (Suspected Serious Injury: 2)
- Total Crashes Exceeded the Speed Limit: 2

Recommendations:

a. Speed limit signs and speed radars, since some crashes have exceeded the speed limit.
b. Safety barriers due to unrecoverable slope on the roadside.
c. Chevrons for the curve.
d. HFST before the curve.
e. Increased width of pavement markings due to a high number of crashes.

4.3.5 SR-150

4.3.5.1 Milepoint: 33.0-33.5

Figure 4.80: SR-150 From Milepost 33.0-33.5

Description:

- AADT: 514
- Speed Limit: 55
- Total Crashes: 3 (Suspected Serious Injury: 3)
- Total Crashes Exceeded the Speed Limit: 0

Recommendations:

a. Clear zone improvements due to rigid obstacles on the roadside.
b. Safety barriers due to rigid obstacles on the roadside.
c. Chevrons for the curve.
d. HFST before the curve.

4.3.5.2 Milepoint: 42.5-43.0

Figure 4.81: SR-150 From Milepost 42.5-43.0

<u>Description:</u>

- AADT: 268
- Speed Limit: 55
- Total Crashes: 2 (Suspected Serious Injury: 1)
- Total Crashes Exceeded the Speed Limit: 0

<u>Recommendations:</u>

a. Clear zone improvements due to rigid obstacles on the roadside.
b. Safety barriers due to rigid obstacles on the roadside.
c. Paved shoulder widening due to narrow shoulders.
d. Increased width of pavement markings due to narrow shoulders.

4.3.5.3 Milepoint: 44.5-45.0

Figure 4.82: SR-150 From Milepost 44.5-45.0

Description:

- AADT: 268
- Speed Limit: 55
- Total Crashes: 1 (Suspected Serious Injury: 1)
- Total Crashes Exceeded the Speed Limit: 0

Recommendations:

a. Clear zone improvements due to rigid obstacles on the roadside.
b. Safety barriers due to rigid obstacles on the roadside.
c. Paved shoulder widening due to narrow shoulders.
d. Increased width of pavement markings due to narrow shoulders.

4.3.5.4 Milepoint: 0.5-1.0

Figure 4.83: SR-150 From Milepost 0.5-1.0

<u>Description:</u>

- AADT: 1396
- Speed Limit: 45
- Total Crashes: 11 (Suspected Serious Injury: 3)
- Total Crashes Exceeded the Speed Limit: 3

<u>Recommendations:</u>

a. Speed limit signs and speed radars, since some crashes have exceeded the speed limit.
b. Chevrons for the curve.
c. HFST before the curve.
d. Paved shoulder widening due to narrow shoulders.
e. Increased width of pavement markings due to narrow shoulders.

4.3.5.5 Milepoint: 27.0-27.5

Figure 4.84: SR-150 From Milepost 27-27.5

<u>Description:</u>

- AADT: 717
- Speed Limit: 55
- Total Crashes: 4 (Fatal Injury: 1)
- Total Crashes Exceeded the Speed Limit: 0

<u>Recommendations:</u>

a. Chevrons for the curve.
b. HFST before the curve.
c. Safety barriers due to unrecoverable slope.

4.3.5.6 Milepoint: 5.0-5.5

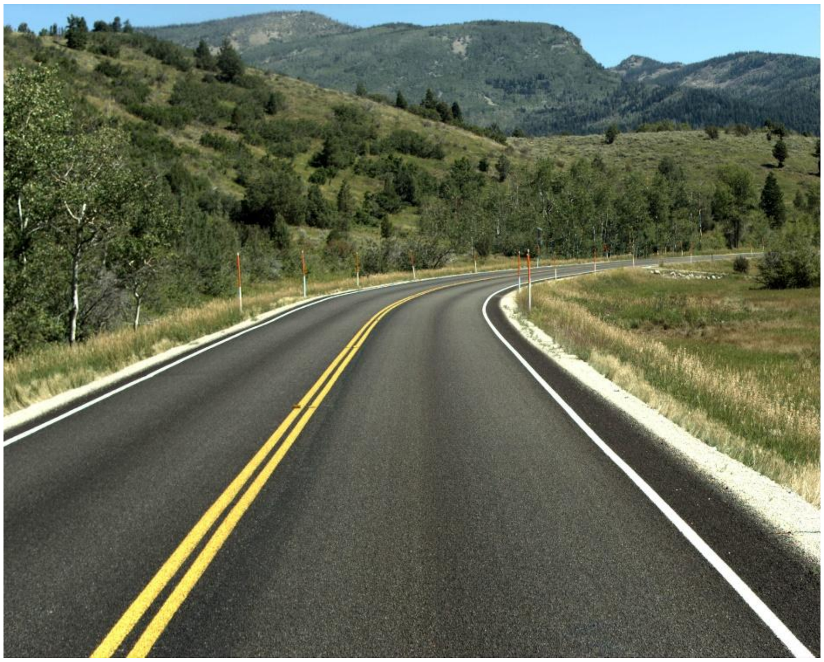

Figure 4.85: SR-150 From Milepost 5.0-5.5

<u>Description:</u>

- AADT: 1640
- Speed Limit: 55
- Total Crashes: 9 (Suspected Serious Injury: 2)
- Total Crashes Exceeded the Speed Limit: 4

<u>Recommendations:</u>

a. Speed limit signs and speed radars, since some crashes have exceeded the speed limit.
b. Chevrons for the curve.
c. HFST before the curve.
d. Paved shoulder widening due to narrow shoulders.
e. Increased width of pavement markings due to narrow shoulders.

4.3.5.7 Milepoint: 15.0-15.5

Figure 4.86: SR-150 From Milepost 15.0-15.5

<u>Description:</u>

- AADT: 717
- Speed Limit: 55
- Total Crashes: 1 (Suspected Serious Injury: 1)
- Total Crashes Exceeded the Speed Limit: 0

<u>Recommendations:</u>

a. Chevrons for the curve.
b. HFST before the curve.
c. Paved shoulder widening due to narrow shoulders.
d. Increased width of pavement markings due to narrow shoulders.

4.3.5.8 Milepoint: 17.5-18.0

Figure 4.87: SR-150 From Milepost 17.5-18.0

<u>Description:</u>

- AADT: 717
- Speed Limit: 55
- Total Crashes: 1 (Suspected Serious Injury: 1)
- Total Crashes Exceeded the Speed Limit: 0

<u>Recommendations:</u>

a. Clear zone improvement due to rigid obstacles on the roadside.
b. Chevrons for the curve.
c. HFST before the curve.
d. Paved shoulder widening due to narrow shoulders.
e. Increased width of pavement markings due to narrow shoulders.

4.3.5.9 Milepoint: 14.5-15.0

Figure 4.88: SR-150 From Milepost 14.5-15.0

<u>Description:</u>

- AADT: 901
- Speed Limit: 55
- Total Crashes: 1 (Suspected Serious Injury: 1)
- Total Crashes Exceeded the Speed Limit: 0

<u>Recommendations:</u>

a. Chevrons for the curve.
b. HFST before the curve.
c. Paved shoulder widening due to narrow shoulders.
d. Increased width of pavement markings due to narrow shoulders.

4.3.5.10 Milepoint: 29.5-30.0

Figure 4.89: SR-150 From Milepost 29.5-30

<u>Description:</u>

- AADT: 934
- Speed Limit: 55
- Total Crashes: 1 (Suspected Serious Injury: 1)
- Total Crashes Exceeded the Speed Limit: 0

<u>Recommendations:</u>

a. Chevrons for the curve.
b. HFST before the curve.
c. Safety barriers due to the unrecoverable slope.
d. Shoulder rumble strips.

4.3.6 I-15

4.3.6.1 Milepoint: 140.0-140.5

Figure 4.90: I-15 From Milepost 140.0-140.5

Description:

- AADT: 23028
- Speed Limit: 75
- Total Crashes: 26 (Fatal Injury: 2, Suspected Serious Injury: 2)
- Total Crashes Exceeded the Speed Limit: 6

Recommendations:

a. Speed limit signs and speed radars, since some crashes have exceeded the speed limit.
b. HFST before the curve.
c. Clear zone improvement due to rigid obstacles on the roadside.
d. Safety barriers due to rigid obstacles on the roadside.
e. Cautionary signs indicating “Risk Ahead” before entering the zone due to a high number of crashes.

4.3.6.2 Milepoint: 185.0-185.5

Figure 4.91: I-15 From Milepost 185-185.5

Description:

- AADT: 20102
- Speed Limit: 80
- Total Crashes: 28 (Fatal Injury: 1, Suspected Serious Injury: 2)
- Total Crashes Exceeded the Speed Limit: 0

Recommendations:

a. Chevrons for the curves.
b. HFST before the curve.
c. Cautionary signs indicating "Risk Ahead" before entering the zone due to a high number of crashes.

4.3.6.3 Milepoint: 194.5-195.0

Figure 4.92: I-15 From Milepost 194.5-195.0

<u>Description:</u>

- AADT: 13595
- Speed Limit: 80
- Total Crashes: 15 (Fatal Injury: 1, Suspected Serious Injury: 1)
- Total Crashes Exceeded the Speed Limit: 0

<u>Recommendations:</u>

a. Chevrons for the curves.
b. HFST before the curve.
c. Cautionary signs indicating "Risk Ahead" before entering the zone due to a high number of crashes.

4.3.6.4 Milepoint: 394.0-394.5

Figure 4.93: I-15 From Milepost 394.0-394.5

Description:

- AADT: 12968
- Speed Limit: 80
- Total Crashes: 4 (Fatal Injury: 1, Suspected Serious Injury: 1)
- Total Crashes Exceeded the Speed Limit: 1

Recommendations:

a. Speed limit signs and speed radars, since some crashes have exceeded the speed limit.
b. Safety barriers due to unrecoverable slope on the roadside.

4.3.6.5 Milepoint: 195.0-195.5

Figure 4.94: I-15 From Milepost 195.0-195.5

<u>Description:</u>

- AADT: 13595
- Speed Limit: 80
- Total Crashes: 14 (Suspected Serious Injury: 2)
- Total Crashes Exceeded the Speed Limit: 1

<u>Recommendations:</u>

a. Speed limit signs and speed radars, since some crashes have exceeded the speed limit.
b. Cautionary signs indicating “Risk Ahead” before entering the zone due to a high number of crashes.

4.3.6.6 Milepoint: 198.5-199.0

Figure 4.95: I-15 From Milepost 198.5-199.0

<u>Description:</u>

- AADT: 13595
- Speed Limit: 80
- Total Crashes: 4 (Suspected Serious Injury: 2)
- Total Crashes Exceeded the Speed Limit: 1

<u>Recommendations:</u>

a. Speed limit signs and speed radars, since some crashes have exceeded the speed limit.
b. Cautionary signs indicating "Risk Ahead" before entering the zone.

4.3.6.7 Milepoint: 196.5-197.0

Figure 4.96: I-15 From Milepost 196.5-197.0

<u>Description:</u>

- AADT: 13595
- Speed Limit: 80
- Total Crashes: 8 (Suspected Serious Injury: 2)
- Total Crashes Exceeded the Speed Limit: 1

<u>Recommendations:</u>

a. Speed limit signs and speed radars, since some crashes have exceeded the speed limit.
b. Cautionary signs indicating "Risk Ahead" before entering the zone.

4.3.6.8 Milepoint: 142.5-143.0

Figure 4.97: I-15 From Milepost 142.5-143.0

<u>Description:</u>

- AADT:23028
- Speed Limit: 80
- Total Crashes: 5 (Fatal Injury: 2, Suspected Serious Injury: 1)
- Total Crashes Exceeded the Speed Limit: 2

<u>Recommendations:</u>

a. Speed limit signs and speed radars, since some crashes have exceeded the speed limit.
b. Chevrons for the curve.
c. HFST before the curve.
d. Clear zone improvement due to rigid obstacles on the roadside.
e. Safety barriers due to rigid obstacles on the roadside.

4.3.6.9 Milepoint: 398.5-399.0

Figure 4.98: I-15 From Milepost 398.5-399.0

Description:

- AADT: 12968
- Speed Limit: 80
- Total Crashes: 41 (Suspected Serious Injury: 1)
- Total Crashes Exceeded the Speed Limit: 0

Recommendations:

a. Chevrons for the curve.
b. HFST before the curve.
c. Safety barriers due to unrecoverable slope on the roadside.

4.3.6.10 Milepoint: 182.0-182.5

Figure 4.99: I-15 From Milepost 182.0-182.5

Description:

- AADT: 18605
- Speed Limit: 80
- Total Crashes: 7 (Suspected Serious Injury: 2)
- Total Crashes Exceeded the Speed Limit: 0

Recommendations:

a. Cautionary signs indicating "Risk Ahead" before entering the zone.

4.3.7 I-80

4.3.7.1 Milepoint: 47.0-47.5

Figure 4.100: I-80 From Milepost 47.0-47.5

Description:

- AADT: 9918
- Speed Limit: 80
- Total Crashes: 13 (Fatal Injury: 1, Suspected Serious Injury: 2)
- Total Crashes Exceeded the Speed Limit: 2

Recommendations:

a. Speed limit signs and speed radars, since some crashes have exceeded the speed limit.
b. Chevrons for the curves.
c. HFST before the curve.
d. Cautionary signs indicating "Risk Ahead" before entering the zone due to a high number of crashes.

4.3.7.2 Milepoint: 191.5-191.9

Figure 4.101: I-80 From Milepost 191.5-191.9

<u>Description:</u>

- AADT: 17218
- Speed Limit: 80
- Total Crashes: 32 (Suspected Serious Injury: 3)
- Total Crashes Exceeded the Speed Limit: 0

<u>Recommendations:</u>

a. Chevrons for the curves.
b. HFST before the curve.
c. Cautionary signs indicating "Risk Ahead" before entering the zone due to a high number of crashes.

4.3.7.3 Milepoint: 34.5-35.0

Figure 4.102: I-80 From Milepost 34.5-35.0

Description:

- AADT: 9960
- Speed Limit: 80
- Total Crashes: 8 (Fatal Injury: 1, Suspected Serious Injury: 1)
- Total Crashes Exceeded the Speed Limit: 1

Recommendations:

a. Speed limit signs and speed radars, since some crashes have exceeded the speed limit.
b. Safety barriers due to unrecoverable slope.

4.3.7.4 Milepoint: 37.0-37.5

Figure 4.103: I-80 From Milepost 37.0-37.5

<u>Description:</u>

- AADT: 23028
- Speed Limit: 80
- Total Crashes: 5 (Fatal Injury: 1, Suspected Serious Injury: 1)
- Total Crashes Exceeded the Speed Limit: 0

<u>Recommendations:</u>

a. Safety barriers due to unrecoverable slope and fatal crashes.

4.3.7.5 Milepoint: 28.5-29.0

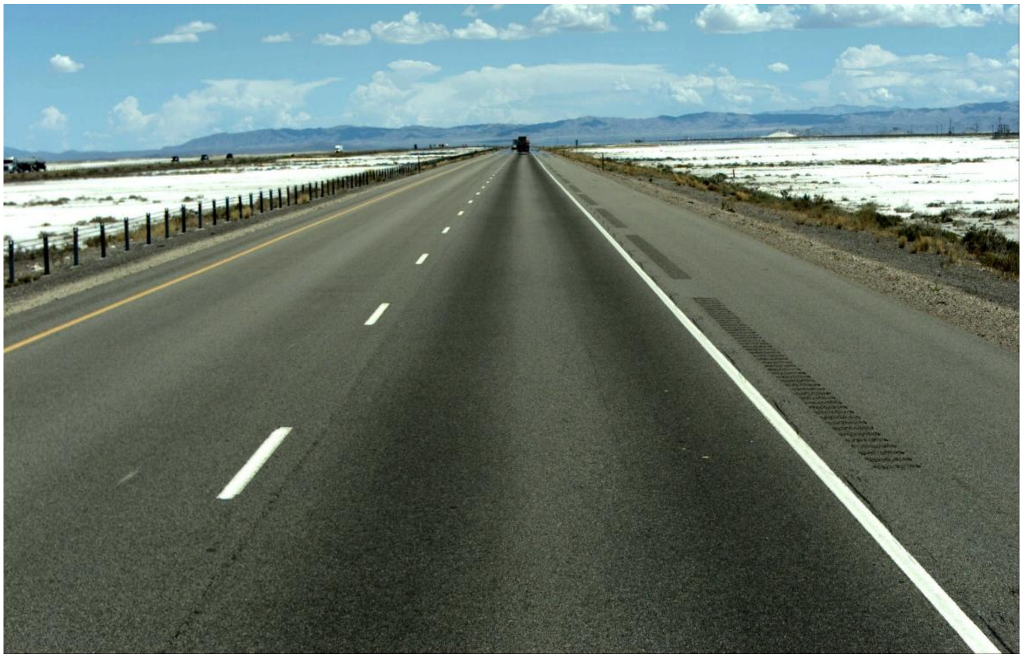

Figure 4.104: I-80 From Milepost 28.5-29.0

<u>Description:</u>

- AADT: 9960
- Speed Limit: 80
- Total Crashes: 3 (Fatal Injury: 2)
- Total Crashes Exceeded the Speed Limit: 0

<u>Recommendations:</u>

a. Safety barriers due to unrecoverable slope and fatal crashes.

4.3.7.6 Milepoint: 70.0-70.5

Figure 4.105: I-80 From Milepost 70.0-70.5

<u>Description:</u>

- AADT: 11063
- Speed Limit: 80
- Total Crashes: 6 (Fatal Injury: 1, Suspected Serious Injury: 1)
- Total Crashes Exceeded the Speed Limit: 1

<u>Recommendations:</u>

a. Speed limit signs and speed radars, since some crashes have exceeded the speed limit.
b. Chevrons for the curves.
c. HFST before the curve.

4.3.7.7 Milepoint: 82.0-82.5

Figure 4.106: I-80 From Milepost 82.0-82.5

<u>Description:</u>

- AADT: 13063
- Speed Limit: 80
- Total Crashes: 8 (Fatal Injury: 1, Suspected Serious Injury: 1)
- Total Crashes Exceeded the Speed Limit: 2

<u>Recommendations:</u>

a. Speed limit signs and speed radars, since some crashes have exceeded the speed limit.
b. Chevrons for the curves.
c. HFST before the curve.

4.3.7.8 Milepoint: 78.0-78.5

Figure 4.107: I-80 From Milepost 78.0-78.5

Description:

- AADT: 13063
- Speed Limit: 80
- Total Crashes: 4 (Fatal Injury: 1, Suspected Serious Injury: 1)
- Total Crashes Exceeded the Speed Limit: 0

Recommendations:

a. Safety barriers due to unrecoverable slope.
b. Chevrons for the curves.
c. HFST before the curve.

4.3.7.9 Milepoint: 167.5-168.0

Figure 4.108: I-80 From Milepost 167.5-168

<u>Description:</u>

- AADT: 17485
- Speed Limit: 70
- Total Crashes: 10 (Suspected Serious Injury: 2)
- Total Crashes Exceeded the Speed Limit: 1

<u>Recommendations:</u>

a. Speed limit signs and speed radars, since some crashes have exceeded the speed limit.
b. HFST before the curve.
c. Cautionary signs indicating “Risk Ahead” before entering the zone due to a high number of crashes.

4.3.7.10 Milepoint: 149.5-150.0

Figure 4.109: I-80 From Milepost 149.5-150.0

<u>Description:</u>

- AADT: 18719
- Speed Limit: 65
- Total Crashes: 19 (Suspected Serious Injury: 2)
- Total Crashes Exceeded the Speed Limit: 2

<u>Recommendations:</u>

a. Speed limit signs and speed radars, since some crashes have exceeded the speed limit.
b. Chevrons for the curve.
c. HFST before the curve.
d. Cautionary signs indicating “Risk Ahead” before entering the zone due to a high number of crashes.

4.4 Model Evaluation on Pathway Images

After transferring labels and relabeling images from Pathway to scale the analysis for future inclusion of other routes, the performance of the computer vision model for classifying four roadside features is evaluated. The results of this evaluation are presented below.

4.4.1 Clear Zone

For the clear zone width classification, the computer vision model trained on the Pathway images exhibited an accuracy of 83.8%. The confusion matrix illustrating the performance of this model is shown in Figure 4.110.

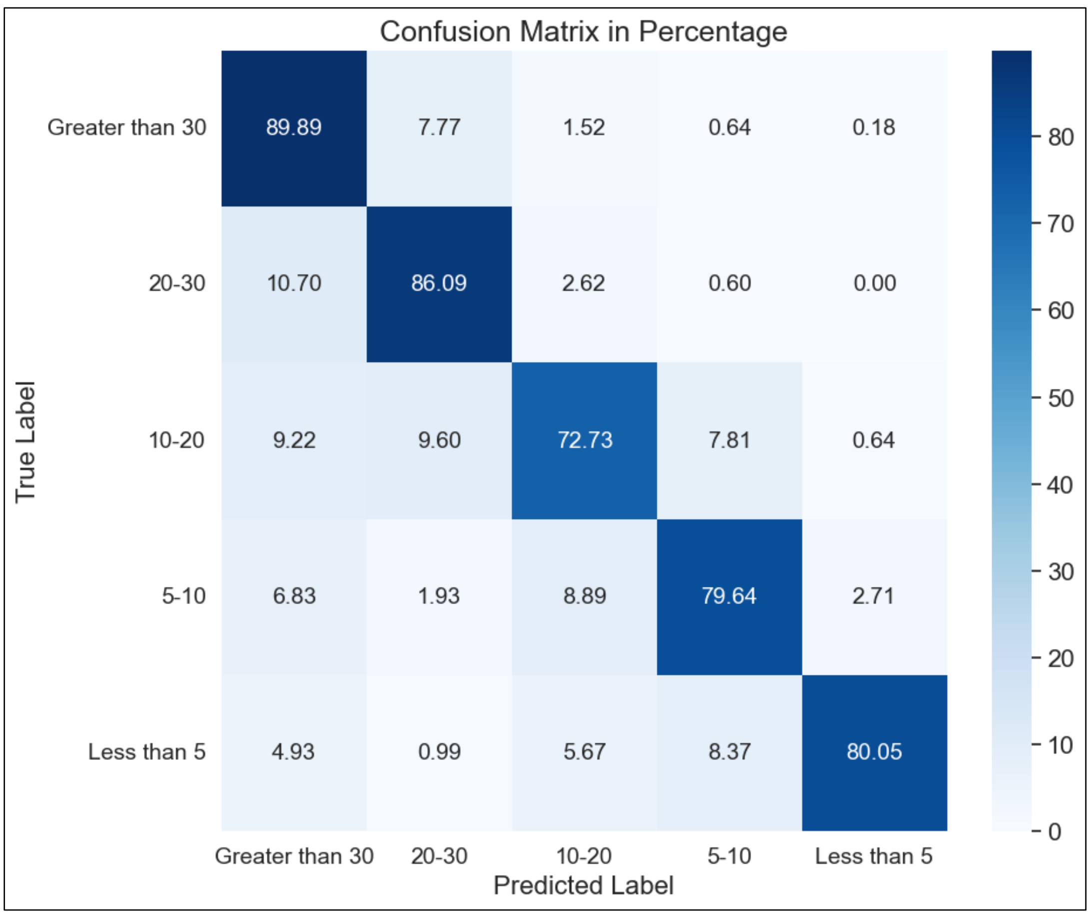

Figure 4.110: Confusion Matrix for Clear Zone Width Classification

4.4.2 Rigid Obstacles

The computer vision model demonstrated an accuracy of 86.1% in classifying rigid obstacles. The confusion matrix displaying the model's performance is presented in Figure 4.111.

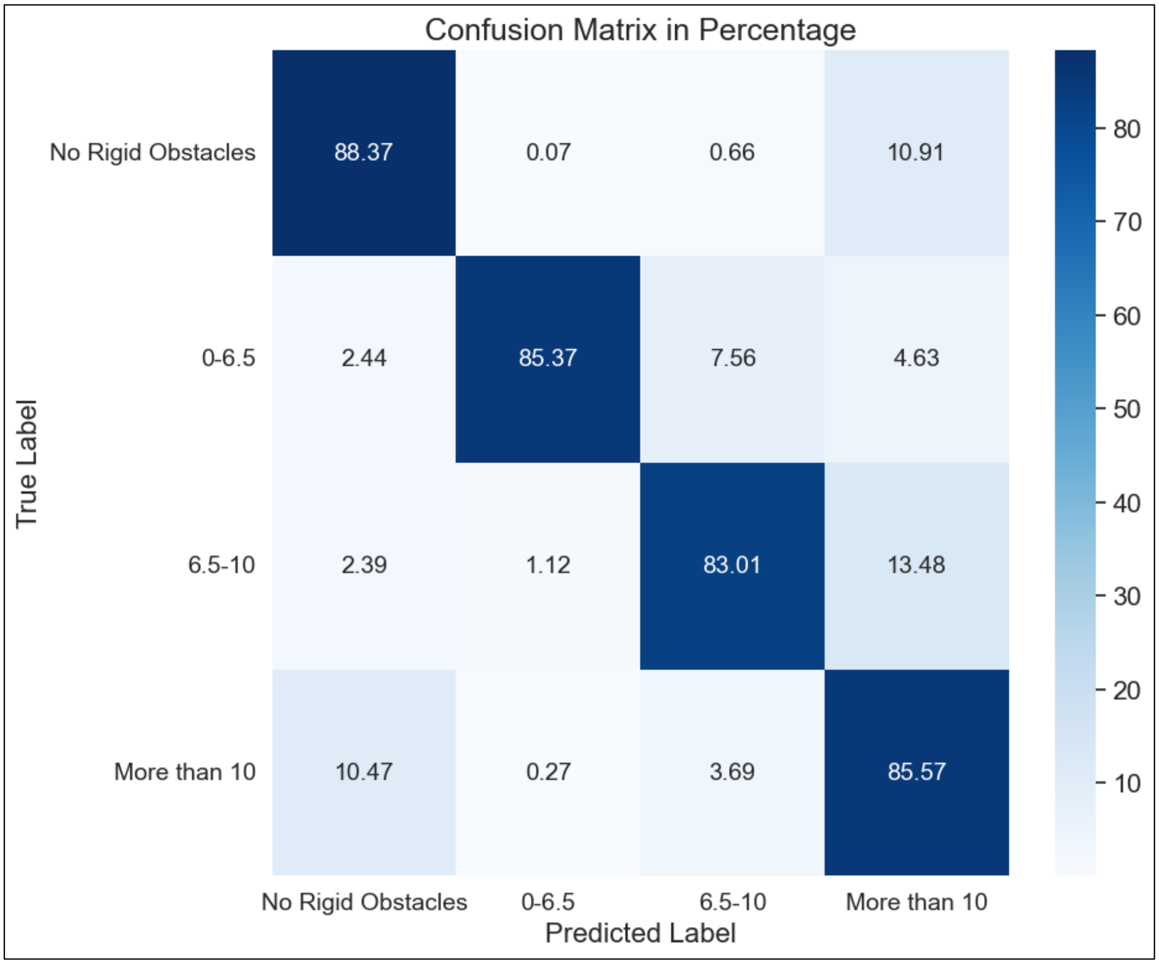

Figure 4.111: Confusion Matrix for Rigid Obstacle Distance Classification

4.4.3 Side Slope

The accuracy of the computer vision model for classifying side slopes was 83.9%. The performance of this model is depicted in the confusion matrix shown in Figure 4.112.

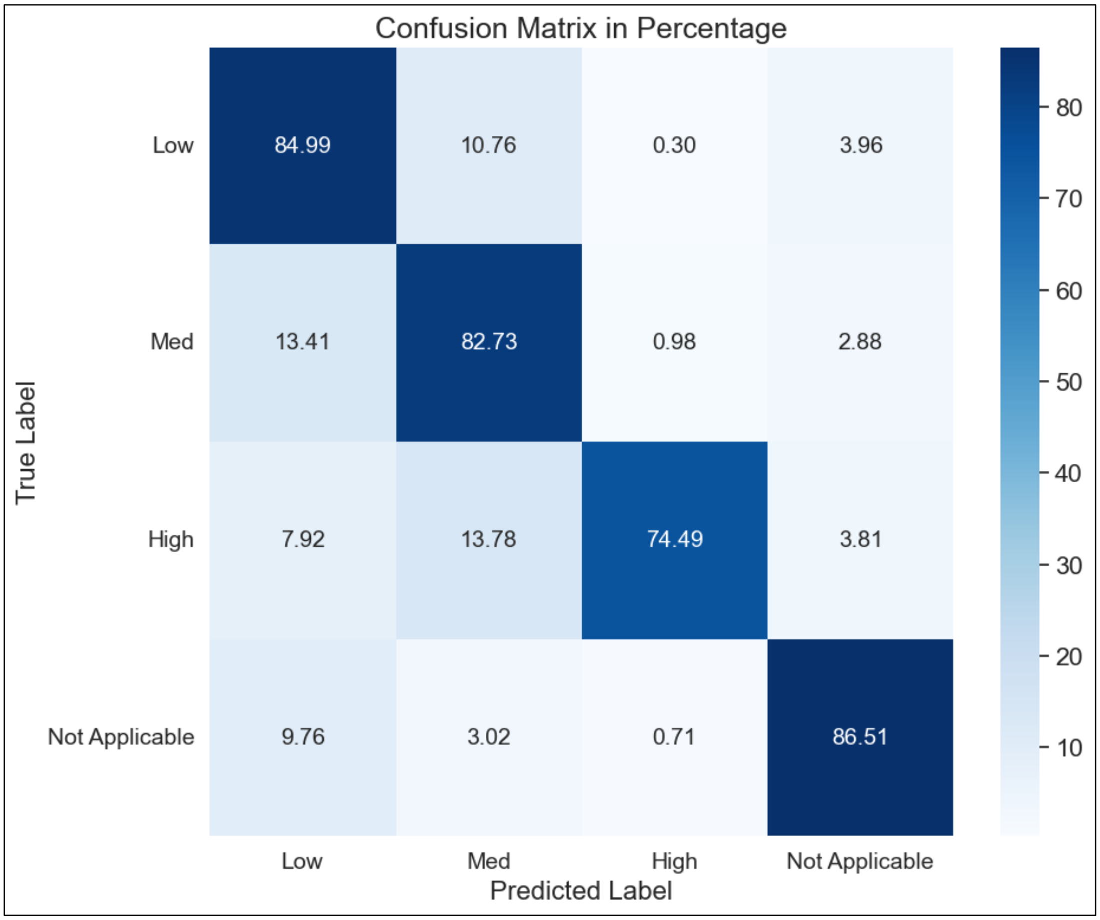

Figure 4.112: Confusion Matrix for Side Slope Classification

4.4.4 Safety Barriers

The computer vision model achieved an accuracy of 97.9% in classifying safety barriers. The confusion matrix showing the model's performance is presented in Figure 4.113.

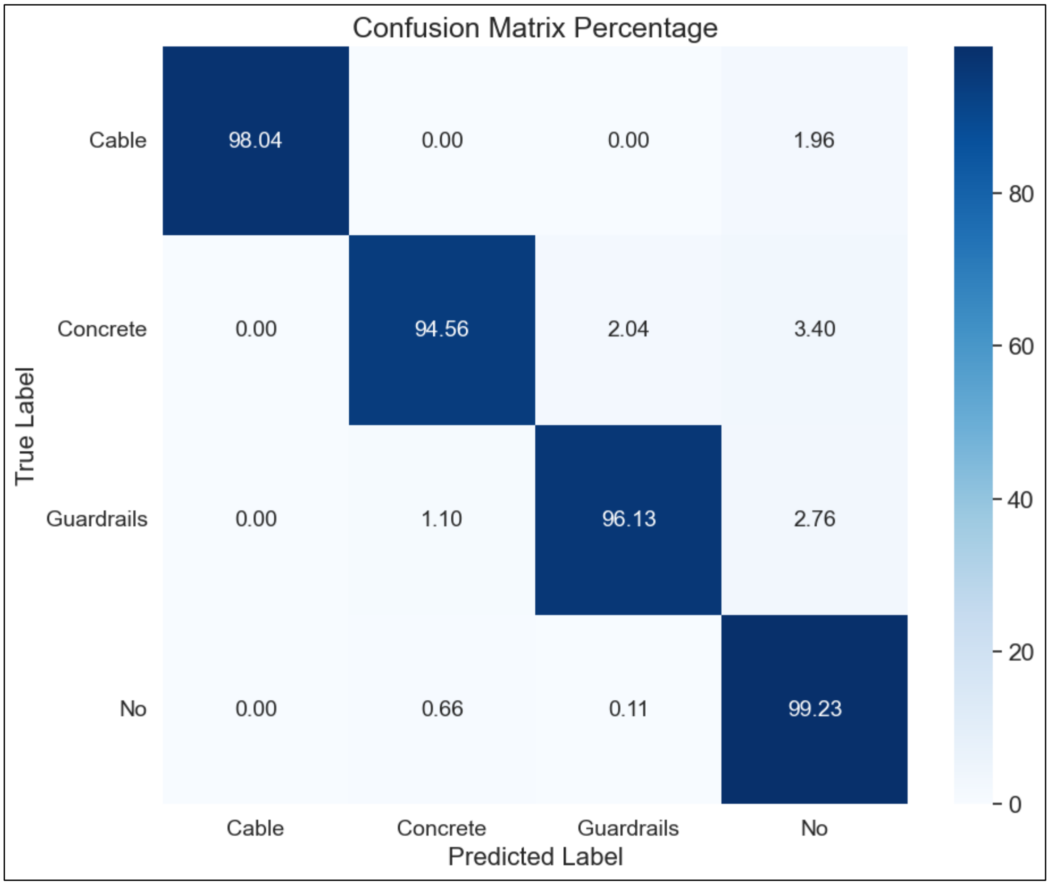

Figure 4.113: Confusion Matrix for Safety Barriers Classification

4.5 Summary

We examined rural RD crash patterns across non-interstate and interstate roads. For both non-interstate and interstate roads, significant relationships emerged between roadside features, safety ratings, and crash and severity rates, with narrower clear zones, closer rigid obstacles, steeper side slopes, and higher safety ratings associated with increased crash risk. The findings emphasize the critical role of clear zones, side slopes, rigid obstacles, and safety barriers in rural RD crashes. The computer vision model achieved high classification accuracies in identifying these roadside features, contributing to a reliable analysis. Prioritized hotspots along each route were identified, paving the way for targeted safety recommendations to mitigate crash severity and frequency.

5.0 CONCLUSIONS

5.1 Summary

This project aims to assist UDOT in identifying hazardous locations on Utah highways and prioritizing safety improvement projects. The study utilizes the computer vision model developed from UDOT's project, Automated Safety Assessment of Rural Roadways using Computer Vision (Mashhadi et al., 2023), to extract roadside features from images. Initially, the model was trained on images collected by Mandli, UDOT's asset collection contractor, covering five rural roads in Utah (US-6, SR-10, SR-12, US-40, and SR-150). To extend the analysis to two additional roads (I-15 and I-80), the model was retrained using images collected by Pathway, UDOT's new data collection contractor. Labels from the Mandli images for the initial five routes were transferred to Pathway images, and additional images from these routes and the new routes were labeled. The retrained model was then used to extract roadside information for all seven routes. The model achieved notable classification accuracies: 83.8% for clear zones, 86.1% for rigid obstacles, 83.9% for side slopes, and 97.9% for safety barriers, demonstrating the effectiveness of computer vision techniques in providing a scalable and efficient approach to safety assessments.

The roadside feature data extracted by the computer vision model was then integrated with crash data provided by UDOT. This combined dataset was used to analyze the impact of four key roadside features—clear zones, rigid obstacles, side slopes, and safety barriers—on rural RD crashes. The analysis was conducted across three distinct categories: non-interstate roads (US-6, SR-10, SR-12, US-40, and SR-150), interstate roads (I-15 and I-80), and a combined dataset of both interstate and non-interstate roads. The analysis focused exclusively on rural road segments, with urban areas excluded.

The research revealed significant relationships between roadside features and crash severity. On non-interstate roads, narrower clear zones were strongly associated with higher rates of severe and fatal injuries. This trend persisted when analyzing both road types together, where narrower clear zones were consistently linked to an increase in severe injury rate. The proximity of rigid obstacles was found to increase the rate of severe injuries on non-interstate roads. On interstate roads, close proximity to rigid obstacles was associated with a higher risk of both severe and fatal injuries, indicating that greater distance from these obstacles may reduce crash severity across both road types. When both roads were combined, the distance from rigid obstacles was found to be associated with severe injury rate. The steepness of side slopes emerged as a critical factor influencing crash severity across all road types. On non-interstate roads, steeper side slopes were associated with higher crash rate, severe injury rate, and fatal injury rate. A similar trend was observed on interstate roads, where steep side slopes correlated with increased severe and fatal injury rates. This trend remained consistent when both road types were combined, reinforcing the significant impact of side slope steepness on crash severity. Higher safety ratings, which indicate worsening road conditions, were linked to increased crash rates and severe injury rates on non-interstate roads. On interstate roads, higher safety ratings were associated with increased rates of both severe and fatal injuries. When data from both roads were combined higher safety ratings were found to be associated with an increase in crash rate and severe injury rate. Safety barriers were highly effective in reducing crash severity. Safety barriers proved to be highly effective in significantly reducing crash severity, with a 73% reduction in severe injuries and a 90% reduction in fatal injuries across both interstate and non-interstate roads combined.

The study further separated cases with and without restraint to evaluate their impact on crash outcomes in relation to roadside features. In restraint-use cases, clear zone width showed a negative correlation with severe injury rate when both interstate and non-interstate roads were combined, though no significant relationship was observed when analyzing interstate and non-interstate roads separately. Distance from rigid obstacles, in restraint-use cases, were found to be significantly correlated with both severe and fatal injury rates, but only on interstate roads. For side slopes, steep slopes were positively correlated with an increase in crash rate, severe injury rate, and fatal injury rate on non-interstate roads. On interstate roads, steep slopes were positively correlated with higher severe injury rate, while in the combined dataset, they were associated with both severe and fatal injury rate. Safety ratings continued to be positively associated with crash and severe injury rates on non-interstate roads and in the combined dataset. On interstate roads, higher safety ratings were linked to increase in both severe and fatal injury rates.

In the analysis of non-restraint cases, clear zone width showed a negative correlation with crash rate and fatal injury rate on non-interstate roads, and with crash, severe injury, and fatal injury rates in the combined dataset of both road types. Rigid obstacles were found to be negatively correlated with crash rate on non-interstate roads and in the combined dataset of both road types. Similarly, side slopes were associated with higher crash rates on non-interstate roads and in the combined dataset. No significant relationships were observed on interstate roads alone. The t-test analysis further emphasized the importance of seat belt use, showing that restraints significantly reduced fatal and severe injuries while increasing the likelihood of non-injury outcomes. Hotspot identification, validated through Utah's crash cost analysis and the New South Wales approach, successfully pinpointed critical locations for safety interventions.

In conclusion, this research provides valuable insights into the critical role of roadside features in influencing crash severity and offers practical recommendations for safety improvements on Utah highways.

5.2 Limitations and Challenges

The use of computer vision technology has significantly enhanced the availability of roadside feature data, facilitating more detailed analysis. However, several limitations and challenges persist.

First, this approach depends on high-quality roadside images with clear visibility of both roadside conditions and lane markings. Low-quality images can lead to inaccurate detection of roadside features. Additionally, roadside conditions, including vegetation, are subject to change over time, requiring periodic retraining of the model with updated images to ensure accurate feature extraction and safety rating assignments. A notable challenge lies in the occurrence of false positives and false negatives in assessing roadside conditions. Computer vision algorithms may inaccurately classify non-hazardous features as hazardous or fail to detect actual hazards. Such errors can lead to unwarranted maintenance expenses or leave dangerous conditions unaddressed. Therefore, human verification is essential before taking action on identified road segments in need of improvement.

Furthermore, this study focuses exclusively on roadside features in rural RD crashes, without considering driver behavior or weather conditions. Therefore, the model should be used as a complementary tool rather than a complete replacement for comprehensive safety evaluations. Additionally, the statistical analysis is limited to rural RD crashes, excluding data from urban crash segments or urban roadside conditions, which narrows the study's focus and applicability to rural contexts only. Moreover, the roadside features analyzed are based on images from 2023, which may not completely reflect the precise conditions at the time each crash occurred.

6.0 RECOMMENDATIONS AND IMPLEMENTATION

6.1 Recommendations

Based on the analysis conducted on roadside features and their impact on rural RD crashes, several key recommendations are proposed to improve safety on Utah highways. The hotspot identification process, which used rankings of the severity rates, led to the selection of the top ten hazardous locations along each route. Safety measures are recommended for these top ten locations based on an extensive literature review and by analyzing the condition of the roadway from the images. The main safety improvements recommended are:

a. Speed Limit Control: Speed limit signs are recommended in locations where there is a high incidence of crashes involving vehicles exceeding the speed limit. These signs, along with speed radars, should be implemented to encourage compliance with speed regulations.

b. Clear Zone Improvement: Widening clear zones is recommended in areas where rigid obstacles are in close proximity to the roadway, posing a higher risk of collision. This improvement will help reduce crash severity by providing a larger recovery area for errant vehicles.

c. Safety Barriers Installation: Safety barriers are recommended to be installed or upgraded in locations with unrecoverable slopes or where rigid obstacles are located near the road, provided there is sufficient shoulder width. Installing these barriers can reduce the severity of crashes, especially in hazardous areas.

d. HFST: HFST is recommended for application on curves, where vehicle skidding and loss of control are more likely. This treatment is effective in reducing crash frequency and severity on curved sections of the roadway.

e. Pavement Marking Improvements: Increasing the width of pavement markings is recommended for areas with narrow shoulders. These improvements will enhance lane visibility and help prevent lane departures, particularly in poor weather conditions.

f. Rumble Strips: Rumble strips are recommended on hotspots where they are currently not present, provided there is sufficient shoulder width. They provide guidance and increase driver awareness, especially on long, straight sections where driver attention may lapse.

g. Chevrons: Chevrons are recommended for installation on curves to provide clear guidance to drivers and help reduce the likelihood of vehicles departing the roadway.

h. Cautionary Signs: Cautionary signs indicating "Risk Ahead" are recommended in areas experiencing a high number of crashes. They are also suggested for locations that appear safer, have minimal risk, and where other safety improvements may not be justified. These signs serve as reminders for drivers to remain cautious.

In addition to engineering-focused recommendations, educational efforts are crucial to enhancing roadway safety. Public awareness campaigns can inform drivers about the risk of RD crashes and preventive measures. Integrating educational outreach with infrastructure improvements can promote safer driving practices and help reduce RD crash risks across Utah's highways.

6.2 Implementation Plan

This research project and associated improvements to the roadside safety model provide three key points of value for enhancing Utah's roadway safety:

a) Model Adaptation for Pathway Images: The model was successfully adapted to work with the new images provided by Pathway, allowing for more efficient and accurate roadside feature extraction.

b) Inclusion of Interstate Highways: The model was expanded to include interstate highways, whereas previously, it was only trained and tested on rural non-interstate highways. This broadens the applicability of the model to all roadway types in Utah, making it a more comprehensive tool for roadside safety analysis.

c) Correlation and Impact Analysis: The correlation and impact of key roadside conditions such as slope, clear zone width, fixed objects, and barriers were examined. This detailed analysis allows for better-targeted safety improvements based on the specific roadside conditions contributing to crashes.

This model provides a new method for conducting risk-based analysis for roadside safety. By identifying unsafe roadside conditions based on actual field conditions rather than relying solely on crash events, we gain significant advantages in improving roadside safety. While similar analysis was previously possible with the United States Road Assessment Program (usRAP) data, the new model offers several improvements, including:

a. More Frequent and Lower-Cost Updates: Results can now be updated more frequently at a lower cost due to the efficiency of the automated machine learning model.

b. Adaptability: The model's outputs can be modified, recalibrated, or adjusted to account for new conditions or variables, providing a flexible tool that can evolve with changing needs.

c. Consistency: Outputs are consistent across the state, eliminating the variability that comes from human raters' judgments.

d. Granularity: The model can collect ratings at a higher granularity based on image collection intervals, providing more detailed insights into roadside conditions.

Effective implementation of this model will require a dedicated team with specific roles. A group of data analysts and machine learning specialists will be necessary to process and run the model, ensuring that the data is analyzed accurately and updated efficiently. Field technicians will play a crucial role in the regular collection of roadside images, maintaining up-to-date and comprehensive data coverage. To handle the large volume of images and ensure timely processing, specialized hardware such as high-performance computers with GPU capabilities will be required.

The implementation phase involves running the model for all state highways to provide a statewide roadside safety score. This will help assess the condition of roadways across Utah and identify priority areas for improvement. The UDOT Traffic & Safety Division will determine the most effective strategy moving forward. Both the usRAP data and the model from this research have value, but there is overlap in what they provide. The image-based model, with its ability to deliver sub-scores beyond just the hazard rating, offers more comprehensive information that can be used either independently or as a replacement for the usRAP-collected roadside hazard ratings.

REFERENCES

Abdel-Rahim, A., Chang, K., Mohamed, M., Skinner, A., & Kassem, E. (2018). *Safety Impacts of Using Wider Pavement Markings on Two-Lane Rural Highways in Idaho*. Idaho. Transportation Department.

Administrations, F. H. (2019). KABCO Injury Classification Scale and Definitions. *Online at: Https://Safety. Fhwa. Dot. Gov/Hsip/Spm/Conversion_tbl/Pdfs/Kabco_ctable_by_state. Pdf. Accessed on November 30*.

Alam, M. S., & Tabassum, N. J. (2023). Spatial pattern identification and crash severity analysis of road traffic crash hot spots in Ohio. *Heliyon*, *9*(5). https://doi.org/10.1016/j.heliyon.2023.e16303

Alsayed, A. R., & Manzi, G. (2019). A comparison of monotonic correlation measures with outliers. *WSEAS Transactions on Computers*, *18*(1), 223–230.

ATSSA. (2011). *Cost Effective Local Road Safety Planning and Implementation*. http://www.bts.gov/publications/national_transportation_statistics/html/table_01_06.html

Avelar, R., Geedipally, S., Das, S., Wu, L., Kutela, B., Lord, D., & Tsapakis, I. (2020). *Evaluation of Roadside Treatments to Mitigate Roadway Departure Crashes: Technical Report*. Texas A&M Transportation Institute.

Brilakis, I., Fathi, H., & Rashidi, A. (2011). Progressive 3D reconstruction of infrastructure with videogrammetry. *Automation in Construction*, *20*(7), 884–895.

Cai, X., Rahmati, Y., Jain, S., & Fishelson, J. (2023). Machine Learning Methods to Analyze and Predict Crash Injury Severity Based on Contributing Factors for Southeast Michigan. In *Transportation Research Record* (Vol. 2677, Issue 3, pp. 83–94). SAGE Publications Ltd. https://doi.org/10.1177/03611981221113569

Calvo-Poyo, F., de Oña, J., Garach Morcillo, L., & Navarro-Moreno, J. (2020). Influence of wider longitudinal road markings on vehicle speeds in two-lane rural highways. *Sustainability*, *12*(20), 8305.

Choudhary, J., Ohri, A., & Kumar, B. (2015). Spatial and statistical analysis of road accidents hot spots using GIS. *3rd Conference of Transportation Research Group of India (3rd CTRG)*.

Dai, F., Rashidi, A., Brilakis, I., & Vela, P. (2013). Comparison of image-based and time-of-flight-based technologies for three-dimensional reconstruction of infrastructure. *Journal of Construction Engineering and Management*, *139*(1), 69–79.

Daniello, A., & Gabler, H. C. (2011). Fatality risk in motorcycle collisions with roadside objects in the United States. *Accident Analysis and Prevention*, *43*(3), 1167–1170. https://doi.org/10.1016/j.aap.2010.12.027

David Merritt, Scott Himes, & R.J. Porter. (2021). *High Friction Surface Treatment Site Selection and Installation Guide*.

Deef-Allah, E., Broaddus, K., & Abdelrahman, M. (2022). Life cycle cost analysis of high friction surface treatment applications. *Transportation Research Record*, *2676*(7), 512–526.

Dissanayake, S., & Galgamuwa, U. (2017). Estimating crash modification factors for lane departure countermeasures in Kansas. *Final Report, Kansas Department of Transportation, Topeka, Kansas*.

Dissanayake, S., & Roy, U. (2014). Crash Severity Analysis of Single Vehicle Run-off-Road Crashes. *Journal of Transportation Technologies*, *04*(01), 1–10. https://doi.org/10.4236/jtts.2014.41001

Donnell, E. T., Porter, R. J., Li, L., Hamilton, I., Himes, S., & Wood, J. (2019). *Reducing roadway departure crashes at horizontal curve sections on two-lane rural highways*. United States. Federal Highway Administration. Office of Safety.

Elvik, R. (1995). The safety value of guardrails and crash cushions: a meta-analysis of evidence from evaluation studies. *Accident Analysis & Prevention*, *27*(4), 523–549.

Elvik, R. (2007). State-of-the-art approaches to road accident black spot management and safety analysis of road networks. *Institute of Transport Economics, Norvegian Centre for Transport Research.*, *Report 883*. https://www.toi.no/publications/state-of-the-art-approaches-to-road-accident-black-spot-management-and-safety-analysis-of-road-networks-article19461-29.html

Ewan, L., Al-Kaisy, A., & Hossain, F. (2016). Safety effects of road geometry and roadside features on low-volume roads in Oregon. *Transportation Research Record*, *2580*, 47–55. https://doi.org/10.3141/2580-06

Farhadmanesh, M., Rashidi, A., Subedi, A. K., & Marković, N. (2024). A Computer Vision-Based Standalone System for Automated Operational Data Collection at Non-Towered Airports. *IEEE Access*.

FHWA. (2013). *2013 National Roadway Safety Awards Noteworthy Practices Guide*. *FHWA-SA-14-002*.

Gayah, V. V., & Donnell, E. T. (2014). Establishing Crash Modification Factors and Their Use. *Pennsylvania Department of Transportation, Harrisburg, Pa.*, *FHWA-PA-2014-005-PSU WO 6*,. www.mautc.psu.edu

Guin, A., Rodgers, M. O., & Hunter, M. P. (2018). *Centerline Rumble Strips Safety Impact Evaluation—Phase 2*. Georgia. Department of Transportation. Office of Performance-Based ….

Han, L., Du, Z., Wang, S., & Chen, Y. (2022). Analysis of traffic signs information volume affecting driver's visual characteristics and driving safety. *International Journal of Environmental Research and Public Health*, *19*(16), 10349.

Hassandokht Mashhadi, A., Rashidi, A., & Marković, N. (2024). A GAN-Augmented CNN Approach for Automated Roadside Safety Assessment of Rural Roadways. *Journal of Computing in Civil Engineering*, *38*(2), 04023043.

Himes, S., Gross, F. B., Persaud, B., & Eccles, K. A. (2017). *Safety evaluation of edge-line rumble stripes on rural two-lane horizontal curves*. United States. Federal Highway Administration.

Holdridge, J. M., Shankar, V. N., & Ulfarsson, G. F. (2005). The crash severity impacts of fixed roadside objects. *Journal of Safety Research, 36*(2), 139–147.

Hossain, A., Sun, X., Islam, S., Alam, S., & Hossain, M. M. (2023). *Identifying roadway departure crash patterns on rural two-lane*.

Hussein, M., Sayed, T., El-Basyouny, K., & de Leur, P. (2020). Investigating safety effects of wider longitudinal pavement markings. *Accident Analysis & Prevention*, *142*, 105527.

Islam, M., & Pande, A. (2020). Analysis of Single-Vehicle Roadway Departure Crashes on Rural Curved Segments Accounting for Unobserved Heterogeneity. *Transportation Research Record*, *2674*(10), 146–157. https://doi.org/10.1177/0361198120935877

Jalayer, M., & Zhou, H. (2016a). Evaluating the safety risk of roadside features for rural two-lane roads using reliability analysis. *Accident Analysis and Prevention*, *93*, 101–112. https://doi.org/10.1016/j.aap.2016.04.021

Jalayer, M., & Zhou, H. (2016b). Overview of Safety Countermeasures. *Ite Journal*. https://onlinepubs.trb.org/Onlinepubs/trr/1991/1302/1302-003.pdf

Jalayer, M., Zhou, H., & Das, S. (2019). Exploratory Analysis of Run-Off-Road Crash Patterns. In *Data Analytics for Smart Cities* (pp. 183–200). Auerbach Publications. https://doi.org/10.1201/9780429434983-8

Kirk, A. (2008). *Evaluation of the effectiveness of pavement rumble strips*. University of Kentucky Transportation Center.

Lee, J., & Mannering, F. (2002). Impact of roadside features on the frequency and severity of run-off-roadway accidents: an empirical analysis. *Accident Analysis & Prevention*, *34*(2), 149–161.

Li, N., Park, B. B., & Lambert, J. H. (2018). Effect of guardrail on reducing fatal and severe injuries on freeways: Real-world crash data analysis and performance assessment. *Journal of Transportation Safety and Security*, *10*(5), 455–470. https://doi.org/10.1080/19439962.2017.1297970

Lord, D., Brewer, M. A., Fitzpatrick, K., Geedipally, S. R., & Peng, Y. (2011). ANALYSIS OF ROADWAY DEPARTURE CRASHES ON TWO-LANE RURAL ROADS IN TEXAS. *Texas Department of Transportation*, *FHWA/TX-11/0-6031-1*.

Mashhadi, A. H., Rashidi, A., & Markovic, N. (2023). AUTOMATED SAFETY ASSESSMENT OF RURAL ROADWAYS USING COMPUTER VISION. *Technical Report, Utah. Dept. of Transportation. Research Division*.

Matsumoto, H., Mori, Y., & Masuda, H. (2021). Extraction of guardrails from mms data using convolutional neural network. *International Journal of Automation Technology, 15*(3), 258–267.

Merritt, D. K., Lyon, C., Persaud, B., & Torres, H. N. (2020). *Developing crash-modification factors for high-friction surface treatments*. United States. Federal Highway Administration.

Miles, J. D., Carlson, P. J., Eurek, R., Re, J., & Park, E. S. (2010). *Evaluation of potential benefits of wider and brighter edge line pavement markings.* Texas Transportation Institute.

Mohamed, M. (2018). *Safety Impact of Wider Pavement Edge Line Markings*. University of Idaho.

Obaid, I., Alnedawi, A., Aboud, G. M., Tamakloe, R., Zuabidi, H., & Das, S. (2023). Factors associated with driver injury severity of motor vehicle crashes on sealed and unsealed pavements: Random parameter model with heterogeneity in means and variances. *International Journal of Transportation Science and Technology*, *12*(2), 460–475.

Peng, Y., Geedipally, S., & Lord, D. (2012). Effect of roadside features on single-vehicle roadway departure crashes on rural two-lane roads. *Transportation Research Record*, *2309*, 21–29. https://doi.org/10.3141/2309-03

Pigman, J. G., & Agent, K. R. (1991). *Guidelines for installation of guardrail* (Issue 1302).

Qawasmeh, B., & Eustace, D. (2022). Effectiveness of Cable Median Barriers in Preventing Cross Median Crashes and Related Casualties in the United States-A Systematic Review. *International Road Federation World Meeting & Exhibition*, 345–354.

Roque, C., Moura, F., & Lourenço Cardoso, J. (2015). Detecting unforgiving roadside contributors through the severity analysis of ran-off-road crashes. *Accident Analysis and Prevention*, *80*, 262–273. https://doi.org/10.1016/j.aap.2015.02.012

Satterfield, C., McGee, H. W., & Hanscom, F. R. (2009). Horizontal Curve Safety. In *Federal Highway Administration (FHWA)* (Issue FHWA-HRT-09-003,). https://highways.dot.gov/public-roads/marapr-2009/low-cost-safety-improvements-horizontal-curves

Spearman, C. (1904). The Proof and Measurement of Association between Two Things. *The American Journal of Psychology*, *15*(1), 72–101. https://doi.org/10.2307/1412159

Sperry, R., Latterell, J., & McDonald, T. (2008). Best Practices for Low-Cost Safety Improvements on Iowa's Local Roads. In *Iowa Department of Transportation* (Issue FHWA Project BPSG (383)). www.ctre.iastate.edu

Stephens Jr, L. B. (2005). Barrier guide for low volume and low speed roads (No. FHWACFL/TD-05-009). *Federal Highway Administration*.

Taylor, H. W. (2005). Preventing roadway departures. *Public Roads*, *69*(1).

Wu, H., Han, Z., Murphy, M. R., & Zhang, Z. (2015). Empirical Bayes before–after study on safety effect of narrow pavement widening projects in Texas. *Transportation Research Record*, *2515*(1), 63–69.

Xie, Q., Li, D., Yu, Z., Zhou, J., & Wang, J. (2019). Detecting trees in street images via deep learning with attention module. *IEEE Transactions on Instrumentation and Measurement*, *69*(8), 5395–5406.

Zhou, H., Jalayer, M., & Pour-Rouholamin, M. (2015). Preventing Vehicle Departures from Roadways. *AMERICAN TRAFFIC SAFETY SERVICES ASSOCIATION*. www.atssa.com

Zou, Y., Tarko, A. P., Chen, E., & Romero, M. A. (2014). Effectiveness of cable barriers, guardrails, and concrete barrier walls in reducing the risk of injury. *Accident Analysis and Prevention*, *72*, 55–65. https://doi.org/10.1016/j.aap.2014.06.013

APPENDIX A: PREPROCESSING

Preprocessing is a crucial step in machine learning that involves transforming raw data into a format that can be effectively utilized by machine learning models. In the context of image classification, various preprocessing techniques are available, but for this research, we are specifically focusing on cropping as a key method for preparing roadway images. This approach allows us to remove irrelevant parts of the images, enabling our analysis to focus exclusively on the roadside features that are critical for our study.

In this project, we systematically crop all images from Pathways to their bottom right section, where the relevant roadside features are typically located. By applying a consistent cropping technique across all images, we ensure uniformity in the layout, which is vital for achieving accurate and reliable results. This uniformity not only enhances the precision of our analysis but also optimizes the processing time. By eliminating irrelevant parts of the images, we streamline the analysis, allowing the model to focus solely on the essential features, thereby improving both efficiency and accuracy. Figure A-1 provides an example of the image cropping process, illustrating how the irrelevant portions of the image are removed to retain only the relevant roadside features, which are crucial for our analysis.

Figure A-1: Image Cropping

Figure A-2 shows the Python implementation for cropping the images:

```python
from PIL import Image
import os
from tqdm import tqdm

def crop_and_save_images(source_path, target_path, crop_params):
    """
    Recursively crop images from source_path to target_path maintaining the folder structure.
    """
    for root, dirs, files in os.walk(source_path):
        # Determine the path in the target directory
        rel_path = os.path.relpath(root, source_path)
        target_dir = os.path.join(target_path, rel_path)

        # Create the target directory if it does not exist
        if not os.path.exists(target_dir):
            os.makedirs(target_dir)

        for file in tqdm(files):
            # Check if the file is an image (by extension, could be improved)
            if file.lower().endswith(('.png', '.jpg', '.jpeg')):
                try:
                    # Construct full file paths
                    file_path = os.path.join(root, file)
                    target_file_path = os.path.join(target_dir, os.path.splitext(file)[0] + '_Cropped.jpg')

                    # Open, crop, and save the image
                    im = Image.open(file_path)
                    w, h = im.size
                    imCrop = im.crop((int(w * crop_params[0]), int(h * crop_params[1]), int(w * crop_params[2]), int(h * crop_params[3])))
                    imCrop.save(target_file_path, "JPEG", quality=100)
                except Exception as e:
                    print(f"Error processing {file_path}: {e}")

# Set the path to the directory containing the images
source_path = "E:\\Pathway Images\\SR"
# Directory where cropped images will be saved
target_path = "F:\\Pathway Images\\SR_Cropped"

# Crop parameters as fractions of width and height: (left, upper, right, lower)
crop_params = (0.54, 0.356, 1.0, 0.895)

# Process the images
crop_and_save_images(source_path, target_path, crop_params)

print("Finished processing images.")
```

Figure A-2: Python Implementation for Image Cropping

This Python script processes images within a specified directory by cropping them and saving the cropped versions into a new directory. All images are named based on the route, camera angle (specified as "Perspective"), and milepoint, using a consistent naming convention that includes the prefix "SR" for all routes. For example, an image from SR-10 at milepoint

0.099 is named "SR_10_Perspective_0.099." This uniform naming system helps in effectively managing the images when integrating them into an Excel sheet with classifications.

Here is a brief breakdown of the code:

Imports: The script uses the PIL library for image processing, os for file and directory operations, and tqdm for showing a progress bar.

Function crop_and_save_images: This is the core function that processes images in the source directory, crops them according to the specified parameters, and saves them in the target directory while preserving the original directory structure.

- source_path: The directory containing the images to be cropped.
- target_path: The directory where the cropped images will be saved.
- crop_params: A tuple of four values specifying the fraction of the width and height of the image to be used for cropping.

Script Parameters:

- source_path: Set to "E:\\Pathway Images\\SR", which is the directory containing the images.
- target_path: Set to "E:\\Pathway Images\\SR_Cropped," where the cropped images will be saved.
- crop_params: The crop parameters (0.54, 0.356, 1.0, 0.895) are used to specify the part of the image to retain after cropping.

Output: The script will save cropped images in the target directory, appending _Cropped.jpg to each file name.

APPENDIX B: APPLICATION

Figure B-1 shows a snapshot of the application:

```python
import numpy as np
import cv2
import glob
import os
from sklearn.model_selection import train_test_split
from sklearn import preprocessing
from keras.applications.vgg16 import VGG16
import xgboost as xgb
from sklearn import metrics
from tqdm import tqdm

def load_and_preprocess_images_in_batches(image_paths, batch_size=32, size=256)
    """
    Load and preprocess images in batches.
    """
    for start in range(0, len(image_paths), batch_size):
        end = min(start + batch_size, len(image_paths))
        batch_paths = image_paths[start:end]
        images = []

        for img_path in batch_paths:
            img = cv2.imread(img_path, cv2.IMREAD_COLOR)
            if img is not None:
                img = cv2.resize(img, (size, size))
                img = cv2.cvtColor(img, cv2.COLOR_RGB2BGR)
                images.append(img)
            else:
                print(f"Failed to read image: {img_path}")

        yield np.array(images, dtype=np.float32) / 255.0

def load_images_and_labels(base_folder):
    """
    Load image paths and corresponding labels.
    """
    images = []
    labels = []

    for directory_path in glob.glob(os.path.join(base_folder, "*")):
        label = directory_path.split("\\")[-1]
        for img_path in glob.glob(os.path.join(directory_path, "*.jpg")):
            images.append(img_path)
            labels.append(label)

    return np.array(images), np.array(labels)

# Load image paths and labels
base_folder = "E:/Final Model/Clear zone/train"
train_images, train_labels = load_images_and_labels(base_folder)

```

Figure B-1: Snapshot of Application

The process begins by importing essential libraries for numerical operations, image processing, data manipulation, and model evaluation. Key tools include the VGG16 pre-trained model from Keras for feature extraction and XGBoost for classification tasks.

Initially, images are loaded and preprocessed in batches. This involves reading the images, resizing them, converting their color format, and normalizing pixel values to a range between 0.0 and 1.0, which is crucial for handling large datasets efficiently.

Images and their corresponding labels are then loaded from a specified directory. The file paths of the images are stored, and labels are derived from directory names. The process ensures that the number of images and labels is accurately collected and verified.

Next, the labels are encoded from text to integers using a label encoder. The dataset is split into training and validation sets, with the class distribution maintained in both sets to ensure proper model training.

The VGG16 model, pre-trained on ImageNet, is employed without its fully connected layers. The model's layers are set to non-trainable, allowing it to serve as a feature extractor. Features from the images are extracted in batches, which is particularly efficient for large datasets.

The extracted features are then used to train an XGBoost classifier. After training, predictions are made for the validation set. The predicted labels are inverse-transformed back to their original form, and the model's performance is evaluated using accuracy, precision, and recall metrics.

This approach enables efficient handling and processing of large image datasets by utilizing pre-trained deep learning models for feature extraction and machine learning models for classification.

APPENDIX C: PROCESSING IMAGES

Figure C-1 shows the Python implementation for using the trained model for prediction.

```python
import numpy as np
import cv2
import glob
import os
import pandas as pd
from keras.applications.vgg16 import VGG16
from tqdm import tqdm
from sklearn.preprocessing import LabelEncoder
import xgboost as xgb

SIZE = 256  # Resize images

# Load the pre-trained VGG16 model
VGG_model = VGG16(weights='imagenet', include_top=False, input_shape=(SIZE, SIZE, 3))
for layer in VGG_model.layers:
    layer.trainable = False

# Function to load and preprocess images
def load_and_preprocess_image(path):
    img = cv2.imread(path, cv2.IMREAD_COLOR)
    img = cv2.resize(img, (SIZE, SIZE))
    img = cv2.cvtColor(img, cv2.COLOR_RGB2BGR)
    img = img / 255.0
    return img

# Function to parse the filename to extract the prefix and mile point
def parse_filename(filename):
    # Example filename: "SR_15_Perspective_100.002_Cropped_Cropped.jpg"
    parts = filename.split('_')
    prefix = parts[0] + '_' + parts[1]  # e.g., SR_15 or SR_80
    mile_point = float(parts[3])  # Adjust index as per your filename format
    return prefix, mile_point

# Load your trained XGBoost model and LabelEncoder
# Assuming these are loaded correctly as `model` and `le`

# Directory containing images to predict
image_directory = "G:/SR test"
image_paths = glob.glob(os.path.join(image_directory, "*.jpg"))
image_paths.sort(key=lambda x: parse_filename(os.path.basename(x)))

# Batch processing parameters
batch_size = 32
results = []

# Predicting in batches
for start in tqdm(range(0, len(image_paths), batch_size)):
    end = start + batch_size
    batch_paths = image_paths[start:end]
    batch_images = np.array([load_and_preprocess_image(path) for path in batch_paths])

    # Extract features using the VGG model
    features = VGG_model.predict(batch_images)
    features = features.reshape(features.shape[0], -1)

    # Predict using the XGBoost model
    batch_predictions = model.predict(features)
    batch_predictions = le.inverse_transform(batch_predictions)

    # Append predictions and print results
    for img_path, prediction in zip(batch_paths, batch_predictions):
        file_name = os.path.basename(img_path)
        results.append((file_name, prediction))
        print(f"Predicted {prediction} for {file_name}")

# Create DataFrame and save results
df_predictions = pd.DataFrame(results, columns=["File_name", "Prediction"])
df_predictions.to_csv("clear zone predictions.csv", index=False)

print("Prediction completed")
```

Figure C-1: Python Implementation for Prediction

The process begins by importing necessary libraries for numerical operations, image processing, file handling, and model operations. The VGG16 model is loaded without its fully connected layers, and the layers are set to non-trainable for feature extraction.

A function is defined to load and preprocess images by resizing, converting color formats, and normalizing pixel values. Another function parses file names to extract route prefixes and milepoints, aiding in organizing and sorting images.

The application assumes the XGBoost model and label encoder are pre-loaded. Image paths from the specified directory are gathered and sorted based on parsed file names. Images are processed in batches where features are extracted using the VGG16 model, and predictions are made with the XGBoost model. Predicted labels are then inverse-transformed to their original form.

The predictions and file names are compiled into a data frame and saved to a CSV file. The process concludes with a confirmation message indicating successful completion.